Amino Acid Synthesis in Meteoritic Parent Bodies of Carbonaceous Chondrites

Amino Acid Synthesis in Meteoritic Parent Bodies of Carbonaceous Chondrites

By

Alyssa Cobb, B.Sc.

A Thesis
Submitted to the School of Graduate Studies
in Partial Fulfilment of the Requirements
for the Degree
Master of Science

McMaster University

Master of Science (2013) McMaster University

(Physics and Astronomy)

(Collaborative Graduate Program in Astrobiology) Hamilton, Ontario

TITLE: Amino Acid Synthesis in Meteoritic Parent Bodies of Carbonaceous Chondrites

AUTHOR: Alyssa Cobb, B.Sc. (Colorado School of Mines)

SUPERVISOR: Ralph E. Pudritz

NUMBER OF PAGES: xv, 119

Abstract

The class of meteorites called carbonaceous chondrites are examples of material from the solar system which have been relatively unchanged from the time of their initial formation. We investigate the carbonaceous chondrite subclasses CI, CM, CR, CV, and CO, which contain high levels of water and organic material, including amino acids. These subclasses span petrologic types 1 through 3, indicating the degree of internal chemistry undergone by the meteoritic parent body. The goal of this thesis is two-fold: to obtain a comprehensive view of amino acid abundances and relative frequencies in carbonaceous chondrites, and to recreate these patterns via thermodynamic computational models.

We collate available amino acid abundance data for a variety of meteorites to identify patterns in total abundance and relative frequencies. We consider only a set of 20 proteinogenic α-amino acids created via a specific chemical pathway called Strecker synthesis. We plot abundances of individual amino acids for each subclass, as well as total abundances across all subclasses. We see a predominance in abundance and variety of amino acids in the CM and CR subclasses, which contain concentrations of amino acids greater by several orders of magnitude than other carbonaceous subclasses. These subclasses correspond to an aqueous alteration temperature range of 200°C to 400°C. Within the CM2 and CR2 meteorites, we identify trends in the relative frequencies of amino acids in preparation for computational modeling.

Now having a baseline observed amino acid abundance plot, we recreate both the total amino acid abundance pattern as well as the relative frequency of amino acids within the CM2 chondrite subclass using computational models. We use thermodynamic theory of Gibbs free energies to calculate the output of amino acids in a meteoritic parent body assuming chemical equilibrium and some set of initial concentrations of organic material. Our model recreates abundance patterns in the temperature range 200°C to 400°C, $\sim 10^5$ parts-per billion (ppb), and the temperature range 400°C to 500°C, $\sim 10^2$ ppb. Our model does not fit well between temperatures of 150°C to 200°C. Our current model assumes a uniform composition of initial chemical reactants; likely an inhomogeneous composition would be a more accurate physical representation of a parent body. In addition, we match relative frequencies to observed frequencies for each amino acid in the CM2 subclass to well within an order of magnitude.

Acknowledgements

This project represents two years' worth of effort and hard work. It would never have come to pass without the assistance of many people, I am especially grateful to my supervisor, Prof. Ralph Pudritz, for his direction and myriad suggestions regarding the greater context of this project in the fields of astrobiology and astrophysics. Thanks also my committee members Prof. Doug Welch and Prof. Greg Slater.

Much of this research has benefited from the experience of, and/or discussion with, a variety of people. The crowd at NASA Goddard has been an invaluable reference, especially regarding amino acid abundances in meteorites, including Daniel Glavin, Aaron Burton, and Jamie Elsila. Thanks also to Stephen Freeland, at University of Hawai'i, and Jason Hein, at University of California, Merced. We also received assistance from people closer to home. Prof. Paul Ayers, at McMaster University, helped immensely with his expertise in theoretical chemistry. His graduate student, Farnaz Zadeh. Also Darren Fernandes and Lee Bardon, both summer research students who worked on this project with me, and Jeff Emberson, who began the project with Ralph before I arrived. I am also indebted to the Canadian Astrobiology Training Program for the graduate fellowship on which I depend.

I am very grateful to my fellow graduate students Mikhail Klassen and Rory Woods for their regular assistance and expertise in Python and coding in general.

For all the late nights, early mornings, and sweaty afternoons, thank you to the whiskey, pancake, and softball crowds. You guys made this a lot of fun and more bearable than it otherwise might have been. I was being extremely clever and you guys were excellent at standing around looking impressed!

And finally, to my family. The love and encouragement of my parents have followed me across continents and fields of study. I know their unconditional support will continue with whatever I chose to do next.

Dedicated to
Disney & The Doctor

Table of Contents

Chapter 3 Nature's Starships I: Abundance and Relative Frequency of Amino Acids in Meteorites 31

List of Figures

List of Tables

Chapter 1

Introduction

Since the 1960s, certain meteorites have been known to contain a substantial quantity and variety of organic material. A class of meteorite called the carbonaceous chondrites have a composition which is especially rich in carbon, water, and organic molecules. These organics may include, but are not limited to, amino acids, carboxylic acids, aldehydes, nucleobases, phospholipids, and sugars (Hayes, 1967; Chyba et al., 1990; Botta & Bada, 2002, and references therein). The amino acid content of carbonaceous chondrites is of particular note, as these molecules are the building blocks of proteins, which are a necessary component for life on Earth (Chyba et al., 1990; Chyba & Sagan, 1992).

Interest in the origin of amino acids in meteorites has only increased over the last half-century. We know these molecules are being delivered to Earth, and possibly other planetary systems, via meteoritic impacts. How, then, are they being formed? What is involved in the creation of meteoritic parent bodies, and how are these organics being synthesized in their interiors?

Meteorites are thought to originate from larger parent bodies which would have formed during the time of solar system formation. Likely composed primarily of rock and ice, these parent bodies would be on the order of a few tens of kilometers in diameter. The closest analogues we have for these bodies are present-day asteroids. Meteorites found on Earth are likely fragments of their larger parent bodies, ejecta from collisions with parent bodies in the protoplanetary disk (Sephton & Botta, 2005; Gaidos & Selsis, 2007). Carbonaceous chondrites are thought to originate from type C asteroids, which are water-rich and likely came from the outer regions of the asteroid belt (Morbidelli et al., 2012, and references therein).

Given some basic understanding of the formation of meteorites, researchers may now model meteoritic parent bodies in an effort to constrain their internal chemistry. Young et al. (1999), Schulte & Shock (2004) and Travis & Schubert (2005) model parent bodies as agglomerations of ice, rock, and various interstellar organic material present during formation. The radionuclide decay of isotopes such as ^{26}Al in their interiors keeps the temperature near the core high enough to melt water. Once liquid water is present, there are a variety of internal chemical processes which cause the organic material initially present to alter into new substances. These processes are collectively called aqueous alteration. See Grimm & McSween Jr. (1989); McSween Jr. & Weissman (1989); Weiss & Elkins-Tanton (2013, and references therein) for a review.

One example of this internal chemistry is Strecker synthesis. Strecker synthesis is a well known process which creates amino acids and may be easily recreated in a laboratory environment. The constituents are common in the interstellar medium and in molecular clouds. As laid out in Botta & Bada (2002) and Botta (2005), the Strecker reaction of hydrogen cyanide (HCN), ammonia (NH_3), and an aldehyde (R-CHO) in aqueous solution (H_2O) produces an intermediary called an aminonitrile. Aminonitriles then undergo a one-way process called hydrolysis, resulting in the synthesis of α-amino acids. All of the necessary reactants for Strecker synthesis have been detected in the spectra of comets, which are thought to be remnants of the earliest phases of protoplanetary disks. We can use cometary data, then, as a rough analog for molecular concentrations.

Early theory for the exogenous delivery of organic material to the early Earth was developed by Chyba & Sagan (1992). The early Earth underwent a brief period of intense meteoritic bombardment approximately 4 billion years ago. This bombardment would have provided the Earth with significant quantities of water, carbon, and organic material, including amino acids. In this way, meteorites are likely to be a key factor in the origin and evolution of life on Earth (Chyba & Sagan, 1992, 1997; Engel & Perry, 2008).

An early criticism of this theory was the damage organic material would experience during entry into Earth's atmosphere. Numerous studies have been performed showing that organic material, including amino acids, does in fact survive the intense temperatures, pressures, and shocks of atmospheric entry. These dangers to biomolecules certainly exist, but there are a several mitigating factors which allow for their survival and safe deposition on Earth. Among these are the extremely short duration of entry, obliqueness of impact, and atmospheric drag (Grimm & McSween Jr., 1989; McSween Jr. & Weissman, 1989; Chyba et al., 1990; Chyba & Sagan, 1992; Ehrenfreund et al., 2002).

The primary purpose of this thesis is to model the synthesis of amino acids in the interiors of meteoritic parent bodies with the intent of accounting for observed amino acid concentrations and relative frequencies in meteorites. This work begins with a thorough literature search to create an amino acid landscape, describing the abundances and relative frequencies of amino acids in a variety of carbonaceous chondrite subclasses. Once we know the frequency patterns and concentrations of amino acids, we use a chemical thermodynamics software program based on a minimization of Gibbs free energy to predict an outcoming set of amino acids for some set of initial conditions. In this retrospective fashion we constrain the alteration conditions (temperature, pressure, and initial concentrations of organics) involved in the Strecker synthesis of biomolecules.

Chapter 2

Background

2.1 Observational Background

Meteorites provide a geologic and chemical record of organic materials across space and time. Meteoritic parent bodies formed during the formation of the solar system and contain materials present at that time. There are a wide variety of meteorite types, all composed of a wide range of varying materials. Being inhomogeneous in nature, different compositions of meteorite are thought to indicate the degree of mixing of materials when their parent bodies were formed. There is a range in alteration temperatures associated with different minerals found in meteorites, and we can use these alteration temperatures to further categorize meteorite samples. The class of meteorites called carbonaceous chondrites is of particular interest with respect to the origin of biomolecules. Representing a mere 4% of all meteorite falls (Glavin et al., 2011), carbonaceous chondrites are relatively undifferentiated from the material with which they were originally formed. They contain exceptionally high concentrations of water, carbon, and other organic materials, relative to other meteorite classes.

Carbonaceous chondrites are further divided into subclasses based on their composition and mineralogy. Subclasses are designated with a pair of letters based on the name of a representative meteorite fall of the type in question. The subclasses we consider in this work are CI (Ivuna-like), CM (Mighei-like), CR (Renazzo-like), CV (Vigarano-like), and CO (Ornans-like).

In addition, each meteorite is identified with a number 1-6 which indicates petrologic type. This number reflects the degree of post-formation processing which has taken place inside the meteoritic parent body. Aqueous alteration, which refers collectively to a variety of internal chemical processes which create hydrous minerals and organic molecules when liquid water interacts with rocky material in the interior of parent bodies, occurs at lower processing temperatures ($\sim 150°$C to $400°$C), increasing as we move from types three through one. Thermal metamorphism, referring to any alteration process which changes one mineral into another with no contributions from water, occurs at higher temperatures ($\sim 600°$C to $950°$C), increasing as we move from types four through six (Sephton, 2002; Weisberg et al., 2006; Taylor, 2011; Weiss & Elkins-Tanton, 2013). For an illustrative chart, see Fig. 3.1. Observations agree with expectations in regard to organic content; amino acids have been found in significant quantities among aqueously altered type 1 and 2 chondrites, and, to a lesser extent, type 3 chondrites.

It has been proposed that different subclasses of carbonaceous chondrite not only share similar chemical and mineralogical makeups, but may actually share origins. Ehrenfreund et al. (2001), Glavin et al. (2011), and Gail et al. (2013), for example, discuss the possibility that all carbonaceous chondrites within a single subclass originate from the same meteoritic parent body. The cause of different subclasses could be that their sources are physically different parent bodies. Gail et al. (2013) and Weiss & Elkins-Tanton (2013) have also discussed the possibility that different petrologic types originate from different layers of a parent body. For example, locations near the core of a parent body might lead to thermal metamorphism (petrologic types 4-6), due to the higher temperatures and limited water content, whereas type 3 meteorites associated with cooler temperatures might originate from material near the surface of a parent body. In this work, we refer to the above theory as the onion shell model for chondrite parent bodies. The onion shell model is well reviewed in Weiss & Elkins-Tanton (2013, and references therein), and the fluid flow within such a body is discussed in Young et al. (1999).

Carbonaceous chondrites have a wide variety of properties which help classify them. Some contain more water, while others may have a greater organic carbon content. The structure of a carbonaceous chondrite may be generalized to an extent; all but a single type contain structures called chondrules. Chondrules are near-spherical objects on the order of a few millimeters in size. It is these objects which are examples of molten material residue from the time of the formation of the solar system. Over time, aqueous alteration (or thermal metamorphism, depending on the temperature and water content) took place and led to the creation of organic material (Hayes, 1967; Botta & Bada, 2002; Taylor, 2011).

CI-type meteorites, like most carbonaceous chondrites, contain near solar abundances of various metals, including magnesium, silicon, and calcium. CI meteorites are unique among carbonaceous chondrites in that they are the only subclass in which no chondrules are found. They have a high content of both water and carbon, both in the form of carbonates and organic carbon, such as amino acids. Their carbon content may be as great as 3% by weight. The water and carbon content likely indicate that these meteorites have undergone the highest degrees of aqueous alteration. Petrologically speaking, these chondrites are all type 1 and have never experienced temperatures higher than $\sim 200°$C. Their parent bodies may have been located near the edges of the protoplanetary disk. They are the most primitive examples of carbonaceous chondrite. (Hayes, 1967; Botta & Bada, 2002; The Catalogue of Meteorites, 2012; Meteoritical Bulletin Database, 2013).

Carbonaceous chondrites of the CM subclass are distinguished by the presence of numerous small chondrules, most no larger than 0.3 mm. The remainder of a CM meteorite is composed of a fine-grained silicate matrix, up to 70% by volume. Like CI-types, they also contain a variety of metals in near-solar abundances, and contain considerable quantities of nickel. They are very abundant in hydrated minerals, and contain 1.8% to 2.6% by weight of carbon. CM chondrites are primarily petrologic type 2, though a few type 1 CM chondrites have also been identified. They show slightly less water content than the CI-types, and contain the greatest concentrations of organic content of all subclasses (Hayes, 1967; Botta & Bada, 2002; The Catalogue of Meteorites, 2012; Meteoritical Bulletin Database, 2013).

CR-type meteorites contain numerous, large chondrules, on the order of 1 mm in size, which occupy approximately 50% of the available volume. The remaining 50% is composed of a fine-grain matrix which may be well hydrated. They have the second highest levels of metals in all carbonaceous chondrite subclasses, between 5% and 8% by volume. Most CR meteorites are petrologic type 2, and contain a correspondingly high level of organic material, rivaling that of the CM subclass (Hayes, 1967; Botta & Bada, 2002; The Catalogue of Meteorites, 2012; Meteoritical Bulletin Database, 2013).

CV chondrites contain large chondrules–up to several millimeters in size–and are composed of up to 40% by volume of a silicate matrix. These meteorites are characterized by their numerous and easily recognizable large chondrules and show little to no evidence of aqueous alteration; they contain relatively little water and organic material. This subclass also contains calcium-aluminum inclusions (CAIs). All known samples of CV carbonaceous chondrite belong to petrologic type 3, and contain approximately 0.2% to 1.0% carbon by weight (Hayes, 1967; Botta & Bada, 2002; The Catalogue of Meteorites, 2012; Meteoritical Bulletin Database, 2013).

Similar to the CV subclass, CO-type chondrites show little to no evidence for aqueous alteration. They contain few organic molecules. It is thought the CO-types likely formed in the same region of the solar system as the CVs. CO-types also contain CAIs, but they are slightly smaller in size and fewer in number than CAIs in CV meteorites. All known samples of CO chondrites are also petrologic type three, with a percent by weight of carbon between 0.2 and 1.0 (Hayes, 1967; Botta & Bada, 2002; The Catalogue of Meteorites, 2012; Meteoritical Bulletin Database, 2013).

There are a few additional subclasses of carbonaceous chondrite which we do not consider in this work. The CB (Bencubbin-like) and CK (Karoonda-like) meteorites are both characterized by a lack of internal aqueous alteration. They are associated with petrologic types 3 (for CB-types) and 4, 5, and 6 (for CK-types), and the higher temperatures of thermal metamorphism, where it is too hot to retain liquid water. CB-types may contain some amino acids, but this classification is extremely young and there is no available amino acid data on CB meteorites at the time of writing this thesis[1]. CH chondrites are so named for their extremely high metal content, which may be as high as 40%. CH-types seem to be type 3 meteorites, and have a correspondingly low organic content (Hayes, 1967; Botta & Bada, 2002; The Catalogue of Meteorites, 2012; Meteoritical Bulletin Database, 2013).

---

[1] A new paper was just published, Burton et al. (2013), which includes the first amino acid abundance data for carbonaceous chondrite subclasses CH and CB. There is insufficient time before thesis submission to add these data to this thesis. For reference and for future work, there is more information in CH and CB subclasses now available.

2.2 Theory

2.2.1 Proteinogenic α-Amino Acids

There are hundreds of amino acids found on Earth. In this work, we consider a specific subset: the α-variety of proteinogenic amino acids. α-amino acids are so named for the location of their amino groups. The general structure of an amino acid is 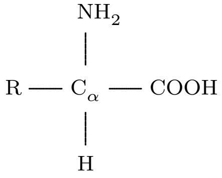 $\mathrm{R} - \underset{\displaystyle \mathrm{H}}{\overset{\displaystyle \mathrm{NH_2}}{\mathrm{C}_\alpha}} - \mathrm{COOH}$, with the R group indicating the side chain. It is this side chain which varies and creates the different amino acids. The 'α' signifies that the amino group (NH_2) of the amino acid is attached at the α carbon. The α carbon is the first carbon; the carbon to which the carboxyl group (COOH) and side chain (R) attach (Pizzarello, 2009; Pizzarello & Holmes, 2009; Hein, 2012, private communication). Note that the Strecker synthesis processes which we discuss below create only α-amino acids.

Amongst the wide variety of α-amino acids, we consider only those amino acids which are proteinogenic. Proteinogenic amino acids are a set of 20 amino acids which are coded for directly by our genetic code. They are an essential part of life on Earth, as they are the building blocks and precursors to proteins. These 20 amino acids are: alanine, arginine, asparagine, aspartic acid, cysteine, glutamic acid, glutamine, glycine, histidine, isoleucine, leucine, lysine, methionine, phenylalanine, proline, serine, threonine, tryptophan, tyrosine, and valine.

2.2.2 Parent Body Processes: Strecker Synthesis

As mentioned earlier, once liquid water is present in the meteoritic parent body, it and any organic materials present can undergo aqueous alteration to produce amino acids. In this work, we focus on one particular type of aqueous alteration, a process called Strecker synthesis. Strecker synthesis is defined as reactions between aldehydes or ketones with hydrogen cyanide, ammonia, and water to create amino acids or hydroxy acids, respectively (Schulte & Shock, 1995; Botta et al., 2002; Sephton & Botta, 2005; Elsila et al., 2007). Strecker theory is a promising avenue of investigation when considering the synthesis of extraterrestrial amino acids; all requisite reactants exist among the volatile content of comets, which we use as an analogue for meteoritic parent bodies (Schulte & Shock, 2004; Alexander, 2011).

In this research, we confine our attention to the formation and concentrations of α-amino acids created by these particular chemical pathways known as Strecker reactions. Strecker synthesis reactions for amino acids are defined specifically in the following manner: aldehyde molecules, in aqueous solution, with hydrogen cyanide and ammonia, react to produce amino acids. The simplest example of a Strecker pathway involves glycine, the simplest amino acid. The Strecker reaction resulting in the formation of glycine is shown in the following series of steps in Figure 2.1, as outlined in Schulte & Shock (1995), Rimola et al. (2010), and Hein (2012, private communication). Note that, following convention, carbon (C) and hydrogen (H) atoms are not written into place for each biomolecule. Any junction of two or more bonds that is not otherwise labeled has a C atom at the core. Carbon always makes 4 bonds, so when not otherwise labeled, any bonds not shown around a carbon atom may be assumed to be hydrogen.

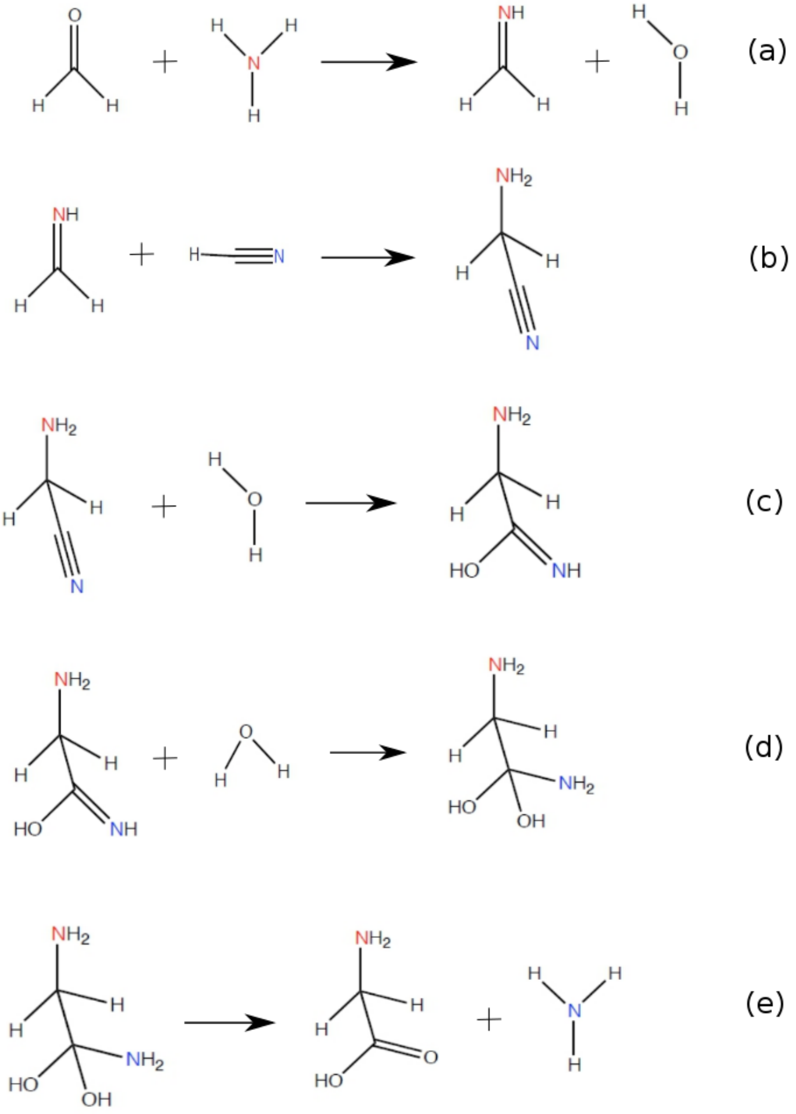

Figure 2.1: Steps involved in Strecker synthesis of glycine, as outlined in Schulte & Shock (1995), Rimola et al. (2010), and Hein (2012, private communication). Line (a) shows step 1. Initial reactants are formaldehyde (CH_2O) and ammonia (NH_3), which combine to produce methanimine ($NHCH_2$) and water (H_2O). Line (b) shows step 2, in which methanimine and hydrogen cyanide (HCN) produce an aminoacetonitrile (NH_2CH_2CN). Lines (c), (d), and (e) collectively show step 3, a one-way process called hydrolysis. Line (c) shows the reaction between an aminoacetonitrile and one water molecule, creating NH_2CH_2COHNH. Line (d) shows the effect of a second water molecule, creating $NH_2CH_2COHOHNH_2$. Line (e) shows the last disassembly into the products glycine (NH_2CH_2COOH) and ammonia. The red N indicates the atom originated from the original ammonia molecule in line (a). The blue N indicates the atom originated from the HCN molecule destroyed in line (b).

Step 1, shown on line (a) of Figure 2.1, shows us the first step in the Strecker synthesis of glycine. In this step, formaldehyde (CH_2O) and ammonia (NH_3) react to create methanimine ($NHCH_2$) and a water molecule (H_2O). The nitrogen atom of the ammonia molecule (shown in RED) and one of its hydrogen atoms double bonds to the carbon of the aldehyde molecule. The displaced oxygen atom joins with the two remaining hydrogens from ammonia, creating a water molecule.

Line (b) shows step 2 of this reaction. The methanimine molecule and hydrogen cyanide (HCN) produce an aminoacetonitrile (NH_2CH_2CN). The H atom of the hydrogen cyanide joins the NH at the top of the large methanimine molecule. The remainder of the HCN (the carbon triple bonded to nitrogen) joins the central carbon of methanimine. The two carbons are joined by a single bond. The blue color indicates the nitrogen atom originated from the HCN molecule.

Step 3 is shown in three stages, lines (c), (d), and (e). These three lines collectively show a one-way process called hydrolysis. In line (c), a water molecule breaks down into an OH portion and a single H atom. The OH forms a single bond with the bottom carbon of the aminoacetonitrile, occupying one of the hydrogen bonds previously involved in a triple bond between carbon and nitrogen. The H joins with the N atom, and this bond is now a double rather than a triple, since the extra bond has been given to the OH. The resulting product is now NH_2CH_2COHNH.

In line (d) we see the effects of the addition of a second water molecule to the larger molecule, NH_2CH_2COHNH. Again, the water donates an OH, which becomes single bonded to the lower carbon, and an H, which joins the NH, creating another amine group, which is now also single bonded to the lower carbon. The product is now $NH_2CH_2COHOHNH_2$.

Line (e) show the last stage, in which the previous molecule $NH_2CH_2COHOHNH_2$ disassembles into glycine and an ammonia molecule. The lower amine group (with the blue N) separates, and takes with it an H from one of the OH segments. This produces an ammonia molecule. The remaining hydrogen-less O atom becomes double bonded to the lower carbon. This new molecule is the amino acid glycine (NH_2CH_2COOH) (Schulte & Shock, 1995; Rimola et al., 2010; Hein, 2012, private communication).

It is important to note that even though one ammonia molecule is destroyed initially and one is created at the end, it is chemically inaccurate to depict this reaction as occurring without ammonia altogether. The initial N, contributed by ammonia, remains in the amino acid. It is the N contributed by HCN molecule which later breaks off from the amino acid and produces the new ammonia molecule (Hein, 2012, private communication).

There are additional possible synthesis pathways which we do not consider in this work. Michael addition, for example, may be responsible for the formation of β-amino acids in parent bodies (Ehrenfreund et al., 2001; Martins et al., 2007a; Glavin & Dworkin, 2009). β-amino acids are characterized by the location of their amino groups. In α-amino acids, amino groups attach at the α-carbon location; amino groups of β-amino acids attach at the β-carbon, which is the carbon immediately adjacent to the α-carbon in the carbon chain. For example, the amino group of α-alanine is attached to the α-carbon, as in 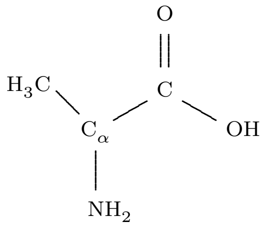. In β-alanine, the amino group is attached to the β-carbon, the second carbon molecule away from the carboxyl group (COOH), as in 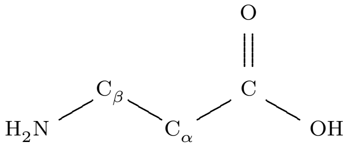

. Clearly, there are not β-versions of each amino acid. Glycine, for example, has no β configuration, as there is only a single carbon atom available for attachments. Since we are currently only considering the formation of α-amino acids via Strecker synthesis, we do no take the Michael addition pathway into account. We also do not consider the alternate Strecker pathway mentioned above, in which the reactants are ketones and the products are hydroxy acids. For example, a Strecker reaction taking place with a simple ketone rather than formaldehyde, and also reacting with no ammonia present, creates glycolic acid rather than glycine (Peltzer et al., 1984; Schulte & Shock, 1995; Ehrenfreund et al., 2001).

It is because we consider Strecker-type synthesis with aldehydes only that we do not consider a few additional amino acids, such as amino-isobutyric acid and isovaline. These two amino acids are non-proteinogenic, yet are both extremely abundant in carbonaceous chondrites. They are synthesized via Strecker-type reactions, yet their precursors are ketones, rather than aldehydes. Our current analysis is somewhat limited in this sense. Future work might adapt this research to include pathways such as Michael addition and the alternate Strecker model. This would allow for the identification of abundance patterns for additional amino acids prevalent in meteorites. For example, in petrographic type 1 chondrites, β- and γ-amino acids (in which the amino group attaches at the third carbon) are more abundant than α-amino acids (Burton et al., 2013).

2.2.3 Strecker Reactions for Proteinogenic Amino Acids

We adapt the Strecker reaction layout following convention. See, for example, Peltzer et al. (1984); Schulte & Shock (1995); Botta et al. (2002); Elsila et al. (2007); Pizzarello & Holmes (2009); Rimola et al. (2010). We write the general form of a Strecker-type reaction as:

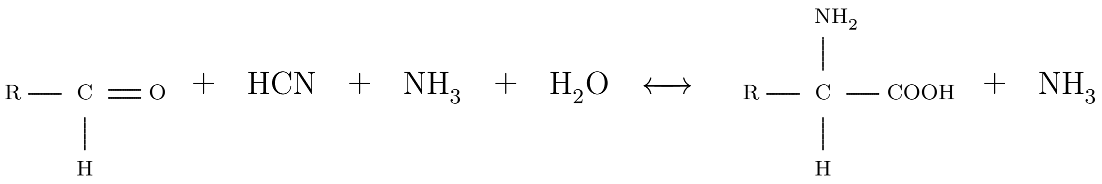

$$\mathrm{R-\underset{\displaystyle H}{\underset{|}{C}}=O} + HCN + NH_3 + H_2O \longleftrightarrow \mathrm{R-\underset{\displaystyle H}{\underset{|}{\overset{\displaystyle NH_2}{\overset{|}{C}}}}-COOH} + NH_3$$

which shows an aldehyde (R-CHO), hydrogen cyanide (HCN), ammonia (NH_3), and water (H_2O) reacting to create an amino acid (NH_2-RCH-COOH) and an ammonia molecule. It is significant to note in this reaction that the R groups of the aldehyde and amino acid are identical. They are not arbitrary indicators showing side chain locations in aldehydes and amino acids; they are structurally identical. For any given Strecker reaction, the side chains of the reactant aldehyde and the product amino acid are the same. We can use this fact to solve for the requisite aldehyde necessary to synthesize each amino acid.

For example, the structure of glycine is

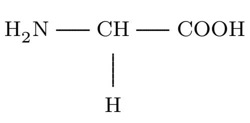

$$\mathrm{H_2N-\underset{\displaystyle H}{\underset{|}{CH}}-COOH}$$

. The

$\mathrm{H_2N - CH - COOH}$ part is common to all amino acids. The central carbon is the α carbon, and it is here the R group attaches. The structure of formaldehyde is

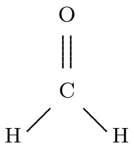

. Again, the $O=C-H$ is common to all aldehydes.

It is the R group which attaches to the center carbon that makes each aldehyde unique. In the case of glycine, the R group is a single H atom, in both the aldehyde and the amino acid.

Using this rigorous definition of Strecker synthesis to identify the requisite aldehydes necessary to create each amino acid allows us to create a list of Strecker reactions. The following series of reactions, shown in Table 2.1, gives the Strecker-type reactions for 17 of the 20 proteinogenic amino acids. The table lists the requisite aldehyde, additional reactants, and the resulting amino acid. In this work we do not consider the amino acids cysteine or methionine, as they are the only 2 proteinogenic amino acids which contain sulfur. Neither do we consider the amino acid proline; this amino acid is the exception to the Strecker pathway. In all other cases, the R group from the aldehyde is identical to the R group of the amino acid; proline may not be formed in this way. Of the 17 amino acids listed below, there are nine which are early-type: glycine, alanine, aspartic acid, glutamic acid, valine, serine, isoleucine, leucine, and threonine. These follow the classification according to Higgs & Pudritz (2009). (Proline would be the tenth and final early-type amino acid, were it included in our simulations.) The remaining amino acids lysine, phenylalanine, arginine, histidine, asparagine, glutamine, tyrosine, and tryptophan are referred to as late-type. Again, this classification follows Higgs & Pudritz (2009), and also includes cysteine and methionine, which are not included in this work. Higgs & Pudritz (2009) suggest the early 10 amino acids as being abundant in the environment on early Earth and hypothesize that this resulted in their appearance and incorporation into the genetic code and early Earth proteins. Their hypothesis is that the late 10 were perhaps more scarce, and were only incorporated into the genetic code when biosynthetic pathways developed which synthesized them.

Table 2.1: Strecker-type reactions for 17 proteinogenic amino acids. In each case, the list includes the requisite aldehyde (additionally labeled with its common name below its molecular formula), a hydrogen cyanide molecule (HCN), an ammonia molecule (NH_3), a water molecule (H_2O), the resulting amino acid (additionally labeled with its common name below its molecular formula), and another ammonia molecule.

$$\underset{\text{formaldehyde}}{CH_2O} + HCN + NH_3 + H_2O \longleftrightarrow \underset{\text{glycine}}{C_2H_5NO_2} + NH_3$$

$$\underset{\text{acetaldehyde}}{C_2H_4O} + HCN + NH_3 + H_2O \longleftrightarrow \underset{\text{alanine}}{C_3H_7NO_2} + NH_3$$

$$\underset{\text{isobutyraldehyde}}{C_4H_8O} + HCN + NH_3 + H_2O \longleftrightarrow \underset{\text{valine}}{C_5H_{11}NO_2} + NH_3$$

$$\underset{\text{3−methylbutanal}}{C_5H_{10}O} + HCN + NH_3 + H_2O \longleftrightarrow \underset{\text{leucine}}{C_6H_{13}NO_2} + NH_3$$

$$\underset{\text{2−methylbutanal}}{C_5H_{10}O} + HCN + NH_3 + H_2O \longleftrightarrow \underset{\text{isoleucine}}{C_6H_{13}NO_2} + NH_3$$

$$\underset{\text{phenylacetaldehyde}}{C_8H_8O} + HCN + NH_3 + H_2O \longleftrightarrow \underset{\text{phenylalanine}}{C_9H_{11}NO_2} + NH_3$$

$$\underset{\text{glycolaldehyde}}{C_2H_4O_2} + HCN + NH_3 + H_2O \longleftrightarrow \underset{\text{serine}}{C_3H_7NO_3} + NH_3$$

$$\underset{\text{2−hydroxypropanal}}{C_3H_6O_2} + HCN + NH_3 + H_2O \longleftrightarrow \underset{\text{threonine}}{C_4H_9NO_3} + NH_3$$

$$\underset{\text{hydroxy−phenylacetaldehyde}}{C_8H_8O_2} + HCN + NH_3 + H_2O \longleftrightarrow \underset{\text{tyrosine}}{C_9H_{11}NO_3} + NH_3$$

$$\underset{\text{3−oxopropanamide}}{C_3H_5NO_2} + HCN + NH_3 + H_2O \longleftrightarrow \underset{\text{asparagine}}{C_4H_8N_2O_3} + NH_3$$

$$\underset{\text{4−oxobutanimide}}{C_4H_7NO_2} + HCN + NH_3 + H_2O \longleftrightarrow \underset{\text{glutamine}}{C_5H_{10}N_2O_3} + NH_3$$

$$\underset{\text{indol-3-ylacetaldehyde}}{C_{10}H_9NO} + HCN + NH_3 + H_2O \longleftrightarrow \underset{\text{tryptophan}}{C_{11}H_{12}N_2O_2} + NH_3$$

$$\underset{\text{3-oxopropanoic-acid}}{C_3H_4O_3} + HCN + NH_3 + H_2O \longleftrightarrow \underset{\text{aspartic-acid}}{C_4H_7NO_4} + NH_3$$

$$\underset{\text{4-oxobutanoic-acid}}{C_4H_6O_3} + HCN + NH_3 + H_2O \longleftrightarrow \underset{\text{glutamic-acid}}{C_5H_9NO_4} + NH_3$$

$$\underset{\text{5-aminopentanal}}{C_5H_{11}NO} + HCN + NH_3 + H_2O \longleftrightarrow \underset{\text{lysine}}{C_6H_{14}N_2O_2} + NH_3$$

$$\underset{\text{N-(4-oxobutyl)guanidine}}{C_5H_{11}N_3O} + HCN + NH_3 + H_2O \longleftrightarrow \underset{\text{arginine}}{C_6H_{14}N_4O_2} + NH_3$$

$$\underset{\text{imidazole-4-acetaldehyde}}{C_5H_6N_2O} + HCN + NH_3 + H_2O \longleftrightarrow \underset{\text{histidine}}{C_6H_9N_3O_2} + NH_3$$

2.2.4 Initial Concentrations of Organics

Table 2.2 lists concentrations of organics found in comets. These values give us a set of initial reactant concentrations to use when modeling amino acid synthesis. The molecules for which we have concentration data include ammonia, hydrogen cyanide, hydrogen sulfide, formaldehyde, acetaldehyde, and glycolaldehyde, all normalized to percent water. Note that in our current model, we have excluded the amino acids cysteine and methionine. These two amino acids each contain a sulfur atom, which originates from a hydrogen sulfide molecule (H_2S). We include H_2S in Table 2.2 as a reference point for when our model is adapted to include sulfur. Cometary data are taken from Bockelee-Morvan et al. (2000), Ehrenfreund & Charnley (2000), Bockelee-Morvan et al. (2004), Crovisier et al. (2004), and Mumma & Charnley (2011).

Cometary data were gathered primarily via spectroscopic surveys, both in radio and infrared. Some data come directly from in situ measurements taken during flyby missions. Radio surveys have detected molecular lines for the following species involved in Strecker synthesis: formaldehyde, acetaldehyde, glycolaldehyde, hydrogen cyanide, and ammonia (Crovisier et al., 2004; Mumma & Charnley, 2011). Infrared analyses have detected molecular lines of water, formaldehyde, hydrogen cyanide, and ammonia (Mumma & Charnley, 2011).

There are a few other aldehydes in our model (butyraldehyde, propionaldehyde, pentanaldehyde) for which we have no cometary data available. In these cases, we estimate initial concentrations for use in our model. In some cases, the aldehydes have been identified and quantified in meteorites, rather than comets, and we extrapolate from there. These values are listed below, in Table 2.3. See Jungclaus et al. (1976), Pizzarello & Holmes (2009), and Monroe & Pizzarello (2011) for meteoritic concentrations.

Table 2.2: Concentrations of organic molecules from cometary data, detection either via spectroscopic surveys or in situ measurements taken during flyby. For specific notes on detection methods, see in-table references. Values are normalized to percent water.

Species	Formula	Hale-Bopp	Halley	Hyakutake	Lee
Water	H_2O	100	100	100	100
Ammonia	NH_3	0.7[1], 0.7-1.8[3], 0.7[4,5]	0.1-2[3], 1.5[4,5]	0.5[3], 0.5[4,5]	
Hyd.Cyanide	HCN	0.25[1], 0.25[3], 0.25[4,5]	0.1[3], 0.1[4,5]	0.1[3], 0.1-0.2[4,5]	0.1-0.3[4]
Hyd.Sulfide	H_2S	1.5[1], 1.5[3], 1.5[4]	0.04[3], 0.4[4]	0.8[3], 0.8[4]	< 0.9[4]
Formaldehyde	HCHO	0.066/1.1[1], 1[3], 1.1[4,5]	0-5[3], 4[4,5]	0.2-1[3], 1[4,5]	1.3[4]
Acetaldehyde	CH_3CHO	0.025[2], 0.25[1], 0.02[4,5]			
Glycolaldehyde	CH_2OHCHO	< 0.4[2]			

Species	Formula	LINEAR	Ikeya-Zhang	73P/SW3
Water	H_2O	100	100	100
Ammonia	NH_3		< 0.2[4]	< 0.3[5]
Hyd.Cyanide	HCN	0.1[4], 0.1-0.6[5]	0.1-0.2[4]	0.25[5]
Hyd.Sulfide	H_2S	0.3[4], 1.15[5]	0.8[4]	0.25[5]
Formaldehyde	HCHO	0.6[4], 0.24[5]	0.4[4]	0.14[5]
Acetaldehyde	CH_3CHO			
Glycolaldehyde	CH_2OHCHO			

[1] Bockelee-Morvan et al. (2000)
[2] Crovisier et al. (2004)
[3] Ehrenfreund & Charnley (2000)
[4] Bockelee-Morvan et al. (2004)
[5] Mumma & Charnley (2011)

Table 2.3: Concentrations of organic molecules from meteoritic data. Values were originally reported in either nanomoles/gram or micrograms/gram, and have been converted to nanomoles/mole using the molecular weights of each species. Values below are all listed in ppb.

Species	Formula	GRA95229	LAP02342	Murchison	Bells	Ivuna
Formaldehyde	HCHO	3273[1]	153[1]	300[1]	961[2]	9102[2]
Acetaldehyde	CH_3CHO	16827[1]	3291[1]	1057[1]; 7000[3]	3114[2]	1832[2]
Butyraldehyde	$CH_3(CH_2)_2CHO$	19917[1]	1478[1]	2322[1]; 1000[3]	3404[2]	1601[2]
Propionaldehyde	CH_3CH_2CHO	19707[1]	5564[1]	1365[1]; 3000[3]	1789[2]	1777[2]
Pentanaldehyde	$CH_3(CH_2)_3CHO$	827[1]	491[1]	112[1]	456[2]	1835[2]

[1] Pizzarello & Holmes (2009)

[2] Monroe & Pizzarello (2011)

[3] Jungclaus et al. (1976)

2.3 Computations

2.3.1 Gibbs Energy

Gibbs energy measures the thermodynamic potential of a thermodynamic system in question; in this case, the thermochemical network of initial reactants present in a meteoritic parent body which are not yet in chemical equilibrium. Gibbs energy (ΔG) is the chemical potential available in a system, and we minimize it when we allow a series of chemical reactions to reach equilibrium. (As Gibbs measures change in potential, it is written with a Δ.)

Each of the Strecker-type reactions listed in Table 2.1 above has some Gibbs free energy of reaction (ΔG_r) associated with it. In this research we assume chemical equilibrium is reached, which allows us to model the series of internal chemical reactions as occurring with a resulting minimum in thermodynamic Gibbs free energies. ΔG_r is calculated via the following equation:

$$\Delta G_r = \Sigma G_f^{products} - \Sigma G_f^{reactants} \tag{2.1}$$

In any system, the Gibbs reaction energy may be calculated as a sum of the Gibbs formation energies of the products minus the sum of the Gibbs formation energies of the reactants, as shown in Eq. 2.1.

In addition to each reaction being associated with a Gibbs reaction energy, each species in our model has some associated Gibbs energy of formation (ΔG_f), as seen above. ΔG_f is a thermochemical property of the species in question, and there are tables of data (see next section) devoted to laboratory and theoretical calculations determining these values.

2.3.2 CHNOSZ and Gibbs Energy Coefficients

Our approach is based on the minimization of Gibbs free energy of the system in question. To obtain a working software program which can compute such a Gibbs minimization, we must first have some information about the Gibbs formation energy of each species. We use a thermochemical database called CHNOSZ as our primary reference (version 0.9-9, 2013-01-01, authored by Jeffrey M. Dick, http://www.chnosz.net/). This database contains the Gibbs energies of formation for an extensive variety of amino acids, aldehydes, and other organics, including ammonia and HCN.

For each of the organic species involved in Strecker-type synthesis, both reactants and products, CHNOSZ contains a set of Gibbs energies of formation. ΔG_f changes with respect to both temperature and pressure, the ranges for which span 0°C to 350°C and 1 to 165 bar, respectively. We plot these formation energies and perform a least squares regression for each species, resulting in a line of best fit. We model each curve as

$$G_f(T,P) = a + bT + cTln(T) + dT^2 + eT^3 + f/T + gP. \tag{2.2}$$

This provides us with a set of Gibbs energy coefficients a through f for each species. Our modeling software, ChemApp, uses Eq. (2.2) as the energy function when it minimizes Gibbs energies. It requires the Gibbs coefficients for each species to perform the global Gibbs energy treatment. Coefficients a through f are input into ChemApp via a data file (see below).

Note the linear dependence of Gibbs energy on pressure. The pressure term in Eq. (2.2), gP, is negligible compared to the temperature dependence, which has both a

T^3 and T^2 dependence, among other terms. As an example, we consider the amino acid alanine. The Gibbs formation energy of alanine decreases characteristically with an increase in temperature, spanning a range of over $100,000$ Joules with a change in temperature of 300°C. Pressure, on the other hand, has minimal effect. A change in pressure by as much as 100 bar changes the Gibbs energy by approximately a single kilojoule. For an illustrative plot, refer to Chapter 4 (Fig. 4.1). Due to the independence of Gibbs energies on pressure, we include neither the coefficient g nor pressure in our current treatment with ChemApp.

2.3.3 CHNOSZ Ancestor

Previously, an undergraduate summer research student, Jeff Emberson, used a database called Thermochemdata, rather than CHNOSZ, as the source for the Gibbs coefficients of each species (see Jeff's undergraduate thesis with Dr. Ralph Pudritz, Emberson (2010)). A difficulty arose shortly after my research here commenced; Jeff's work was limited to a highly selective group of amino acids, the data for which were all contained within Thermochemdata. However, part of my project has been to expand our amino acid landscape, to include a wider variety of amino acids and aldehydes. Many of the new species we consider do not exist in Thermochemdata, and that database is limited to the species already contained within it. The database was constructed using a software program called OrganoBIoGeoTherm (OBIGT), which is now both outdated and inaccessible to us.

OBIGT's progeny software is our new program, CHNOSZ. CHNOSZ functions in effectively the same manner, with an up-to-date and reliable database of thermochemical information for an extensive collection of chemical species, including the majority of species we consider in our treatment.

Darren Fernandes, another undergraduate summer research student who worked on this project, was the first to attempt to perform a linear regression on the Gibbs data for each species, plot the line of best fit as in Eq. (2.2) and receive the Gibbs coefficients as output (see Darren's undergraduate thesis with Dr. Ralph Pudritz, Fernandes (2013)).

When I arrived, in addition to expanding the amino acid landscape, I implemented a coding sequence which would computationally determine the Gibbs coefficients based on data directly from CHNOSZ. This is different from the previous method, which was fit by hand. Our new code receives as input the plot of Gibbs formation energies for a species, performs the least squares fit to the linear regression, and calculates the Gibbs coefficients a-f. These coefficients are listed in Table 2.4.

To validate these coefficients, for each species we calculated G using Eq. (2.2) and the coefficients below at two different temperatures (100°C and 200°C). The calculated Gibbs values were compared to the Gibbs energies contained in CHNOSZ. In all cases, the Gibbs values matched to within 0.1%.

Table 2.4: Gibbs energy coefficients a through f for all species required by our ChemApp model.

Species	**a**	**b**	**c**	**d**	**e**	**f**
Acetaldehyde	-3381515.25	75302.23126	-12613.89718	21.0499590	-0.006597879616	155464435.26
Butyraldehyde	-2431234.39	54624.24219	-9152.808212	15.01928405	-0.004708991756	108144818.5
Formaldehyde	-3680722.855	82603.67332	-13837.02113	23.19983528	-0.007271672388	172609450.6
Propionaldehyde	-2913316.03	64963.15053	-10883.26982	18.03449653	-0.00565340096	131803280.9
Pentanaldehyde	-1959382.621	44288.24780	-7422.546162	12.0043361	-0.003764648820	84490311.9
Glycolaldehyde[2]	-343813.24	3648.2983	-631.89742	0.98099568	-0.00039704802	4254143.8
Ammonia	-897666.9137	19778.34032	-3291.263091	5.149692355	-0.001557004594	44283260.50
HCN	-624042.7135	18477.41857	-3116.925949	5.182277422	-0.001645254927	33517298.56
Water	-233169.6934	304.5868851	-53.49736688	-0.03796895476	1.269310222e-05	-270548.4436
Alanine	1031451.202	-32579.64120	5490.578936	-9.971079920	0.003239965646	-64382528.43
Arginine	1397055.971	-37910.42980	6405.693272	-12.10512083	0.003998128505	-73196899.70
Asparagine	1018313.535	-36048.11595	6081.886186	-11.19959102	0.00367804712	-68281682.34
Aspartic Acid	454306.7993	-27657.83123	4679.05524	-8.833705136	0.002931948072	-50926332.94
Cysteine	864408.5331	-27570.58300	4647.417361	-8.58803092	0.002801313052	-55420343.68
Glutamic Acid	359044.5675	-25145.80366	4251.98428	-8.119593554	0.002700959759	-47300343.8

Glutamine	772741.8061	-30347.31799	5130.007313	-9.680589819	0.003206006409	-57237275.41
Glycine	1420243.66	-41888.92300	7043.162963	-12.47986937	0.004032514295	-81555751.30
Histidine	1886400.326	-48462.26250	8170.165424	-14.93754185	0.004867372862	-95419236.33
Isoleucine	389132.5053	-16510.3132	2807.876121	-5.729344137	0.001903770487	-35960378.63
Leucine	389355.4110	-16678.23472	2836.163561	-5.792171398	0.001922583815	-36667167.66
Lysine	-806.2054093	-8170.705686	1425.514030	-3.523383275	0.001268110311	-12707580.74
Methionine	694950.9569	-23177.03032	3920.319836	-7.612075124	0.002522929468	-46657993.75
Phenylalanine	708981.8676	-21026.38580	3576.953855	-7.209602440	0.002405378819	-43508064.544
Proline	680240.6733	-23134.38205	3919.034936	-7.513161299	0.00249902962	-43603176.38
Serine	815522.7699	-31112.55435	5247.552395	-9.629707841	0.003152626869	-59497795.44
Threonine	291986.4617	-18438.96902	3127.520001	-6.101115881	0.002031217015	-35800477.86
Tryptophan	1043745.253	-26728.32712	4541.88846	-8.980321569	0.00298875490	-54644159.63
Tyrosine	80108.85978	-11350.73517	1975.394250	-4.672322399	0.001656252951	-19137857.82
Valine	611706.5594	-22115.43587	3742.815965	-7.204053426	0.00236461931	-46311060.23
Aminobutyric Acid	-3529209.098	73937.84285	-12387.89701	20.55110260	-0.006432368169	151307640.48

---

[2] Indicates species is not included in CHNOSZ database. Instead we are using Jeff's glycolaldehyde coefficients, based on mixture of acetaldehyde and acetic acid, as in Espinosa-García & Dóbé (2005).

Chapter 3

Nature's Starships I: Abundance and Relative Frequency of Amino Acids in Meteorites

This chapter will be submitted to the journal of Astrobiology as part I of a two-paper set. Authors are Cobb, A. K. and Pudritz, R. E.

Abstract

The class of meteorites called carbonaceous chondrites are examples of material from the solar system which have been relatively unchanged from the time of their initial formation. These meteorites have been classified according to the temperatures and physical conditions of their parent bodies. We collate available data on amino acid abundance in these meteorites and plot the concentrations of different amino acids for each meteorite within various meteorite classes. We focus on meteorites for which a complete set of data for six amino acids (glycine, alanine, serine, aspartic acid, glutamic acid, and valine) is available, and calculate the total amino acid abundance for each meteorite. We also calculate and plot the average concentrations for various amino acids across meteorites separated by subclass and petrologic type, revealing both total and average abundance patterns. We see a predominance in abundance and variety of amino acids in the subclass of carbonaceous chondrites called CM2 and CR2. These meteorites contain concentrations of amino acids greater by several orders of magnitude than other carbonaceous subclasses. A central result of our analysis is that there is an increased abundance in organic material in these classes which corresponds to an optimal temperature range from 200°C to 400°C for amino acid synthesis in parent bodies. This range in temperature also corresponds to a high degree of aqueous alteration, indicating that aqueous synthesis of amino acids took place. Within the CM2 and CR2 meteorites, we additionally identify trends in the relative frequencies of amino acids in preparation for computational modeling. **Key Words:** Amino acid synthesis–Meteorites–Carbonaceous chondrites–Abundance patterns–Petrologic classification–Astrochemistry

3.1 Introduction

Meteorites provide a geological and chemical record of the formation of organic molecules in the early solar system. Amino acids which formed in meteoritic parent bodies are an important source of organic material that was delivered to young planets via meteoritic impacts. Amino acids are the basic building block in proteins used by life on Earth. This extraterrestrial origin of biomolecules suggests one possible way that the prebiotic conditions for life in the universe could have been established, both on our own early Earth and perhaps on other planets (Chyba & Sagan, 1992; Botta & Bada, 2002; Sephton, 2002; Glavin et al., 2011).

The class of meteorites called carbonaceous chondrites is of particular interest with regard to the origin of organic material. Representing approximately 4% of meteorite falls (Glavin et al., 2011), these meteorites are relatively undifferentiated from the original material with which they were created and have an unusually high percentage of both water and amino acids. The carbonaceous chondrites are divided into subclasses and petrologic types based on their composition, mineralogy, and degrees of internal alteration. There are two types of alteration processes, aqueous and thermal. Carbonaceous chondrites which have undergone aqueous alteration show increased levels of organic material, including amino acids (Sephton, 2002; Weisberg et al., 2006; Glavin et al., 2011).

Meteorite classification is based on two characteristics in particular: primarily, their chemical composition, and secondarily, the amounts of aqueous and thermal processing. Aqueous alteration is a general term for the transformation of molecules to organic material in a hydrated environment - exactly what is occurring in the interior of meteoritic parent bodies resulting in the formation of amino acids. Thermal metamorphism, on the other hand, involves processing temperatures too hot to retain a hydrated environment. See Weisberg et al. (2006) and Weiss & Elkins-Tanton (2013) for a review.

The range of temperatures that allows for significant amounts of this aqueous alteration is roughly 150°C - 400°C. At relatively high temperatures, > 600°C, the parent bodies undergo thermal metamorphism instead; no aqueous alteration occurs, and we see little to no synthesis of organics. Petrologically speaking, aqueously altered meteorites are given a classification value of type 1-type 3, and thermally altered meteorites are listed as type 4-type 6 (Sephton, 2002; Weisberg et al., 2006).

There is great diversity amongst carbonaceous chondrite literature regarding petrographic types and their corresponding alteration temperatures. These are well summarized in Grimm & McSween Jr. (1989) and Weiss & Elkins-Tanton (2013, and references therein). Broadly, the different petrographic types are classified based on compositional differences of meteorite samples. In each type, minerals have undergone different levels of melting or other alteration, and each mineral has a unique melting point. Based on which minerals have been differentiated, a meteorite may be classified as having undergone alteration temperatures which reach the melting point of those specific minerals.

The amino acid content of carbonaceous chondrites has become the focus of a variety of studies due to their high organic content. A subclass of carbonaceous chondrite called CM meteorites is of particular interest, as they contain the greatest quantities of amino acids. Murchison meteorite alone contains over 70 different amino acids, many of which are extraterrestrial in origin (Cronin & Pizzarello, 1983; Sephton, 2002; Botta, 2005). There are 20 proteinogenic amino acids which are encoded for directly by the genetic code, and many of these are found in meteorites.

In this work, we investigate the abundance patterns of proteinogenic amino acids found in carbonaceous chondrites. We collate available data on amino acid concentration in a variety of carbonaceous chondrites. The data are shown graphically to more easily distinguish patterns in amino acid abundance across meteorite subclasses. We show figures of amino acid concentration per meteorite class and per amino acid, as well as a total amino acid concentration per meteorite. We average total amino acid concentrations per meteorite class to observe overall abundance trends across the carbonaceous chondrites.

In addition to identifying abundance patterns, we also investigate the relative frequencies of amino acids within two subclasses of carbonaceous chondrites. Higgs & Pudritz (2009) examined a limited set of carbonaceous chondrite data. They found an empirical relation between relative frequency of some amino acids and their Gibbs free energy of reaction. The order they found related to the amino acids they called 'early type', referring to the set of amino acids likely present on early Earth. These amino acids are glycine, alanine, aspartic acid, glutamic acid, valine, serine, isoleucine, leucine, proline, and threonine.

This examination extrapolates patterns of amino acid synthesis across a range of temperatures which define individual meteorite subclasses. We also show the relative abundance patterns of amino acids in various meteorites based on environmental factors and internal chemistry during organics formation. Our analysis of these data shows that there exists a 'sweet spot' in temperature range, which corresponds to specific meteorite classifications. The patterns which emerge from the cumulative data plots reveal an optimal temperature range of 200°C - 400°C during alteration which corresponds to increased levels of aqueous alteration and the synthesis of amino acids. This pattern leads to conclusions that have several significant implications for theories of amino acid synthesis in meteoritic parent bodies.

3.2 Background

3.2.1 Amino Acids

The goal of this paper is to report the results of our investigation into trends in abundance and relative frequencies of amino acids. We use this information to constrain models of amino acid origin in meteoritic parent bodies. We perform a literature search with the intent of identifying overall patterns in i) amino acid abundances, and ii) relative amino acid frequencies in meteorites. From these, we can infer information about alteration processes in meteoritic parent bodies. The data collated here help provide significant insights into the chemistry behind the formation of these acids.

From the Murchison meteorite alone, we have evidence of over 70 different species of amino acids, the majority of which are extraterrestrial in origin (Cronin & Pizzarello, 1983; Sephton, 2002; Botta, 2005). On Earth, there are 20 proteinogenic amino acids encoded for directly by the genetic code. These 20 are alanine, arginine, asparagine, aspartic acid, cysteine, glutamic acid, glutamine, glycine, histidine, isoleucine, leucine, lysine, methionine, phenylalanine, proline, serine, threonine, tryptophan, tyrosine, and valine.

In the case of amino acids in meteorites, we gather data for only a particular set of amino acids. We consider 13 amino acids created via a set of chemical pathways called Strecker reactions. The 13 acids we consider in this work are alanine, aspartic acid, glutamic acid, glycine, isoleucine, leucine, lysine, phenylalanine, proline, serine, threonine, tyrosine, and valine. Our analysis is limited by the available data; these 13 amino acids are the only acids for which we have a relatively complete set of data across the carbonaceous chondrite subclasses.

Strecker-type synthesis produces amino acids through chemical reactions between aldehyde (R-CHO) molecules, hydrogen cyanide (HCN), and ammonia (NH_3) in aqueous solution. For the purposes of this paper, we consider only the α-amino acid species produced via Strecker-type synthesis. The side chain of an α-amino acid is attached to the α carbon, the first carbon adjacent to the carboxylic group. The initial reactants in Strecker processes combine to create aminonitriles as intermediaries, which themselves undergo a one-way process called hydrolysis, resulting in the formation of α-amino acids.

$$\underset{\text{methanal}}{CH_2O} + \underset{\text{cyanide}}{\overset{\text{hydrogen}}{HCN}} + \underset{\text{water}}{H_2O} + \underset{\text{ammonia}}{NH_3} \longleftrightarrow \underset{\text{glycine}}{C_2H_5NO_2} + \underset{\text{ammonia}}{NH_3}$$

In the above example of a Strecker pathway, we see a mass balance reaction for formaldehyde (also known as methanal) reacting with hydrogen cyanide, water, and ammonia. The products of this reaction are the amino acid glycine and another ammonia molecule. Note that Strecker-like pathways may also occur utilizing ketones rather than aldehydes. In this case, ketones, HCN, NH_3, and water react to form cyanonitriles and eventually α-hydroxy acids.

The α-, β-, and γ- nomenclature for amino acids is designed to indicate the placement of the side chain of an amino acid. Side chains, also called R groups, connecting to the amino acid via the alpha carbon are referred to as α-amino acids. It is possible to produce β-amino acids, e.g. through the Michael addition pathways, or γ-amino acids. Glavin et al. (2006), Glavin et al. (2011) and Martins et al. (2007a), for example, detected β-alanine and γ-amino-isobutyric acid during analyses of carbonaceous chondrites. Murchison meteorite and its impressive array of amino acids also includes β-amino acids, γ-amino acids, and non-proteinogenic α-amino acids (meaning they are not used as subunits in the building of proteins), e.g. β-alanine, γ-amino-n-butyric acid, amino-isobutyric acid, norvaline, and isovaline (Sephton, 2002). Laboratory analyses of retrieved falls has revealed the presence of a significant number of amino acids and other organic material, such as aldehydes and carboxylic acids, within meteorites. Having outlined the amino acid content of meteorites, the most immediate question to ask is how they got there.

3.2.2 Meteoritic Classification

Meteorites are broadly split into one of three categories based on a coarse initial description: iron, stone, and stony-iron. Stony meteorites are further divided into one of two categories: chondrites and achondrites. The chondrites are the most primitive examples of meteorites. They are relatively undifferentiated from the makeup of their parent body material and their chemical composition is of near-solar abundance. These meteorites reflect processes occurring during and following the formation of the solar system. Chondrites contain small spherical inclusions of undifferentiated material, called chondrules. Historically, within the chondrite division are three classes: carbonaceous, ordinary, and enstatite. These terms, while slightly misleading (e.g. 'ordinary' stemming from the fact that these are the most common type), are still used to describe similarities amongst meteorite groups. The carbonaceous chondrites are so named for their $> 5\%$ by weight composition of organic carbon, which results in a predominantly dark appearance (Botta & Bada, 2002; Botta, 2005; Glavin et al., 2011). These meteorites collectively represent some of the most primitive samples of meteorite available. Carbonaceous chondrites may be further divided into subcategories, including CI, CM, CR, CH, CO, CV, CK, and CB, based on their bulk mineralogical composition. Subclass titles are designated based on the name of a representative fall within each group: CI (Ivuna-like), CM (Mighei-like), CR (Renazzo-like), CH (Allan Hills-like), CO (Ornans-like), CV (Vigarano-like), CK (Karoonda-like), and CB (Bencubbin-like). These meteorite classes are additionally categorized into a petrologic type between 1 and 6.

Carbonaceous chondrites are assigned a subclass and a number, based on their bulk chemical makeup and petrologic type.

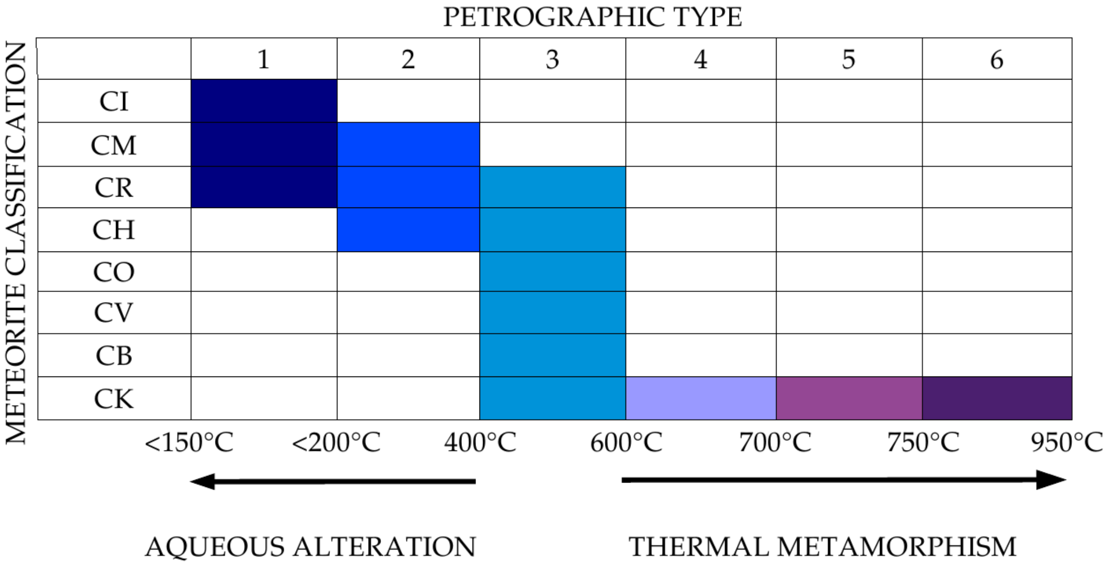

Figure 3.1: Classification of carbonaceous chondrites. Classified according primarily to chemical composition and secondarily to degrees of thermal and aqueous processing. Adapted from Sephton (2002); Taylor (2011).

Figure 3.1 shows the petrologic types associated with each subclass of carbonaceous chondrite. Type 1 meteorites show the highest degree of aqueous alteration amongst chondrites. They formed in the temperature range of 150°C to 200°C. These meteorites have a high water content and significant organic abundance, including amino acids. They are 3-5% carbon by weight and 18% water by weight. Type 2 meteorites are slightly less aqueously altered, associated with a temperature between 200°C to 400°C. These meteorites contain between 0.8-2.5% of carbon by weight, and between 2-16% water. Type 3 contains the most pristine meteorite samples. They are in the middle ground; mid-temperature range, 400°C to 600°C, showing no to relatively insignificant degrees of either aqueous alteration or thermal metamorphism. By weight, they contain 0.2-1% carbon and 0.3-3% water. Type 2 meteorites show an insignificant amino acid abundance corresponding to the limited levels of aqueous processing. Moving from type 3 through type 6, increasing in alteration temperature, shows an increase in the amount of thermal metamorphism and no aqueous alteration (Sephton, 2002; Weisberg et al., 2006). We adapt the alteration temperatures as in Fig. 3.1 as a starting place for petrographic type classifications. There is great disparity among accepted alteration temperatures in chondrites. The temperature boundaries listed here are in agreement with Grimm & McSween Jr. (1989), Sephton (2002), Taylor (2011), and Weiss & Elkins-Tanton (2013, and references therein), and are based on relative temperatures of alteration for the different minerals seen in various chondrite subclasses.

CI, CM, and CR-type meteorites, mostly types 1 and 2, generally contain greater quantities of amino acids and underwent greater degrees of aqueous alteration processing at lower temperatures. CV, CO, CB, and CK-type meteorites are limited to petrologic type 3. These chondrites likely underwent minimal degrees of aqueous alteration at higher temperatures than types 1 and 2. The CK-types, a relatively new subclass, cover a broad range in petrologic types, crossing boundaries between types

3 through 6, moving with increasing alteration temperature and levels of thermal processing, up to 950°C.

The more hydrated environments of the CI/CM/CR meteorites correspond to greater levels of aqueous alteration. Following this classification scheme, we expect to see greater quantities of organic material and amino acids among the aqueously altered meteorites (CI/CM/CR range). However, the most aqueously altered specimens of petrographic type 1 (the CI-types) express lower levels of organics than petrographic type 2 (the CM- and CR-types). Young et al. (1999) and Weiss & Elkins-Tanton (2013, and references therein) suggest possible reasons for this, which include an onion-shell model for meteorite origination and different models of fluid flow within chondrite subclasses. Nevertheless, the presence of organic material in carbonaceous chondrites which predates life on Earth suggests an origin from abiotic chemical evolution.

3.3 Materials and Methods

3.3.1 Meteoritic Amino Acid Data

The presence of organic constituents in meteoritic parent bodies is now widely accepted, and technological advancements allow for more precise and accurate measurements of amino acid concentrations. We are interested in a specific assortment of amino acids. Necessary characteristics include the amino acids being proteinogenic and being α-amino acids. We collated the data from the following sources into a single large table. Figures 3.2 through 3.6 show concentrations of amino acids per meteorite, within each meteorite class. Concentrations are reported in parts-per-billion (ppb); for example, nanograms of amino acid per gram of meteorite. Where applicable, amino acid concentrations initially reported in left and right handed configuration abundances have been combined.

Kaplan et al. (1963) was one of the first research groups to investigate the organic constituent present in stony meteorites. They analyzed the carbonaceous chondrite meteorites Orgueil, Cold Bokkeveld, Mighei, Murray, Felix, Lance, and Warrenton for the following proteinogenic amino acids: arginine, lysine, histidine, aspartic acid, glutamic acid, glycine, alanine, serine, proline, valine, threonine, leucine, tyrosine, phenylalanine, cysteine, and methionine.

The CM-type meteorite Murchison is one of the best studied meteorites of the carbonaceous chondrites. Cronin & Pizzarello (1983) quantified the abundances of the following amino acids: glycine, alanine, valine, proline, leucine, isoleucine, aspartic acid, and glutamic acid. In addition, they presented an amino acid abundance comparison of three different Murchison samples taken from the Field Museum of Natural History in Chicago, Illinois, Collections of Arizona State University, and the Smithsonian Institution National Museum in Washington D.C.

Peltzer et al. (1984) studied amino acids found in Murchison, exclusively those created via Strecker-type pathways. They discovered appreciable quantities of both glycine and alanine.

Around the same time, Shimoyama et al. (1985) investigated organics in Antarctic meteorites, looking specifically into amino acid concentrations on the Yamato meteorite. They found measurable quantities of aspartic acid, threonine, serine, glutamic acid, proline, glycine, alanine, valine, isoleucine, and leucine.

Botta et al. (2002) present amino acid abundance data for a wide variety of CM, CI, CR, CV, and one ungrouped meteorite. Meteorites include CM-types Murchison, Murray, Nogoya, Mighei, and Essebi, CI-types Orgueil and Ivuna, CR-type Renazzo, CV-type Allende, and the ungrouped Tagish Lake meteorite. Proteinogenic amino acids detected were aspartic acid, serine, glutamic acid, glycine, and alanine.

Glavin et al. (2006) present total amino acid abundances in CM meteorites Murchison (to be identified as Murchison USNM 6650 in Glavin et al. (2011)), Lewis Cliffs (LEW) 90500, and Allan Hills (ALH) 83100. Amino acids reported include aspartic acid, glutamic acid, serine, glycine, alanine, and valine. Glavin et al. (2011) present an extensive account of total amino acid abundances in a variety of CI, CM, and CR class meteorites. Of the proteinogenic amino acids, the data include abundances for aspartic acid, glutamic acid, serine, glycine, alanine, and valine. Samples of CI meteorite Orgueil, CM meteorites Meteorite Hills (MET) 01070, Scott Glacier (SCO) 06043, Murchison USNM 5453, and Lonewolf Nunataks (LON) 94102, and CR meteorites Grosvenor Mountains (GRO) 95577, Elephant Moraine (EET) 92042, and Queen Alexandra Range (QUE) 99177 were all analyzed and reported in Glavin et al. (2011). Also included in the Glavin et al. (2011) paper are the data for CM meteorites Murchison USNM 6650 and LEW 90500, though these samples were analyzed in Glavin et al. (2006).

Martins et al. (2007b) perform chemical analyses of the organic content in the carbonaceous chondrite CR-type Shişr 033. They discovered aspartic acid, glutamic acid, serine, glycine, valine, and leucine. Martins et al. (2007a) published another paper in the same year. They investigated the organic content of three Antarctic CR meteorites: EET 92042, Graves Nunataks (GRA) 95229, and GRO 95577, and confirmed and quantified the presence of proteinogenic amino acids aspartic acid, glutamic acid, serine, glycine, alanine, and valine.

Pizzarello & Holmes (2009) analyzed two CR meteorites, LaPaz Icefield (LAP) 02342 and GRA 95229. They reported abundance data for glycine, alanine, valine, isoleucine, leucine, aspartic acid, glutamic acid, serine, threonine, proline, phenylalanine, and tyrosine.

Monroe & Pizzarello (2011) analyzed the CM-type Bells meteorite and found aspartic acid, serine, glutamic acid, glycine, alanine, valine, leucine, and isoleucine.

Burton et al. (2012) reported amino acid abundances for a wide variety of CV meteorites. Analyzed meteorites include CV3 types Allan Hills (ALH) 84028, Elephant Moraine (EET) 96026, LaPaz Icefield (LAP) 02206, Graves Nunataks (GRA) 06101, Larkman Nunataks (LAR) 06317, and Allende, and CO3 types Allan Hills (ALH) A77307, Miller Cliffs (MIL) 05013, and Dominion Range (DOM) 08006. They report abundance data for the following proteinogenic amino acids: aspartic acid, glutamic acid, serine, glycine, alanine, and valine.

Most recently, Chan et al. (2012) investigated the amino acid content of two CO meteorites, Colony and Ornans. They quantified the presence of proteinogenic amino acids alanine, valine, glycine, leucine, aspartic acid, and glutamic acid.

The reported amino acid abundances cited above, and used for our plots below, were obtained by original researchers via a combination of two widely practiced methods of amino acid extraction. These are high-performance liquid chromatography (HPLC) and a combination gas chromatography/mass spectroscopy (GC/MS). Briefly, HPLC measures retention time during elution of meteorite samples which have been hot water and HCl hydrolyzed. GC/MS is used to identify different substances in a sample based on a mass-to-charge ratio and different elution times. For a more in-depth comparison of the methods of amino acid detection and quantification in meteorites, as well as a discussion of their limitations, see Botta & Bada (2002), Glavin et al. (2006), and Martins et al. (2007a).

Using amino acid abundance data from the above sources, we created a series of figures showing amino acid abundances across a range of meteorites and meteorite classes. To visualize more easily the patterns in amino acid spread, the following figures show amino acid abundances on log scales, separated by meteorite class.

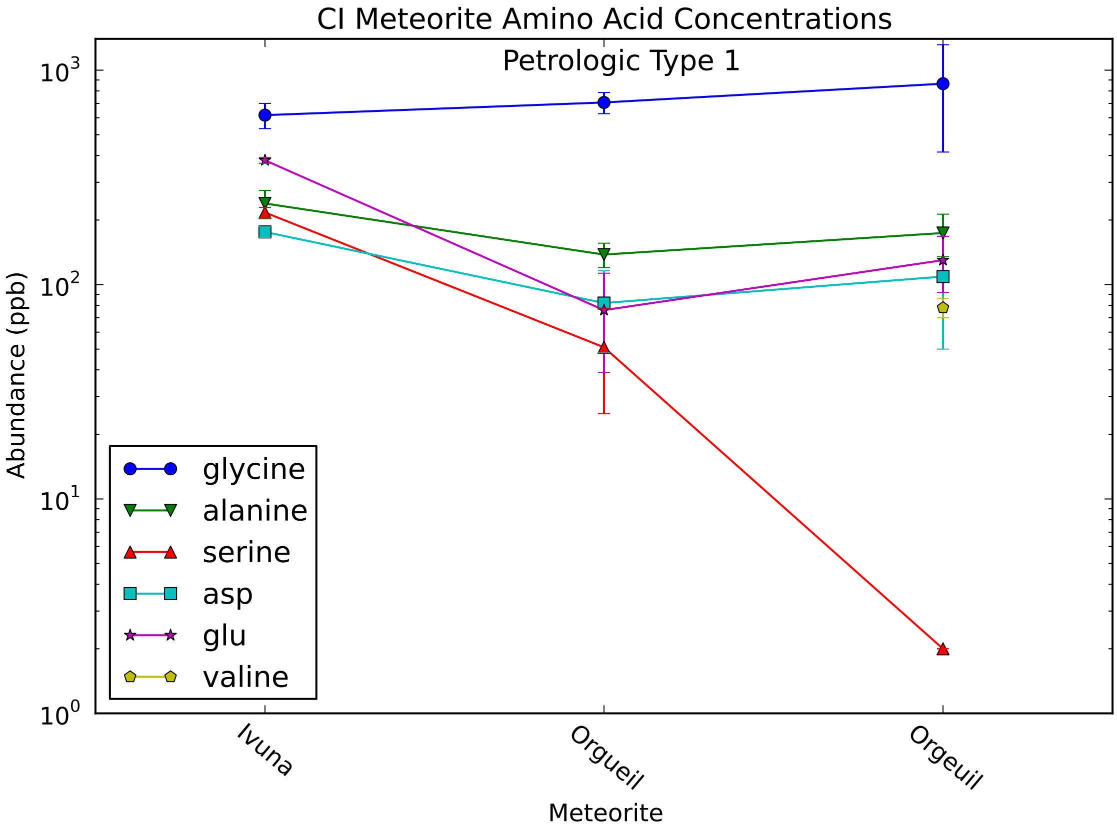

Figure 3.2: Amino acid abundances for three samples of CI meteorite. Concentrations are shown in ppb. See Table

Figure 3.2 shows amino acid concentrations for the CI-type meteorites. There are three CI meteorites shown here, Ivuna and two samples of Orgueil (from separate analyses). All three are petrologic type 1. Glycine is the most abundant amino acid in each meteorite. Alanine, glutamic acid, aspartic acid, and valine remain relatively constant at a mid-level abundance. Serine remains near the bottom in all samples, as well, a pattern that seems to be consistent throughout the meteorite classes. There are no significant fluctuations in concentration for any amino acid.

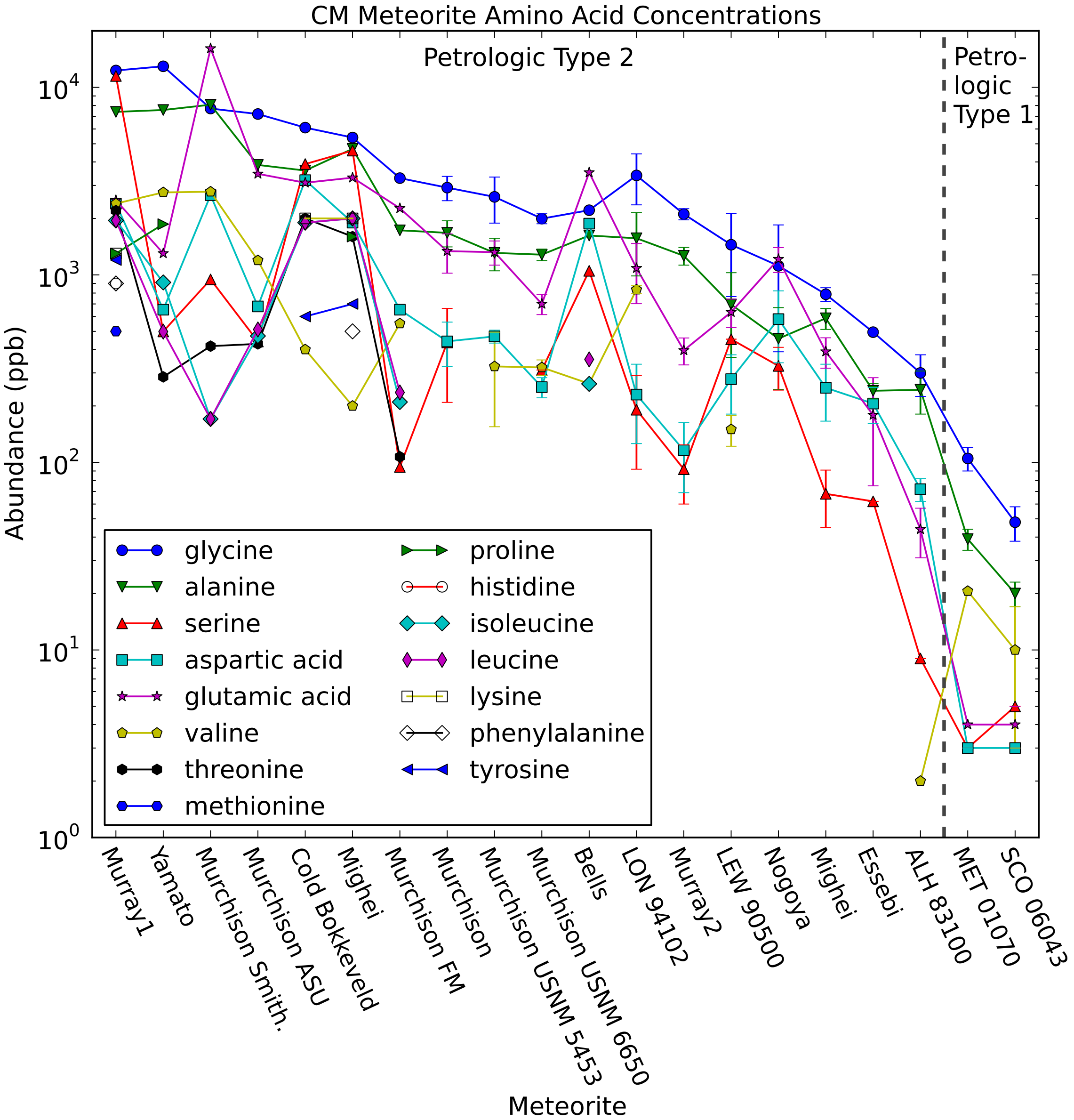

Figure 3.3: Amino acid abundances for 20 samples of CM meteorite. Concentrations are shown in ppb. See Table

Concentrations for the CM class are shown in Figure 3.3. There are 20 sets of data for CM meteorites: two samples of Murray, called Murray 1 and Murray 2, Yamato, six samples of Murchison, called Murchison, Murchison Smith., Murchison ASU, Murchison FM, Murchison USNM 5453, and Murchison USNM 6650, Cold Bokkeveld, Mighei, Bells, LON 94102, LEW 90500, Nogoya, a second sample of Mighei, Essebi, ALH 83100, MET 01070, and SCO 06043. The first 18 are all type 2 meteorites. The last two, MET 01070 and SCO 06043, are type 1. As in Figure 3.2, glycine again rides along the top of Figure 3.3. Alanine follows in a close second for most abundant amino acid of the CMs. Serine remains near the bottom abundance levels in most meteorites. The wider variety of CM-types allows us a broader landscape to observe, which also allows for more variation in amino acid concentration. We see a considerable fluctuation in abundance of numerous amino acids, especially around the Cold Bokkeveld and Mighei meteorites, and again at Bells. In general, we see that the amino acid tracks remain roughly parallel across the CM class.

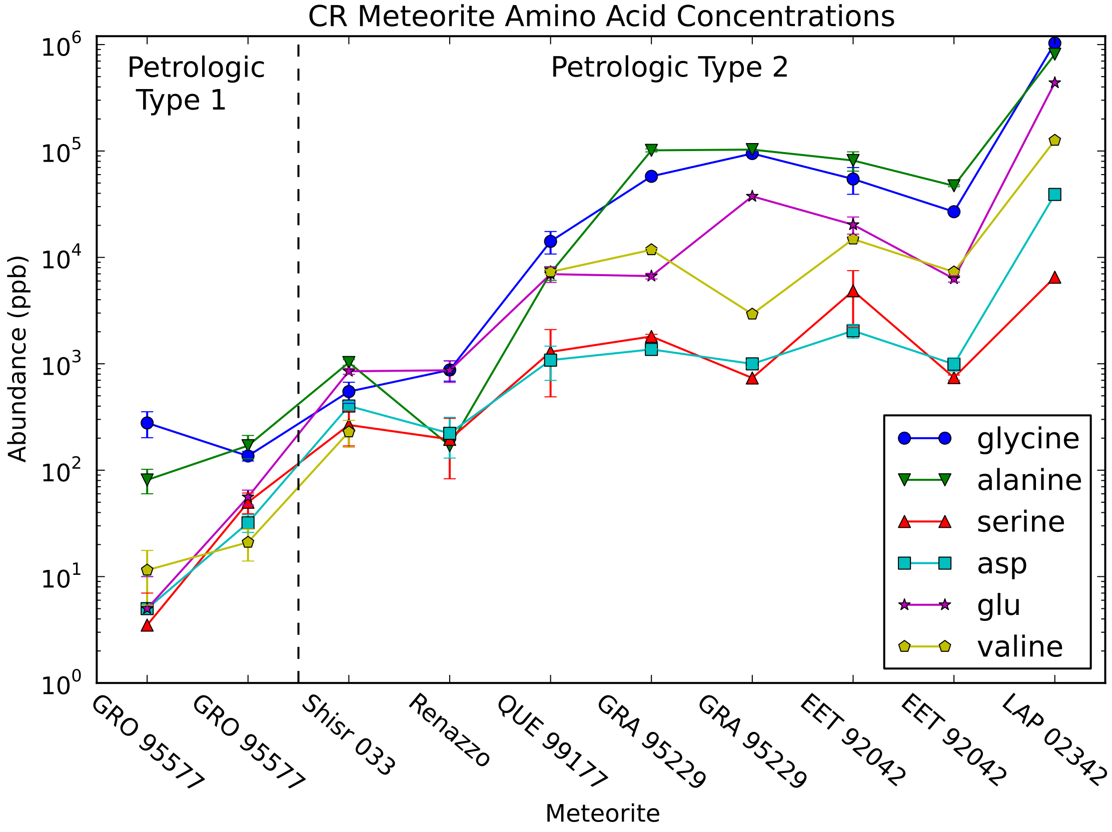

Figure 3.4: Amino acid abundances for 10 samples of CR meteorite. Concentrations are shown in ppb. See Table

Figure 3.4 shows amino acid concentration for the CR class of meteorites. We have 10 meteorite samples for the CRs. One CR meteorite is petrologic type 1, GRO 95577, for which there are two data sets from two separate analyses. The other eight samples are type 2: Shişr 033, Renazzo, QUE 99177, two samples of GRA 95229, two samples of EET 92042, and LAP 02342. Note that QUE 99177 has occasionally been classified as a CR3 type rather than a CR2, such as in Glavin et al. (2011). Amino acid abundances for this meteorite are between 10^3 and 10^4 ppb, well above the average abundance for other type 3 samples. For the purpose of this work, we consider QUE 99177 as a type 2 carbonaceous chondrite. Glycine continues largely to be the most abundant amino acid present, and serine among the least abundant. Valine, aspartic acid, and glutamic acid tracks move roughly parallel near the middle of the abundance range.

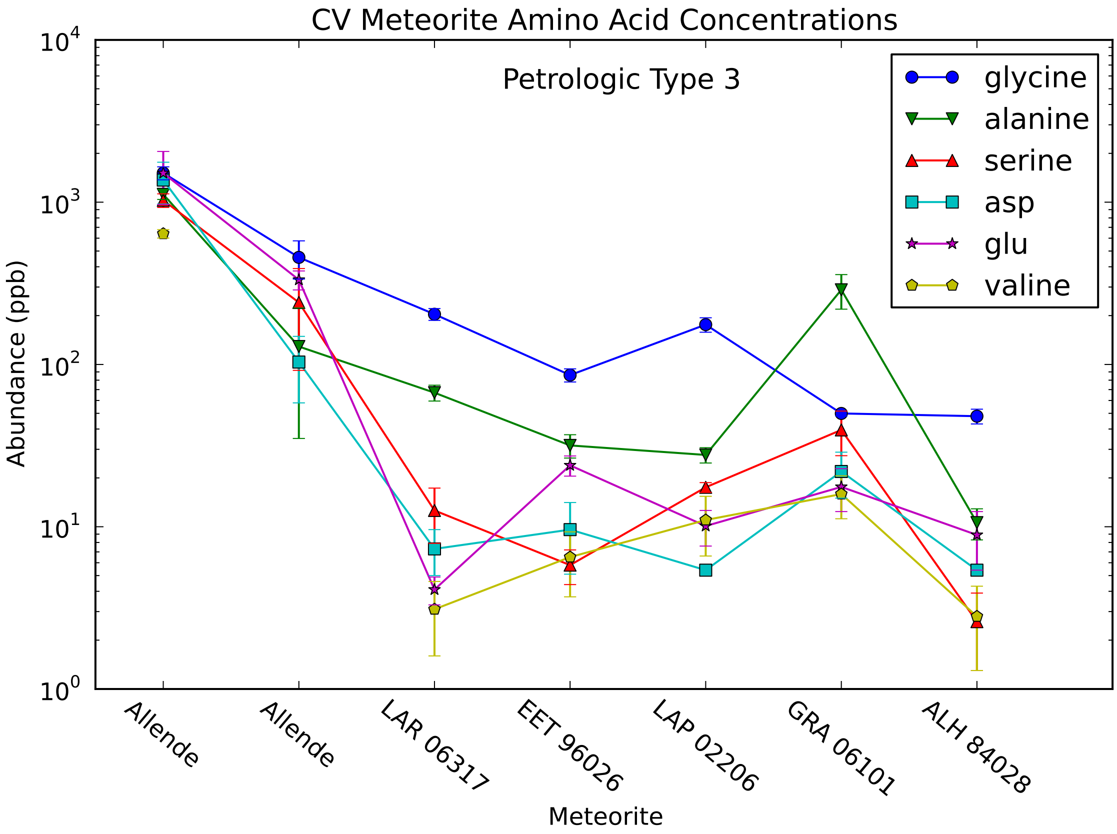

Figure 3.5: Amino acid abundances for seven samples of CV meteorite. Concentrations are shown in ppb. See Table

Figure 3.5 shows concentration data for the CV meteorites. There are seven sets of amino acid abundance data for the CV class, all CV3s. These chondrites are Allende (data from two different analyses), LAR 06317, EET 96026, LAP 02206, GRA 06101, and ALH 84028. Again glycine predominantly leads the abundance data curves. Valine and aspartic acid seem to be the least abundant amino acids amongst the CV-types. Serine, alanine, and glutamic acid trace near the middle. There is a single large spike in alanine values seen in the GRA 06101 meteorite.

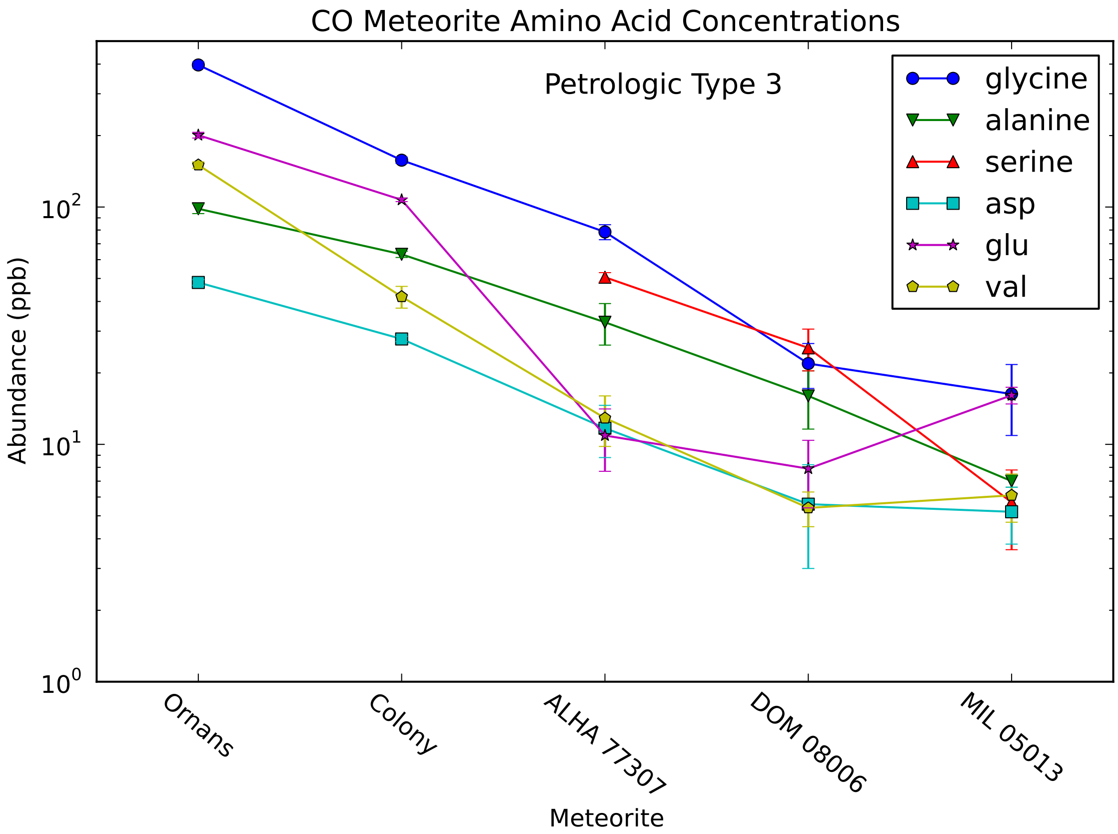

Figure 3.6: Amino acid abundances for five samples of CO meteorite. Concentrations are shown in ppb. See Table

Amino acid concentrations within the CO-type meteorites are shown in Figure 3.6. We have data for five CO3 chondrites: Ornans, Colony, ALHA 77307, DOM 08006, and MIL 05013. Figure 3.6 amino acid concentration tracks are among the most parallel of any meteorite class. Glycine consistently remains one of the most abundant amino acids, among the COs and all other meteorite classifications. In this type, valine and aspartic acid are the least abundant. Alanine, glutamic acid, and serine show some variation.

The data have been separated into different plots based on meteorite classification, CI, CM, CR, CV, and CO. The meteorites in each class have been further organized according to petrologic type. These data, while comprehensive and up-to-date, are difficult to visualize. The data are presented graphically to improve pattern recognition. Overall patterns which emerge include the tendency of glycine to be the most abundant amino acid, and serine, valine, and aspartic acid tend to be the least abundant. Alanine and glutamic acid show significant variation across all classes. In general, amino acid abundance curves track roughly parallel across all meteorites within a given subclass.

3.4 Results

Figures 3.2 through 3.6 are organized into separate plots of amino acid abundance for each meteorite classification. Within each type classification, meteorites are listed according to the broad spectrum of decreasing amino acid concentration. To observe the overall trends total amino acid abundance, we plot in Figure 3.7 the total amino acid concentrations for the entire range of meteorites across all classifications. Each meteorite has a single data point representing the sum of amino acid abundances for six amino acids: glycine, alanine, serine, aspartic acid, glutamic acid, and valine. We have the most complete set of data for these six amino acids. In the cases of multiple sets of abundance data for the same meteorite, amino acid concentrations were averaged. We did not include incomplete sets of abundance data when calculating the sum for each meteorite, as inclusion of extra amino acids for some meteorites and not for others would skew the total abundance pattern.

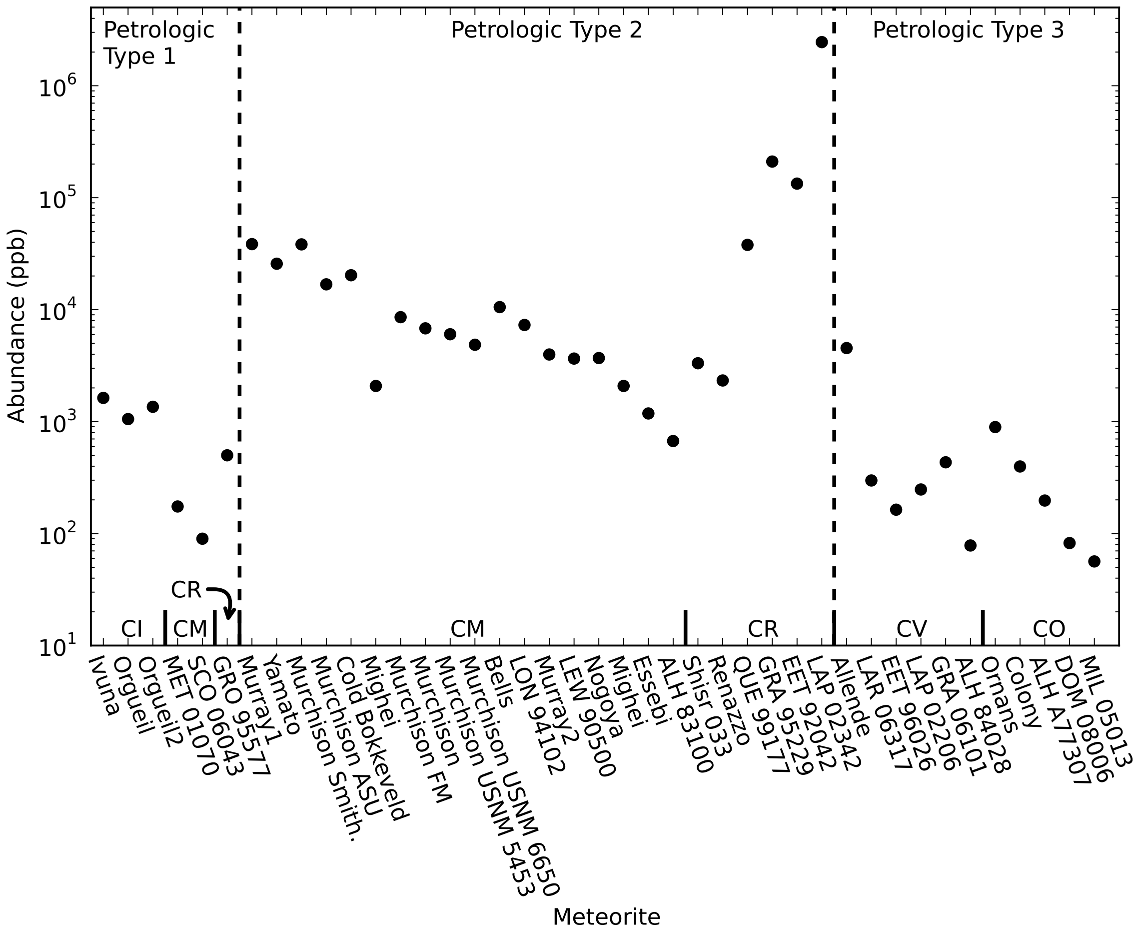

Figure 3.7: Total amino acid abundances for all meteorites. Summed amino acid values include glycine, alanine, serine, aspartic acid, glutamic acid, and valine. Concentrations are shown in ppb.

Within the broader spectrum of amino acid presence in meteorites, the data show general characteristics of abundance among meteorite classes. We see that amino acids are most abundant in the CM and CR meteorite classes. Historically, CMs show the highest quantity of organic materials, though that has changed since the discovery and classification of recent CR-type finds. The average concentration for a single amino acid among CMs is on the order of 10^3 ppb. Most concentrations range from 10^2 to 10^4 ppb, with a few specimens expressing low organic content, around 100 ppb. The CM chondrites contain the greatest variety of amino acids of all investigated subclasses, and previously held the record for greatest concentration.

The CR-types show a similarly broad variety in amino acids, and the full range of amino acids in CR chondrites shows the greatest variation in concentration. Recently, the analysis of three CRs in particular, EET 92042, GRA 95229, and LAP 02342, have increased the average amino acid abundance of the CR class drastically. CR-type concentrations typically range from 10^2 to 10^4 ppb. A few specimens have amino acid abundances in the 10^5 to 10^6 ppb range.

CI-, CV-, and CO-type meteorites cover the middle ground with regard to amino acid variety and abundance. These subclasses tend to contain a much simpler assortment of α-amino acids, primarily the amino acids glycine and alanine. The majority of CI abundance data lay between 10 and 400 ppb, with a single meteorite containing around 800 ppb. CVs average between 10 and 200 ppb, with a single meteorite specimen showing individual amino acid abundances around 10^3 ppb. Amino acids are the least abundant in CO-type meteorites. Levels of each amino acid across the CO class range between 10 and 400 ppb.

3.4.1 Amino Acid Abundance Patterns

Figure 3.8 shows the average concentration by weight of each amino acid per meteorite classification and represents one of the most important findings in this paper. There are fewer samples of meteorite types CI1, CM1/CR1, CV3, and CO3, where we have only a complete set of data for six amino acids. There is a larger set of meteorite samples in the CM2 and CR2 classes, and a broader variety of amino acids for which we have data.

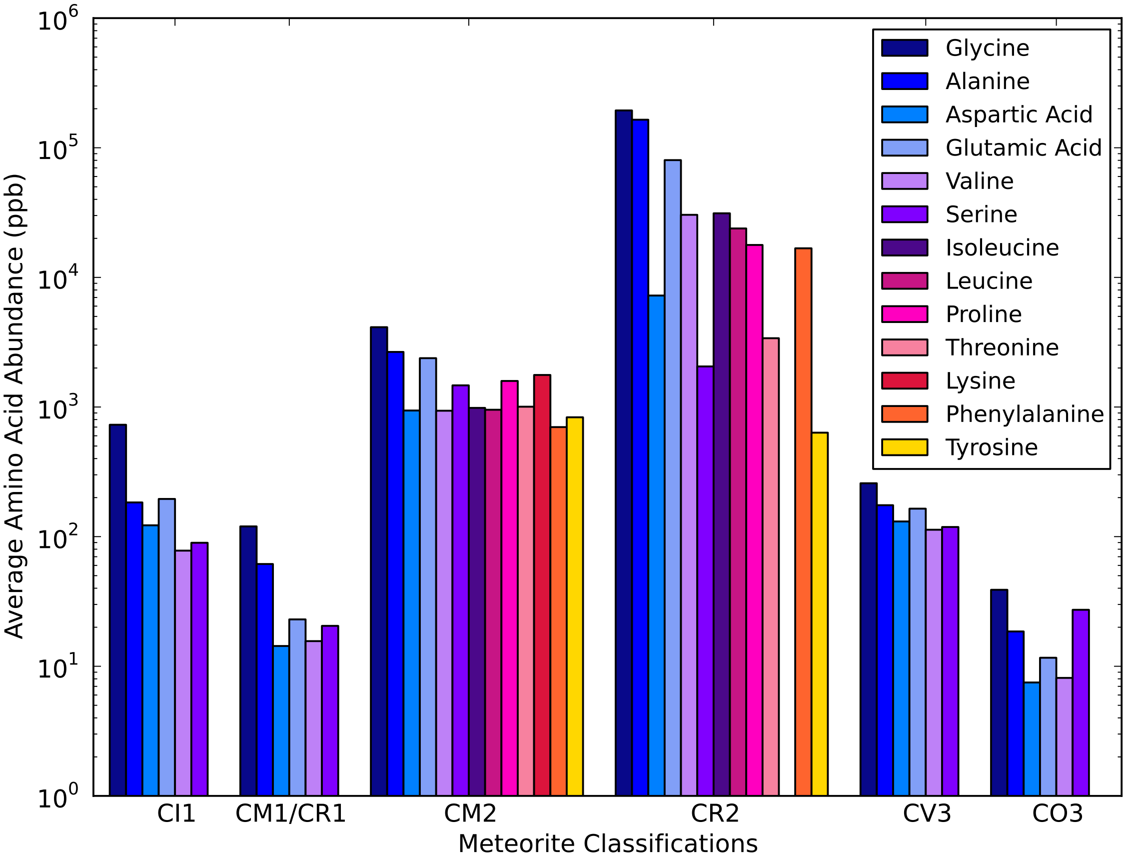

Figure 3.8: Average amino acid abundances separated by meteorite class. There are three meteorite samples of CI1, two samples of CM1, one of type CR1, 18 of CM2, six of CR2, six meteorites of type CV3, and three samples of CO3. The averages for the CM1 and CR1 classes are combined as there are so few samples of each type. CI1, CM1/CR1, CV3, and CO3 only have available and complete data for six amino acids: glycine, alanine, serine, aspartic acid, glutamic acid, and valine. The greater number of samples in the CM2 and CR2 classes allows for a broader spectrum of available amino acid data: glycine, alanine, serine, aspartic acid, glutamic acid, valine, threonine, proline, isoleucine, leucine, lysine, phenylalanine, and tyrosine.

We see that the pattern of relative amino acid abundance roughly follows the classification according to petrologic type. The greatest total abundance of amino acids occurs in CM and CR type 2 meteorites. CI meteorites, all petrologic type 1, do contain a significant quantity of amino acids, though less than the CM2/CR2 by several orders of magnitude. The few meteorites we have of type CM1/CR1 show a similar quantity of total amino acids to CI1, indicating a dependence on formation processes associated with the type 1 petrologic type. As suggested by Figure 3.1, the CO and CV meteorites, all type 3, show relatively little aqueous alteration and associated low abundances of amino acids.

Following the pattern laid out in Figure 3.1, we see an increase in amino acid synthesis associated with greater degrees of aqueous alteration between temperatures 200°C and 400°C. The temperature range between 150°C and 200°C corresponds to the greatest degrees of aqueous alteration, amongst petrologic type 1 meteorites. We see comparatively low abundances of amino acids in the type 1 samples compared to the type 2 meteorites. Martins et al. (2007a) and Glavin et al. (2011) suggest this lack of significant amino acid presence is due to some chemical oxidation process during aqueous alteration. At lower temperatures, there is clearly some external effect causing degradation of amino acids in parent bodies. Whatever the chemical reasoning behind the decline in amino acid concentration, this suggests that the observed peak in amino acid synthesis we see amongst type 2 samples is due to the existence of an optimal temperature range and interior conditions inside meteoritic parent bodies. Cobb and Pudritz (2013b, in prep.) use principles of thermodynamics to examine the trend of amino acid dependence on temperature. As is, we observe a clear relationship between total amino acid abundances and petrologic type. Both the CM2- and CR2-type meteorites show the greatest concentration of amino acids among meteorite classes. This indicates the existence of an optimal temperature range for amino acid synthesis around 200°C to 400°C.

3.4.2 Normalized Amino Acid Relative Frequencies

The data visualized in the previous figures have shown conclusively there exists a greater abundance of amino acids in meteorites of type CM2 and CR2. Given that standing pattern, we now take a closer look at these two classes in particular. Figure 3.9 shows average amino acid frequencies relative to glycine for meteorites in the CM2 class. We normalize all frequencies to glycine. This follows convention as glycine is the simplest, achiral, and one of the most abundant amino acids. The ordering of amino acids follows the pattern in Higgs & Pudritz (2009) of the 10 early type amino acids formed during Miller and Urey's atmospheric discharge experiments. Higgs & Pudritz (2009) found a thermodynamic relationship between Gibbs free energies of reaction and these 10, which are glycine, alanine, aspartic acid, glutamic acid, valine, serine, isoleucine, leucine, proline, and threonine.

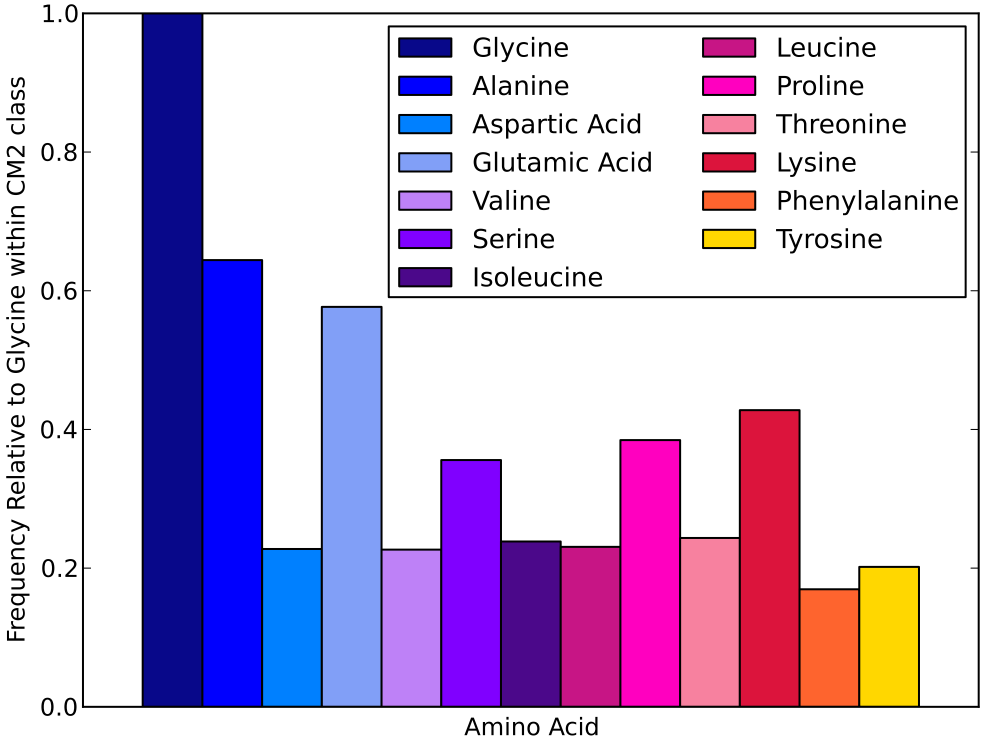

Figure 3.9: Relative amino acid frequencies for the CM2 meteorite class. Abundance values have been averaged over the 18 meteorite samples in this classification. Abundances of 13 amino acids are shown relative to glycine, reported in ppb(amino acid) per ppb(glycine).

Figure 3.10 shows average amino acid frequencies relative to glycine for meteorites in the CR2 class. Note that the normalization to glycine does not include normalization over molecular weight. We follow the nomenclature of Higgs & Pudritz (2009), where relative frequency means the occurrence or abundance of some amino acid species relative to a baseline amino acid, in this case glycine.

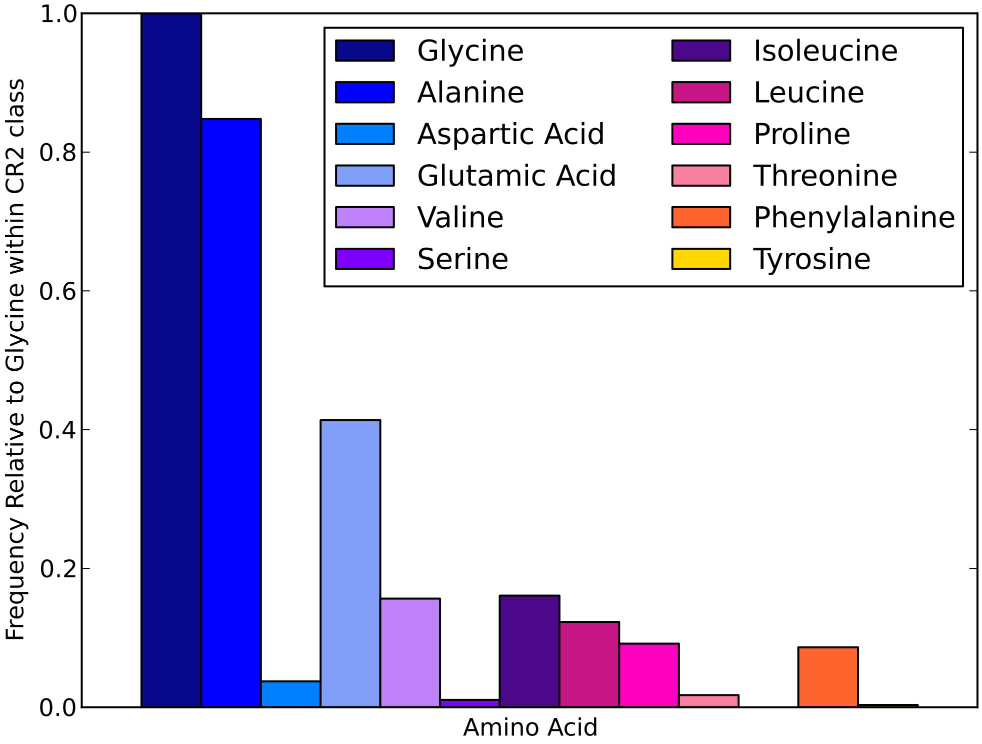

Figure 3.10: Relative amino acid frequencies for the CR2 meteorite class. Abundance values have been averaged over the 6 meteorite samples in this classification. Abundances of 12 amino acids are shown relative to glycine, reported in ppb(amino acid) per ppb(glycine).

In both Figures 3.9 and 3.10 we see a relative predominance of glycine. Glycine is classically one of the most abundant amino acids found on meteorites, it is achiral, and is the easiest to synthesize. Alanine is the second most abundant amino acid in meteorites, followed by glutamic acid. In CM2-types, there are also appreciable quantities of serine, proline, and lysine. Other amino acids present in much smaller quantities are aspartic acid, valine, threonine, isoleucine, leucine, phenylalanine, and tyrosine.

These plots allow us to make comparative statements about relative concentrations within a given meteorite class. Higgs & Pudritz (2009) found that amino acid frequency data for three CM2 meteorites could be correlated with the Gibbs free energy of reaction using a purely thermodynamic relation. In Cobb and Pudritz (2013b, in prep.), we use the frequencies shown in Figures 3.9 and 3.10 as a baseline for our modeling software to examine a much broader class of data using predictive thermodynamic theory.

3.5 Conclusions

This work investigates amino acid abundance patterns and relative frequencies in carbonaceous chondrites. We collated data from a variety of sources covering a range of meteorites, including CI, CM, CR, CV, and CO, and petrologic types 1 through 3. The data represent a wide variety of meteoritic parent body alteration states. Collation of this data allows for identification of patterns and the relationship between amino acid abundance and meteorite classification/petrologic type. We included amino acid abundances for 41 different samples of meteorite, covering five different subclasses of meteorite and three petrologic types. Our results are listed below.

1. We present the data according to physical properties and trends in formation mechanisms. Type 1 meteorites, be they CI, CM, or CR, are the most aqueously altered specimens. Aqueous alteration occurred at low temperatures, 150°C to 200°C, yet we do not observe a peak in total amino acid concentration at this location. All CI meteorites are petrologic type 1. There are only three listed type 1 CM/CR chondrites (two CM1 meteorites, one CR1 meteorite).

2. The type 2 meteorites, associated with alteration temperatures 200°C to 400°C, show the greatest amino acid concentrations of all petrologic groups. The CM2s and CR2s contain the greatest quantities and variety of amino acids of all subclasses.

3. All CV and CO chondrites are type 3, associated with alteration temperatures of 400°C to 600°C. Type 3s are relatively unaltered from the time of their original formation. They have undergone relatively little to no alteration, either aqueous or thermal metamorphism, and show a corresponding lack of amino acids.

4. These data indicate the existence of a 'sweet spot' in temperature for amino acid synthesis in meteoritic parent bodies. The temperature range between 200°C to 400°C corresponds with the greater amino acid abundances by several orders of magnitude.

5. For this optimal temperature range, we identify the relative frequencies of amino acids relative to glycine for the CM2 and CR2 carbonaceous chondrites. In Higgs & Pudritz (2009), relative frequencies are shown to occur according to thermodynamic principles. The more extensive data shown here reinforces the conclusion that an underlying thermodynamic argument may be responsible.

In Cobb and Pudritz (2013b, in prep.), we investigate computationally if temperature and aqueous conditions account for the overall abundance patterns we see in the data as well as for relative frequencies within subclasses.

3.6 Supplementary Material

3.6.1 Amino Acid Data

Table 3.1 gives all relevant values of α-amino acid concentrations used in this research. Reported abundances are listed in parts-per-billion (ppb) format. A blank space in the table indicates that either the amino acid was not looked for or not detected within a meteorite. In some sources, amino acid abundances were reported with D- and L- enantiomers listed individually; the table below shows only combined values. Where applicable, some abundances are also reported with error values associated with each abundance measurement. For extraction procedures, error, and additional information, the authors refer the reader to citations listed for each meteorite.

Table 3.1: Amino acid abundances of various two- to nine-carbon amino acids quantified in an assortment of carbonaceous chondrite meteorites, including CI1, CM1, CR1, CM2, CR2, CR3, CV3, CO3. Amino acid abundances are reported in parts per billion, specifically for α-amino acids. Where applicable, concentrations initially reported separately as D- and L-acids have been added together to show the combined value. For extraction procedures, refer to sources cited for individual meteorites.

	CI1			CM1	
	Ivuna	Orgueil	Orgueil	MET 01070	SCO 06043
Amino Acid	Botta et al. (2002)		Glavin et al. (2011) & Glavin & Dworkin (2009)	Glavin et al. (2011)	
2-carbon					
Glycine	617 ± 83	707 ± 80	865 ± 450	105 ± 15	48 ± 10
3-carbon					
D-,L-alanine	239 ± 36	138 ± 18	174 ± 39	39 ± 5	20 ± 3
D-,L-serine	217 ± 12	51 ± 26	< 2	< 3	< 5
Sarcosine					
4-carbon					
D-,L-aspartic acid	176 ± 10	82 ± 34	109 ± 59	< 3	< 3
Threonine					
D-,L-ABA	12 ± 7	13 ± 11	71 ± 49	23 ± 4	4 ± 1
AIB	46 ± 33	39 ± 37	343 ± 140	37 ± 10	30 ± 9
5-carbon					
D-,L-glutamic acid	380 ± 12	76 ± 37	130 ± 38	< 4	< 4
Methionine					
Proline					
Valine			78 ± 8	< 10.3	9.6 ± 8.1
Isovaline	< 163	< 194	85 ± 5	< 0.9	7.9 ± 0.9
Norvaline			27 ± 2	< 0.4	1.4 ± 0.4
Ornithine					
6-carbon					
Histidine					
Isoleucine					
Leucine					
Norleucine					
Pseudoleucine					
Alloisoleucine					
Lysine					
Amino-adipic acid					
9-carbon					
Phenylalanine					
Tyrosine					

Table 3.1, cont'd: Amino acid abundances of various two- to nine-carbon amino acids quantified in an assortment of carbonaceous chondrite meteorites, including CI1, CM1, CR1, CM2, CR2, CR3, CV3, CO3. Amino acid abundances are reported in parts per billion, specifically for α-amino acids. Where applicable, concentrations initially reported separately as D- and L-acids have been added together to show the combined value. For extraction procedures, refer to sources cited for individual meteorites.

	CR1		CM2			
	GRO 95577	GRO 95577	Yamato 791198	Cold Bokkeveld	Mighei	Murray
Amino Acid	Glavin et al. (2011)	Martins et al. (2008)	Shimoyama et al. (1985)	Kaplan et al. (1963)		
2-carbon						
Glycine	278 ± 76	136 ± 14	12949.6	6100	5400	12300
3-carbon						
D-,L-alanine	81 ± 21	170 ± 42	7572.7	3600	4700	7400
D-,L-serine	< 7	50 ± 11	499.2	3900	4600	11500
Sarcosine			1180.5			
4-carbon						
D-,L-aspartic acid	< 10	32 ± 6	652.2	3200	1900	2400
Threonine			285.9	2000	1600	2200
D-,L-ABA	45 ± 10		8043.4			
AIB	175 ± 15	48 ± 3	66512.4			
5-carbon						
D-,L-glutamic acid	< 10	56 ± 9	1302.1	3100	3300	2500
Methionine						500
Proline			1865.1		1600	1300
Valine	11.5 ± 6.1	21 ± 7	2753	400	200	2400
Isovaline	32.8 ± 3.7	65.5 ± 65.5				
Norvaline	4 ± 0.3		2811.6			
Ornithine						2100
6-carbon						
Histidine						900
Isoleucine			911.6	3800	4000	3900
Leucine			498.4			
Norleucine						
Pseudoleucine						
Alloisoleucine						
Lysine				2000	2000	1300
Amino-adipic acid			2352.9			
9-carbon						
Phenylalanine					500	900
Tyrosine				600	700	1200

Table 3.1, cont'd: Amino acid abundances of various two- to nine-carbon amino acids quantified in an assortment of carbonaceous chondrite meteorites, including CI1, CM1, CR1, CM2, CR2, CR3, CV3, CO3. Amino acid abundances are reported in parts per billion, specifically for α-amino acids. Where applicable, concentrations initially reported separately as D- and L-acids have been added together to show the combined value. For extraction procedures, refer to sources cited for individual meteorites.

	CM2					
	Murchison (FM)	Murchison (ASU)	Murchison (Smith.)	Murchison	Murray	Nogoya
Amino Acid	Cronin & Pizzarello (1983)			Botta et al. (2002)		
2-carbon						
Glycine	3280.6	7206.7	7709.7	2919 ± 433	2110 ± 144	1118 ± 729
3-carbon						
D-,L-alanine	1728.3	3857.6	8080.5	1676 ± 266	1264 ± 137	457 ± 212
D-,L-serine	94.6	441.4	945.8	436 ± 227	92 ± 32	327 ± 84
Sarcosine						
4-carbon						
D-,L-aspartic acid	652.2	678.8	2662	442 ± 118	116 ± 47	581 ± 241
Threonine	107.2	428.8	416.9			
D-,L-ABA	567.2	1660.2	1361.2	642 ± 209	463 ± 68	< 151
AIB	14983.3	10332.6	9394.2	2901 ± 328	1968 ± 350	458 ± 346
5-carbon						
D-,L-glutamic acid	2265.8	3457.6	16125.4	1338 ± 317	396 ± 65	1214 ± 184
Methionine						
Proline						
Valine	550.6	1194.9	2776.5			
Isovaline	6255.8	3245.1	6771.3	808 ± 392	2834 ± 780	< 72
Norvaline	175.7	468.6	292.9			
Ornithine						
6-carbon						
Histidine						
Isoleucine	209.9	472.2	170.5			
Leucine	236.1	511.6	170.5			
Norleucine	118	354	66			
Pseudoleucine	52	380	341			
Alloisoleucine	105	498	131			
Lysine						
Amino-adipic acid						
9-carbon						
Phenylalanine						
Tyrosine						

Table 3.1, cont'd: Amino acid abundances of various two- to nine-carbon amino acids quantified in an assortment of carbonaceous chondrite meteorites, including CI1, CM1, CR1, CM2, CR2, CR3, CV3, CO3. Amino acid abundances are reported in parts per billion, specifically for α-amino acids. Where applicable, concentrations initially reported separately as D- and L-acids have been added together to show the combined value. For extraction procedures, refer to sources cited for individual meteorites.

	CM2					
	Mighei	Essebi	Bells	Murchison USNM 5453	Murchison USNM 6650	LEW 90500
Amino Acid	Botta et al. (2002)		Monroe & Pizzarello (2011)	Glavin et al. (2011)	Glavin et al. (2006) & Glavin & Dworkin (2009)	
2-carbon						
Glycine	788 ± 66	495 ± 6	2212.3	2606 ± 717	1995 ± 122	1448 ± 682
3-carbon						
D-,L-alanine	587 ± 75	241 ± 23	1621.4	1310 ± 259	1282 ± 90	695 ± 332
D-,L-serine	68 ± 23	< 62	1050.9		94 ± 18	454 ± 314
Sarcosine						
4-carbon						
D-,L-aspartic acid	250 ± 84	206 ± 45	1876.7	470 ± 37	252 ± 31	278 ± 97
Threonine						
D-,L-ABA	201 ± 148	< 29		622 ± 128	403 ± 156	431 ± 159
AIB	740 ± 219	208 ± 26		5124 ± 2487	3182 ± 620	2706 ± 377
5-carbon						
D-,L-glutamic acid	390 ± 72	179 ± 104	3516.4	1322 ± 195	700 ± 86	633 ± 110
Methionine						
Proline						
Valine			262.9	325 ± 170	321 ± 31	150 ± 28
Isovaline	295 ± 185	< 29		3321 ± 345	2796 ± 298	1306 ± 83
Norvaline				118 ± 8	27 ± 4	18 ± 2
Ornithine						
6-carbon						
Histidine						
Isoleucine			262.3			
Leucine			354.2			
Norleucine						
Pseudoleucine						
Alloisoleucine						
Lysine						
Amino-adipic acid						
9-carbon						
Phenylalanine						
Tyrosine						

Table 3.1, cont'd: Amino acid abundances of various two- to nine-carbon amino acids quantified in an assortment of carbonaceous chondrite meteorites, including CI1, CM1, CR1, CM2, CR2, CR3, CV3, CO3. Amino acid abundances are reported in parts per billion, specifically for α-amino acids. Where applicable, concentrations initially reported separately as D- and L-acids have been added together to show the combined value. For extraction procedures, refer to sources cited for individual meteorites.

	CM2		CR2			
	ALH 83100	LON 94102	EET 92042	Renazzo	EET 92042	GRA 95229
Amino Acid	Glavin et al. (2006)	Glavin et al. (2011)	Glavin & Dworkin (2009) & Glavin et al. (2011)	Botta et al. (2002)	Martins et al. (2008)	
2-carbon						
Glycine	300 ± 75	3391 ± 1029	54527 ± 15365	875 ± 188	26875 ± 1176	57796 ± 358
3-carbon						
D-,L-alanine	244 ± 63	1568 ± 581	81433 ± 16752	85 ± 85	47077 ± 933	101403 ± 3303
D-,L-serine	< 9	191 ± 99	4851 ± 2657	195 ± 112	742 ± 42	1807 ± 84
Sarcosine						
4-carbon						
D-,L-aspartic acid	72 ± 10	230 ± 104	2044 ± 302	222 ± 92	991 ± 147	1365 ± 16
Threonine						
D-,L-ABA	19 ± 5	896 ± 300	20859 ± 5653	< 89		
AIB	250 ± 40	753 ± 413	56825 ± 15592	< 73	57856 ± 2030	27679 ± 1113
5-carbon						
D-,L-glutamic acid	44 ± 13	1086 ± 384	20268 ± 3716	869 ± 201	6298 ± 436	6673 ± 405
Methionine						
Proline						
Valine	< 2	834 ± 41	14864 ± 927		7297 ± 152	11789 ± 355
Isovaline	< 10	380 ± 40	28610 ± 1663	349 ± 33	11399 ± 11399	13922 ± 13922
Norvaline		522 ± 37	6506 ± 742			
Ornithine						
6-carbon						
Histidine						
Isoleucine						
Leucine						
Norleucine						
Pseudoleucine						
Alloisoleucine						
Lysine						
Amino-adipic acid						
9-carbon						
Phenylalanine						
Tyrosine						

Table 3.1, cont'd: Amino acid abundances of various two- to nine-carbon amino acids quantified in an assortment of carbonaceous chondrite meteorites, including CI1, CM1, CR1, CM2, CR2, CR3, CV3, CO3. Amino acid abundances are reported in parts per billion, specifically for α-amino acids. Where applicable, concentrations initially reported separately as D- and L-acids have been added together to show the combined value. For extraction procedures, refer to sources cited for individual meteorites.

	CR2			CR3	CO3	
	GRA 95229	LAP 02342	Shisr 033	QUE 99177	ALHA 77307	MIL 05013
Amino Acid	Pizzarello & Holmes (2009)		Martins et al. (2007)	Glavin & Dworkin (2009) & Glavin et al. (2011)	Burton et al. (2012)	
2-carbon						
Glycine	94663.3	1032062.4	548 ± 123	14134 ± 3376	78.5 ± 5.7	16.3 ± 5.4
3-carbon						
D-,L-alanine	103077.1	812322.6	1028 ± 64	7133 ± 1049	32.7 ± 6.5	7 ± 0.4
D-,L-serine	735.6	6515.6	266 ± 97	1294 ± 805	50.6 ± 2.3	5.7 ± 2.1
Sarcosine						
4-carbon						
D-,L-aspartic acid	998.3 ± 66.6	39064.9	401 ± 33	1082 ± 384	11.7 ± 2.9	5.2 ± 1.4
Threonine	2144.2	4645.7				
D-,L-ABA	34029.6	240682.1		3300 ± 637	0.2 ± 0.2	0.9 ± 0.5
AIB	49807	353186		14246 ± 3249	1.1 ± 0.4	1.1 ± 0.2
5-carbon						
D-,L-glutamic acid	37518.2	437711.8	851 ± 55	6959 ± 1139	10.9 ± 3.2	16.1 ± 1.3
Methionine						
Proline	7253.2	28322				
Valine	2928.8	125936.3	229 ± 65	7303 ± 345	12.9 ± 3.1	6.1 ± 1.4
Isovaline	14292.3	72984.5	< 12	11098 ± 302		
Norvaline				1927 ± 128	0.2 ± 0.2	0.2 ± 0.2
Ornithine						
6-carbon						
Histidine						
Isoleucine	1180.5	61256.4				
Leucine	2885.7	68470.7	214 ± 30			
Norleucine						
Pseudoleucine						
Alloisoleucine	2623.4	101263.2				
Lysine						
Amino-adipic acid	1611.6	13859.4				
9-carbon						
Phenylalanine	5451.3	28082.3				
Tyrosine	906	< 362.4				

Table 3.1, cont'd: Amino acid abundances of various two- to nine-carbon amino acids quantified in an assortment of carbonaceous chondrite meteorites, including CI1, CM1, CR1, CM2, CR2, CR3, CV3, CO3. Amino acid abundances are reported in parts per billion, specifically for α-amino acids. Where applicable, concentrations initially reported separately as D- and L-acids have been added together to show the combined value. For extraction procedures, refer to sources cited for individual meteorites.

	CO3			CV3		
	DOM 08006	Colony	Ornans	Allende	Allende	ALH 84028
Amino Acid	Burton et al. (2012)	Chan et al. (2012)		Botta et al. (2002)	Burton et al. (2012)	
2-carbon						
Glycine	21.9 ± 4.7	157.5 ± 4.8	396.7 ± 11.6	457 ± 121	1513 ± 139	48 ± 5
3-carbon						
D-,L-alanine	16 ± 4.4	63.2 ± 1.9	98.3 ± 4.5	129 ± 94	1118 ± 78	10.6 ± 2.3
D-,L-serine	25.5 ± 5.1			241 ± 149	1027 ± 99	2.6 ± 1.3
Sarcosine						
4-carbon						
D-,L-aspartic acid	5.6 ± 2.6	27.8 ± 0.7	48.1 ± 1.3	103.5 ± 45.5	1369 ± 394	2.8 ± 2.6
Threonine						
D-,L-ABA	1.4 ± 0.4			< 4	17.4 ± 3.1	0.8 ± 0.6
AIB	2.7 ± 1.4			< 10	6.5 ± 1.7	1.9 ± 1.1
5-carbon						
D-,L-glutamic acid	7.9 ± 2.5	107.2 ± 1.8	200.8 ± 5.6	332.5 ± 44.5	1511 ± 544	8.9 ± 3.5
Methionine						
Proline						
Valine	5.4 ± 0.9	41.9 ± 4.4	150.3 ± 4.6		639 ± 38	2.8 ± 1.5
Isovaline				< 35		
Norvaline	0.2 ± 0.2				3.3 ± 0.6	0.2 ± 0.2
Ornithine						
6-carbon						
Histidine						
Isoleucine						
Leucine						
Norleucine						
Pseudoleucine						
Alloisoleucine						
Lysine						
Amino-adipic acid						
9-carbon						
Phenylalanine						
Tyrosine						

Table 3.1, cont'd: Amino acid abundances of various two- to nine-carbon amino acids quantified in an assortment of carbonaceous chondrite meteorites, including CI1, CM1, CR1, CM2, CR2, CR3, CV3, CO3. Amino acid abundances are reported in parts per billion, specifically for α-amino acids. Where applicable, concentrations initially reported separately as D- and L-acids have been added together to show the combined value. For extraction procedures, refer to sources cited for individual meteorites.

	CV3			
	EET 96026	LAP 02206	LAR 06317	GRA 06101
Amino Acid	Burton et al. (2012)			
2-carbon				
Glycine	86 ± 8	176 ± 18	204 ± 17	49.9 ± 1.8
3-carbon				
D-,L-alanine	31.7 ± 5.2	27.7 ± 3	67 ± 7.5	288.5 ± 69.4
D-,L-serine	5.8 ± 1.4	17.5 ± 1.2	12.6 ± 4.7	39.5 ± 12.1
Sarcosine				
4-carbon				
D-,L-aspartic acid	9.6 ± 4.5	2.7 ± 2.7	7.3 ± 2.3	21.9 ± 6.9
Threonine				
D-,L-ABA	0.6 ± 0.4	0.4 ± 0.1	0.1 ± 0.1	0.6 ± 0.3
AIB	0.8 ± 0.2	0.6 ± 0.3	0.6 ± 0.2	1.2 ± 0.2
5-carbon				
D-,L-glutamic acid	23.9 ± 3.4	10.1 ± 2.5	4.1 ± 0.8	17.6 ± 5.2
Methionine				
Proline				
Valine	6.5 ± 2.8	11 ± 4.4	3.1 ± 1.5	15.9 ± 4.7
Isovaline				
Norvaline	0.2 ± 0.2	0.2 ± 0.2	0.2 ± 0.2	0.2 ± 0.2
Ornithine				
6-carbon				
Histidine				
Isoleucine				
Leucine				
Norleucine				
Pseudoleucine				
Alloisoleucine				
Lysine				
Amino-adipic acid				
9-carbon				
Phenylalanine				
Tyrosine				

3.6.2 Note on Relative Frequencies

The data visualized in all previous figures have shown the greater abundance of amino acids in CM2- and CR2-type meteorites. Amino acid concentrations were reported and plotted in ppb. The relative concentrations in Figures 3.9 and 3.10 have units of ppb(amino acid)/ppb(glycine), consistent with observation. In Cobb and Pudritz (2013b, in prep.) (Ch. 4), we recreate and predict amino acid synthesis and relative abundances based on a minimization of their Gibbs free energies. To compare the computational models to observation, we need units to be in molar form rather than ppb. In preparation for comparison, Figures 3.11 and 3.12 show average amino acid abundances relative to glycine in units of mol(amino acid)/mol(glycine) for the CM2 subclass and CR2 subclass, respectively.

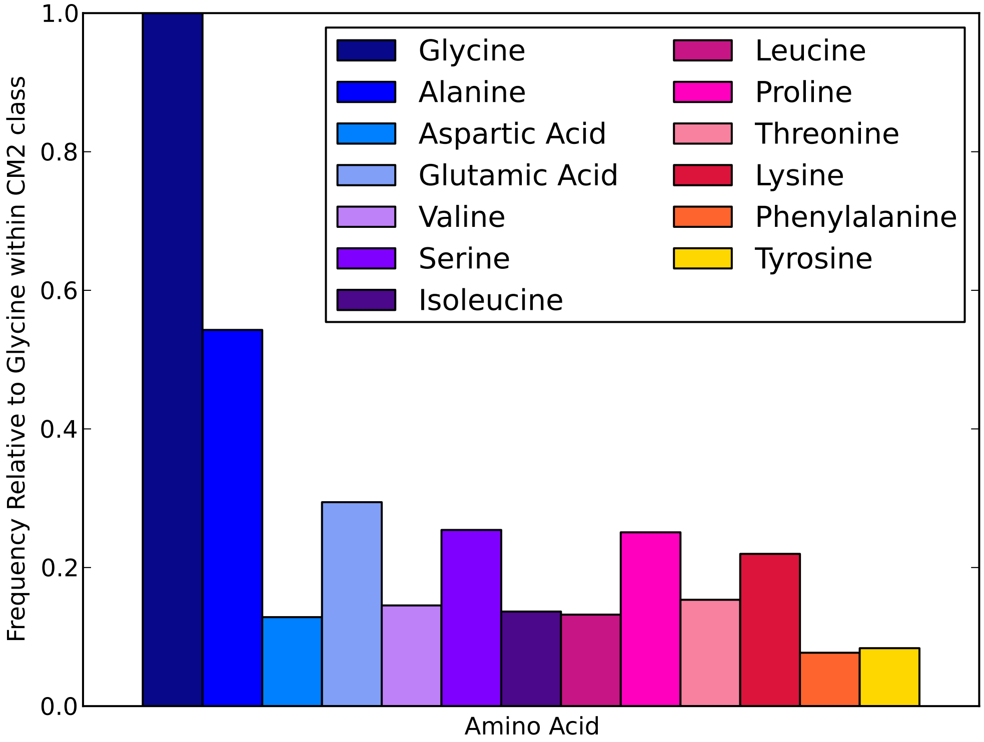

Figure 3.11: Amino acid abundances for the CM2 meteorite class. Abundance values have been averaged over the 18 meteorite samples in this classification. Concentrations of 13 amino acids are shown relative to glycine, reported in mol(amino acid) per mol(glycine).

Figure 3.11 shows average amino acid abundances relative to glycine for meteorites in the CM2 subclass. Figure 3.12 shows average amino acid abundances relative to glycine for meteorites in the CR2 subclass.

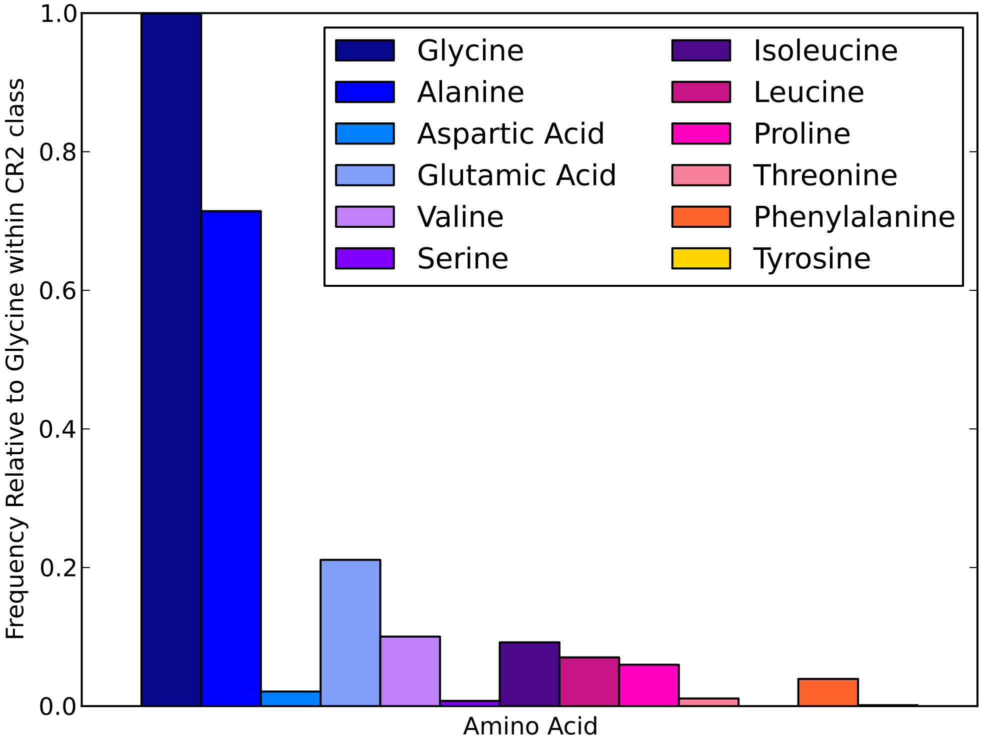

Figure 3.12: Amino acid abundances for the CR2 meteorite class. Abundance values have been averaged over the six meteorite samples in this classification. Concentrations of 12 amino acids are shown relative to glycine, reported in mol(amino acid) per mol(glycine).

In both Figures 3.11 and 3.12 we see a predominance of glycine, followed by alanine, then glutamic acid. The remaining amino acids, serine, proline, lysine, aspartic acid, valine, threonine, isoleucine, leucine, phenylalanine, and tyrosine, are present in smaller quantities.

In Equations 3.1 and 3.2, we show the conversion from ppb relative to glycine to moles relative to glycine. In Equation 3.1 amino acid concentration in ppb [nanograms (ng) amino acid (AA) per grams (g) meteorite (met)] is divided by molecular weight [g(AA)/mol(AA)] multiplied by 10^{-9} to account for the nanogram-to-gram conversion.

In Equation 3.2, mol(AA)/g(met) is divided by mol(glycine)/g(met), resulting in a conversion to mol(AA) per mol(glycine).

$$\frac{ng(AA)}{g(meteorite)}/\frac{g(AA)}{mol(AA)} * 10^{-9} = \frac{mol(AA)}{g(met)} \tag{3.1}$$

$$\frac{mol(AA)}{g(met)}/\frac{mol(glycine)}{g(met)} = \frac{mol(AA)}{mol(glycine)} \tag{3.2}$$

As reported in observation, the original data points for amino acid concentration are shown in ppb [ng(AA)/g(met)]. The converted values were calculated by dividing by the molecular weight [g(AA)/mol(AA)] for each amino acid species and accounting for the nanogram-to-gram conversion before taking the ratio over glycine. This leaves us with concentration relative to glycine in terms of moles rather than ppb [mol(AA)/mol(glycine)]. Note that since the concentration of each amino acid is scaled by its own molecular weight, the plots of converted concentrations in Figures 3.11 and 3.12 do not match the exact abundance patterns in the non-converted plots, Figures 3.9 and 3.10. Figures 3.11 and 3.12 are now in the format which will be compared to the output for Cobb and Pudritz (2013b, in prep.) (Ch. 4).

Chapter 4

Nature's Starships II: Computational Modeling of Amino Acid Synthesis in Meteoritic Parent Bodies of Carbonaceous Chondrites

This chapter will be submitted to the journal of Astrobiology as part II of a two-paper set. Authors are Cobb, A. K. and Pudritz, R. E.

Abstract

The class of meteorite called carbonaceous chondrites is known for having a high water and organic material content, including amino acids. In Cobb & Pudritz (2013a) (Ch. 3), we collated available amino acid abundance data from a variety of carbonaceous chondrite subclasses and differing petrologic groups. Now having a baseline observed amino acid abundance plot, we model both the total amino acid abundance pattern as well as the relative frequency of amino acids within the CM2 chondrite subclass using computational models. We use thermodynamic theory of Gibbs free energies to calculate the output of amino acids in a meteoritic parent body assuming chemical equilibrium and some initial concentration of organic material. We limit our thermodynamic model to include only those proteinogenic α-amino acids which are synthesized via a particular series chemical reactions called Strecker synthesis. Strecker synthesis is defined as the chemical reaction between an aldehyde, ammonia, and hydrogen cyanide in aqueous solution to produce an amino acid. We find excellent agreement between observed total abundances of amino acids and the theoretical yield from our simulation, especially at temperatures in the range 200°C to 500°C. Theoretical abundances return approximately 10^5 parts-per-billion (ppb), which is well within the observed abundance range of $\sim 2 * 10^4 - 5 * 10^5$ ppb, associated with temperatures 200°C to 400°C and petrologic type 2 meteorites. In observation, there is a sharp turnover point shortly after 400°C, in which the observed abundances decrease to $\sim 10^1 - 10^2$ ppb. Theoretical yields also drop, reaching levels as low as 10^2 ppb by 500°C. Our model does not fit well around temperatures 150°C to 200°C. Observationally, total abundances are low, $\sim 10^1 - 10^2$ ppb, associated with petrologic type 1 chondrites. Our model reports a high abundance for this range, $\sim 10^5$ ppb. There are likely additional factors which determine amino acid synthesis in parent

bodies of these meteorites which are not considered in our model. In addition to total abundances, we match relative frequencies to observed frequencies for each amino acid to well within an order of magnitude.

4.1 Introduction

The overarching goal of this work is to thermodynamically model the Strecker-type synthesis of amino acids inside meteoritic parent bodies. Cobb & Pudritz (2013a) took a closer look at overall amino acid abundances and the relative frequencies of amino acids within specific meteorite subclasses. This broad spectrum view of amino acid abundance data provided us with a goal; we now use our modeling software to recreate these observed abundance patterns.

Cobb & Pudritz (2013a) (Ch. 3) presented an extensive collation of available meteoritic data on amino acid abundances and relative frequencies in carbonaceous chondrites. Carbonaceous chondrites are the class of meteorite which contain the highest content of both water and organic materials, including amino acids. Each meteorite is assigned a number 1 through 6 indicating petrologic type, in addition to a subclass designation CI, CM, CR, CV, or CO (CH, CB, and CK are also carbonaceous chondrite subclasses, but these are not considered in this work). Petrologic type carries with it information regarding degrees of internal chemical alteration undergone by the meteoritic parent body. Petrologic type 1 chondrites are the most altered, having undergone significant degrees of what is known as aqueous alteration, which uses the liquid water resources in a parent body to chemically alter its makeup. Petrologic type 2 meteorites have undergone significant degrees of aqueous alteration, as well, though not to the extent of type 1 meteorites. Petrologic type 3 meteorites most closely resemble the solar nebulae in which they formed; they have undergone relatively little to no degrees of alteration. The carbonaceous chondrites subclasses CI, CM, CR, CV, and CO, in particular, are all known to contain high concentrations of water and organics, and their petrologic types vary from 1 to 3.

CI meteorites, all petrologic type 1, are the most aqueously altered carbonaceous chondrites. They are associated with the lowest range in temperatures (150°C to 200°C) and theoretically underwent the greatest degrees of Strecker synthesis, an example of the internal aqueous alteration processes which create amino acids inside parent bodies. The CM and CR subclasses express the highest total amino acid concentrations, greater by several orders of magnitude than any other subclass. They also express the greatest variety of proteinogenic amino acids. These subclasses correspond to petrologic type 2, with a few type 1 exceptions, and are associated with alteration temperatures of 200°C to 400°C. The CV and CO meteorites are all petrologic type 3, associated with temperatures between 400°C and 600°C. These chondrites are the most pristine samples of material we have from the time of the solar system formation. They are relatively unaltered, either via aqueous alteration or thermal metamorphism, which occurs at higher temperatures of $\sim 600^\circ - 900^\circ$C with no water present, and we observe a corresponding lack of amino acids present in the meteorites.

In this work, we investigate the computational synthesis of proteinogenic α-amino acids inside meteoritic parent bodies. Given that parent bodies remain aqueous for more than 1 Myr, and that the time scale for these reactions which synthesize amino acids is no longer than thousands of years, it is a good assumption that processes will have achieved thermodynamic equilibrium, making the Gibbs free energy approach a desirable minimum. Our model inherently assumes this chemical equilibrium, and outputs a series of amino acid concentrations which minimizes the Gibbs free energy. We model parent body interiors using temperatures and pressures cited in previous studies, as well as cometary abundance data of organics for the initial concentrations in our model.

We compare our theoretical amino acid abundances to observed total abundances in different subclasses of carbonaceous chondrite, measured in ppb. Additionally, in Cobb & Pudritz (2013a) we calculated the relative frequencies of various amino acids normalized to glycine, measured in moles of amino acid/moles of glycine. We calculate the pattern of relative frequencies in theoretical yield, and match it to observation.

In this work, we are limited to investigating the abundances of proteinogenic α-amino acids only. The thermochemical database with which we work currently contains data for a specific subset of amino acids, those being proteinogenic α-amino acids. It is important to note that there are appreciable quantities of non-proteinogenic amino acids (such as amino-isobutyric acid and isovaline) and non-α-amino acids (such as β-alanine) detected in carbonaceous chondrites. In addition, we currently only consider amino acids which are synthesized via Strecker-type reactions involving aldehydes. Amino-isobutyric acid and isovaline, while both highly abundant in carbonaceous chondrites, are synthesized via Strecker-type reactions with ketone precursors.

4.2 Theoretical Background

4.2.1 Strecker Chemistry

In this paper we consider the formation of α-amino acids created through the aqueous alteration process called Strecker synthesis. The general form of a Strecker-type reaction may be written as a mass-balance equation,

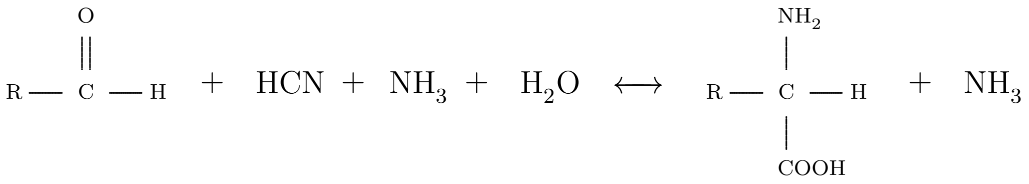

$$\mathrm{R}-\overset{\overset{\displaystyle \mathrm{O}}{\|}}{\mathrm{C}}-\mathrm{H} + \mathrm{HCN} + \mathrm{NH_3} + \mathrm{H_2O} \longleftrightarrow \mathrm{R}-\overset{\overset{\displaystyle \mathrm{NH_2}}{|}}{\underset{\underset{\displaystyle \mathrm{COOH}}{|}}{\mathrm{C}}}-\mathrm{H} + \mathrm{NH_3} \quad (4.1)$$

where an aldehyde (R-CHO) reacts with hydrogen cyanide (HCN) and ammonia (NH_3) in aqueous solution (H_2O) to produce an amino acid (H_2N-RCH-COOH) and a new ammonia molecule. This general form may be used to define the underlying Strecker pathway for each of the proteinogenic amino acids laid out in Cobb & Pudritz (2013a). In each case, the side chain (R group) of a reactant aldehyde will be identical to the R group in the corresponding amino acid. For example, the Strecker pathway for glycine is

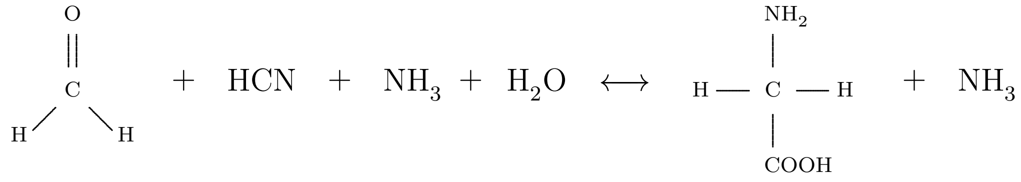

$$\overset{\overset{\displaystyle \mathrm{O}}{\|}}{\underset{\mathrm{H}\diagup\quad\diagdown\mathrm{H}}{\mathrm{C}}} + \mathrm{HCN} + \mathrm{NH_3} + \mathrm{H_2O} \longleftrightarrow \mathrm{H}-\overset{\overset{\displaystyle \mathrm{NH_2}}{|}}{\underset{\underset{\displaystyle \mathrm{COOH}}{|}}{\mathrm{C}}}-\mathrm{H} + \mathrm{NH_3} \quad (4.2)$$

where the reactant aldehyde is formaldehyde (CH_2O) and the product amino acid is glycine ($C_2H_5NO_2$). The R group in both the aldehyde and the amino acid is a single H atom.

This precise treatment of Strecker-type synthesis necessitates the R-group equivalence of the reactant and the product. For each Strecker reaction producing a proteinogenic amino acid, we can balance the incoming atom count with the outgoing atom count to definitively determine the aldehyde required to create an amino acid. Table 4.1 shows various information for 12 of the 13 proteinogenic amino acids considered in Cobb & Pudritz (2013a). We exclude proline from the model due to its inconformity with the basic Strecker-type treatment. With regard to the chemical structures shown below, the common elements among all amino acids are generally located on the top/right hand side of the structures. The common elements are H_2N-C_αH-COOH. The R group of an α-amino acid is everything attached to the α-carbon, which is the first carbon in the chain, excepting the -COOH group. Note that extra carbon-hydrogen bonds are all hidden to improve visual acuity. When reading structures, recall that carbon always makes four bonds; any bonds not shown include an inherent H attachment. For example, each label 'C_α' shows only two/three bonds in the structures. Any bonds not shown attach H atoms to a C atom. Information contained within this table may be combined with the Strecker reaction information listed in Table 2.1 to create a list of complete Strecker-type reactions with molecular structures, as in Eq. (4.2).

Table 4.1: Example set of amino acids. Listed with their common names and molecular formulae, structure, side chains (-R group), and the common name and molecular formula of the reactant aldehyde used in Strecker synthesis of the amino acid.

Name	Amino Acid Structure	R group	Aldehyde
Glycine $C_2H_5NO_2$	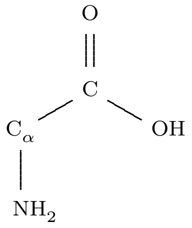	H	Formaldehyde CH_2O
Alanine $C_3H_7NO_2$	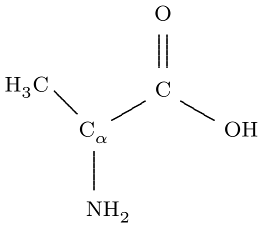	CH_3	Acetaldehyde C_2H_4O
Valine $C_5H_{11}NO_2$	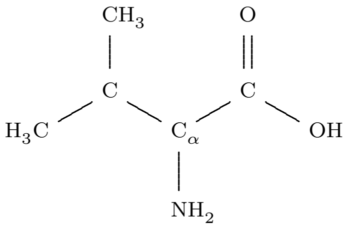	C_3H_7	Isobutyraldehyde C_4H_8O
Leucine $C_6H_{13}NO_2$	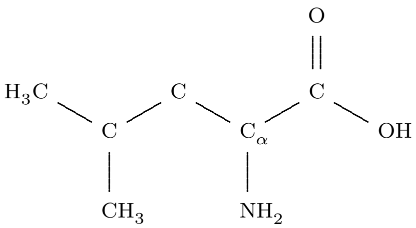	C_4H_9	3-methyl butanal $C_5H_{10}O$

Isoleucine $C_6H_{13}NO_2$	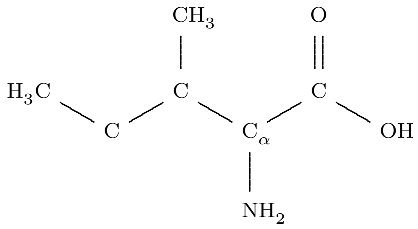	C_4H_9	2-methyl butanal $C_5H_{10}O$
Serine $C_3H_7NO_3$	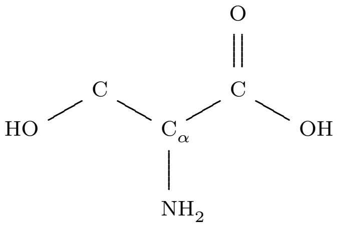	CH_3O	Glycolaldehyde $C_2H_4O_2$
Lysine $C_6H_{14}N_2O_2$	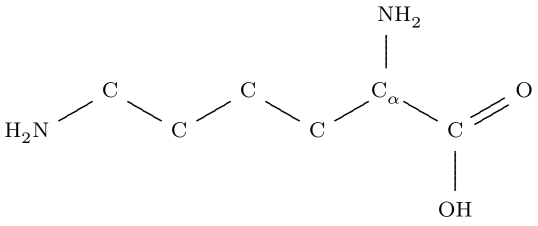	$C_4H_{10}N$	5-aminopentanal $C_5H_{11}NO$
Threonine $C_4H_9NO_3$	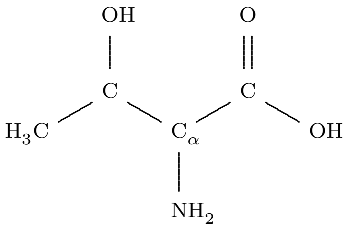	C_2H_5O	2-hydroxy-propanal $C_3H_6O_2$

Tyrosine $C_9H_{11}NO_3$	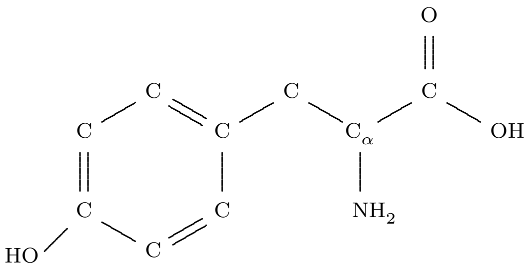	C_7H_7O	p-hydroxyphenyl-acetaldehyde $C_8H_8O_2$
Phenylalanine $C_9H_{11}NO_2$	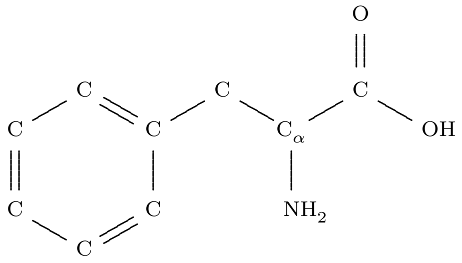	C_7H_7	phenyl-acetaldehyde C_8H_8O
Aspartic acid $C_4H_7NO_4$	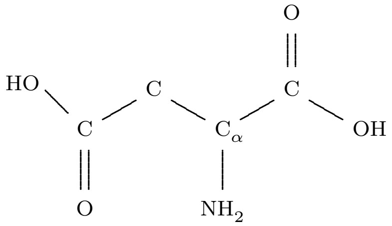	$C_2H_3O_2$	3-oxopropanoic acid $C_3H_4O_3$
Glutamic acid $C_5H_9NO_4$	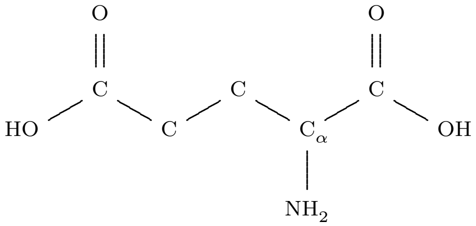	$C_3H_5O_2$	4-oxobutanoic acid $C_4H_6O_3$

4.3 Computational Methods

4.3.1 Gibbs Energies

We use a chemical thermodynamics database called CHNOSZ (version 0.9-9 (2013-01-01), authored by Jeffrey M. Dick, http://www.chnosz.net/) to obtain the Gibbs energies of formation for each species. CHNOSZ contains Gibbs energies for a wide variety of amino acids and aldehydes, in addition to water, ammonia, and hydrogen cyanide, all requisite species involved in the Strecker-type synthesis of amino acids in meteoritic parent bodies.

For each of the chemical species we are interested in (reactants and products), CHNOSZ contains a set of Gibbs formation energies (ΔG_f) which change with respect to both temperature and pressure, spanning 0°C to 350°C and 1 to 165 bar. We plot these values and perform a least squares regression. We model the resulting line of best fit as

$$G_f(T, P) = a + bT + cTln(T) + dT^2 + eT^3 + f/T + gP, \tag{4.3}$$

which provides us with the Gibbs coefficients a through g for each chemical species. Here, temperature must be in Kelvin and pressure in bars, and Gibbs energies return in Joules/mole. Eq. (4.3) is the requisite Gibbs energy function as required by our modeling software, ChemApp. Note the linear dependence of Gibbs energy on pressure; this term is negligible in contrast to the temperature dependence. To illustrate, Fig. 4.1 shows the dependence of Gibbs formation energy of alanine on pressure and temperature. We see the characteristic decrease in Gibbs energy with an increase in temperature. There is an obvious lack of dependence on pressure; three pressure curves are shown (100 bar, 150 bar, and 200 bar), and they vary by approximately a single kilojoule. Therefore, in our computations, we set the pressure to a static value of 100 bar. This value typifies the interiors of planetesimals, and is in fairly good agreement with values cited by various authors, including Dodd (1981), citetSchulte1995, Cohen & Coker (2000), and Warren (2012).

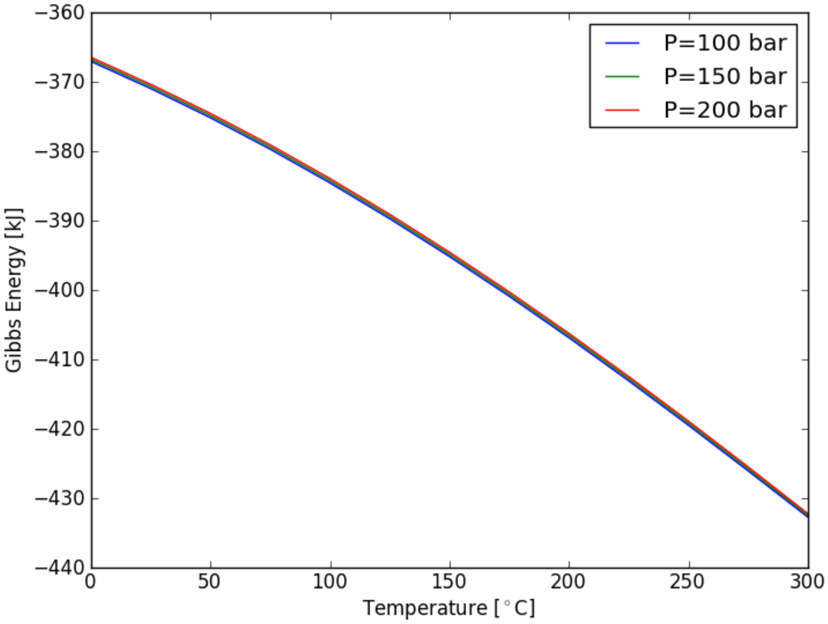

Figure 4.1: A example plot showing Gibbs formation energy dependence on pressure and temperature for the amino acid alanine. Temperature is allowed to vary from 0°C to 300°C. Three curves are shown, representing the Gibbs energies at pressures of 100 bar (blue curve), 150 bar (green curve), and 200 bar (red curve).

Our thermodynamic modeling software, ChemApp, requires the set of coefficients a through f for each chemical species, as from Eq. (4.3). CHNOSZ contains the data necessary to calculate the coefficients for each species in our system, with the exception of glycolaldehyde. All other species we have data for: initial reactants (water, hydrogen cyanide, and ammonia), the other five aldehydes (formaldehyde, acetaldehyde, butyraldehyde, propionaldehyde, and pentanaldehyde), and the 13 amino acids listed previously in Table 4.1. Glycolaldehyde was modeled as a mixture of acetaldehyde and acetic acid, as in Espinosa-García & Dóbé (2005). We use the associated Gibbs coefficients calculated in Emberson (2010).

In addition to species-specific Gibbs formation energies, each Strecker-type reaction we consider has some Gibbs free energy of reaction associated with it (ΔG_r). This ΔG_r may be computed at various temperature and pressure combinations using the Gibbs free energies of formation for each species. These values are related via the relationship

$$\Delta G_r = \Sigma G_f^{products} - \Sigma G_f^{reactants}. \tag{4.4}$$

The values of the Gibbs energies of formation change with temperature and pressure for each species according to Eq. (4.3).

It is important to note that the CHNOSZ database does not contain Gibbs formation energies on all the aldehydes listed in Table 4.1. We have specific coefficients for formaldehyde, acetaldehyde, and glycolaldehyde, which are the Strecker precursors for glycine, alanine, and serine, respectively. All additional aldehydes in Table 4.1 are modeled in ChemApp using the closest related aldehyde for which CHNOSZ contains data. The three substitute aldehydes we use are butyraldehyde, propionaldehyde, and pentanaldehyde. These three, combined with formaldehyde, acetaldehyde, and glycolaldehyde, provide us with a range of species which contain successive numbers of carbon atoms. The carbon count is the primary feature we use to match Strecker aldehydes with available species. For example, the Strecker aldehyde necessary to synthesize valine is isobutyraldehyde. CHNOSZ, however, does not contain an entry for isobutyraldehyde. We model the ChemApp synthesis of valine using butyraldehyde instead, as it is a close substitute and contains an identical number of each atom.

4.3.2 ChemApp

We use a modeling software called ChemApp (distributed by GTT Technologies, http://www.gtt-technologies.de/newsletter) to calculate a theoretical yield of amino acids. ChemApp is a computational subroutine database of chemical thermodynamics which functions assuming a thermodynamic equilibrium of the system in question. For these systems, Gibbs free energy is minimized for a closed chemical system in equilibrium. The model simulates reactions in meteoritic parent bodies at temperatures and pressures that should theoretically exist in parent body interiors as a consequence of radionuclide decay. We use internal conditions in agreement with modeled carbonaceous chondrite parent bodies in Travis & Schubert (2005). Thermal evolution models using radionuclide decay as a heat source have also been considered by Grimm & McSween Jr. (1989).

The functional structure of ChemApp is to read-in a data file containing all relevant information for a given trial, including thermochemical data for all species, temperatures, pressures, and initial organic concentrations. The basic components of every file are the series of basic elements involved in our research: carbon, hydrogen, nitrogen, and oxygen. Each chemical species we consider is defined as the addition of its elemental components. We build a program which reads in the data file, and define a set of ChemApp subroutines at specific internal conditions including temperature, pressure, and chemical composition. When called, the code performs a global minimization of the Gibbs free energy of the system based on the thermochemical input from the data file, which includes the Gibbs coefficients calculated from CHNOSZ data. Our system consists of the species listed in the collective reactions of Table 2.1. ChemApp does not treat each Strecker reaction individually; we manually restrict the pool of possible reactants and products. This pool, while based on and ideally including all species listed in Table 2.1, includes a few aldehyde substitutions, discussed in the previous section. E.g., a butyraldehyde substitution in place of isobutyraldehyde, involved in the synthesis of valine. These substitutions are necessary due to the unavailability of thermochemical data in CHNOSZ for some aldehyde species. The energy minimization is constrained by a mass balance system, and returns a set of molecular concentrations from the entire pool of reactants and products (one concentration value for each molecular species) which minimizes Gibbs free energy.

It is important to note that ChemApp has no inherent system to differentiate between molecular structures. Because each input species is broken down to its elemental form, two systems run with different molecular abundances, but identical elemental abundances, would return equivalent output concentrations. Additionally, our current treatment assumes an ideal solution for each reaction, and we force the chemistry to be in aqueous-phase only, assuming Strecker-type synthesis.

Our current system restricts the possible outcomes of ChemApp to include only those species in which we are interested. The equations laid out in Table 2.1 include every species we consider in our simple model. Sources of initial reactants as well as alternate Strecker products are not considered. For example, we do not include in ChemApp the formation pathways which lead to the formation of aldehydes; we assume some initial concentration. Also, we do not consider the hydroxy acids which Strecker synthesis may also produce. In this way, we have a limited set of initial species and a limited set of possible products. ChemApp reports the resulting abundances of only amino acids and initial reactants which minimize Gibbs energy, without considering alternate products which may detract from amino acid abundances.

In the case of our work in amino acid synthesis, ChemApp receives as input the data file containing the Gibbs coefficients a-f we calculated in Eq. (4.3) for all species considered in any given run. Due to the independence of Gibbs energy on pressure, our current treatment with ChemApp does not allow for a pressure-dependent term. We set the pressure to a value which typifies parent body interiors and hold it constant. Factors which may be varied between ChemApp runs are temperature and the initial concentrations of reactants.

4.3.3 Modeled Internal Conditions and the Onion Shell Model

Our current ChemApp treatment includes a set pressure at 100 bar and a temperature range from 150°C to 500°C in increments of 25°C. McSween Jr. et al. (2002) and Travis & Schubert (2005) model thermal evolution and internal heating processes in meteoritic parent bodies of carbonaceous chondrites. The temperatures we use in ChemApp are in agreement with Travis & Schubert (2005) for the parent bodies of less altered carbonaceous chondrites. The higher temperatures follow the temperatures classifications as laid out in numerous studies, including Sephton (2002), Weisberg et al. (2006), and Taylor (2011), who discuss the temperature ranges associated with different subclasses of carbonaceous chondrite. Our temperature ranges are also in agreement with peak alteration temperatures among carbonaceous chondrite petrologic groups in Weiss & Elkins-Tanton (2013).

We are primarily interested in the effects of varying temperature on amino acid synthesis. As discussed in Cobb & Pudritz (2013a), different subclasses of carbonaceous chondrite may be linked to different parent body formation conditions and therefore different amino acid abundance levels. We vary temperature in our ChemApp runs to recreate the temperature range across meteorite classifications.

Table 4.2 lists concentrations of organics we input into ChemApp. These values were selected based on data regarding concentrations of organics found in comets. The molecules for which we have concentration data include ammonia, hydrogen cyanide, formaldehyde, acetaldehyde, and glycolaldehyde, all normalized to percent water. These concentrations are in agreement with cometary data in Bockelee-Morvan et al. (2000), Ehrenfreund & Charnley (2000), Bockelee-Morvan et al. (2004), Crovisier et al. (2004), and Mumma & Charnley (2011), which are data from a variety of radio and infrared surveys.

There are a few additional aldehydes included in our model for which we have no available cometary data. These are butyraldehyde, propionaldehyde, and pentanaldehyde. In some cases, these organics have been identified and quantified in meteoritic samples. We extrapolate from meteoritic concentrations to obtain the initial concentrations used in our ChemApp model. See Jungclaus et al. (1976), Pizzarello & Holmes (2009), and Monroe & Pizzarello (2011) for meteoritic concentrations.

Table 4.2: Initial concentration of organics used in ChemApp model. Concentrations reported in percent normalized to water. Values are in agreement with Bockelee-Morvan et al. (2000), Ehrenfreund & Charnley (2000), Bockelee-Morvan et al. (2004), Crovisier et al. (2004), and Mumma & Charnley (2011) (for cometary data), and Jungclaus et al. (1976), Pizzarello & Holmes (2009), and Monroe & Pizzarello (2011) (for meteoritic data).

Species	Concentration
Water	100
Ammonia	0.7
Hydrogen cyanide	0.25
Formaldehyde	0.066
Acetaldehyde	0.04
Glycolaldehyde	0.04
Butyraldehyde	0.02
Propionaldehyde	0.012
Pentanaldehyde	0.012

Our current model treats a theoretical parent body as homogeneous; the initial concentrations of reactants are uniform throughout the parent body. This is likely not physically the case in a real parent body. McSween Jr. et al. (2002) and Weiss & Elkins-Tanton (2013, and references therein) review theory of meteorite parent body models. Planetesimals likely formed onion shell structures, with higher temperatures nearest the center, and concentric shells of material at progressively lower temperatures moving outwards toward the surface. They discuss the importance of fluid flow within chondrite parent bodies. Models in Young et al. (1999) and McSween Jr. et al. (2002) allow for the simultaneous existence of metamorphosed rock (near the high temperature center) and aqueously altered regions (toward the surface). Percentages of minerals available for alteration depend on the supply of flowing water. This idea of an onion shell structure is different than our current simplification of a uniform composition. In future work, we would like to expand our model to include water and chemical gradients in a theoretical parent body.

4.4 Results

4.4.1 Total Abundances

In Figure 8 of Cobb & Pudritz (2013a), (see Fig. 3.8) we plot average amino acid abundances in ppb across different carbonaceous chondrite subclasses. This allows us to identify graphically in which subclasses more amino acids are being synthesized. From this figure we identified the petrologic type 2 meteorites, both CM2 and CR2, as containing greater total abundances of amino acids than either the petrologic type 1 or type 3 meteorites.

We use the ChemApp model described above to compute the theoretical yield of amino acids in temperature and pressure conditions analogous to those in the interior of a meteoritic parent body. The results are shown in Fig. 4.2. In the same figure we include total observed concentrations of the different subclasses, indicated in blue, for comparison with our model.

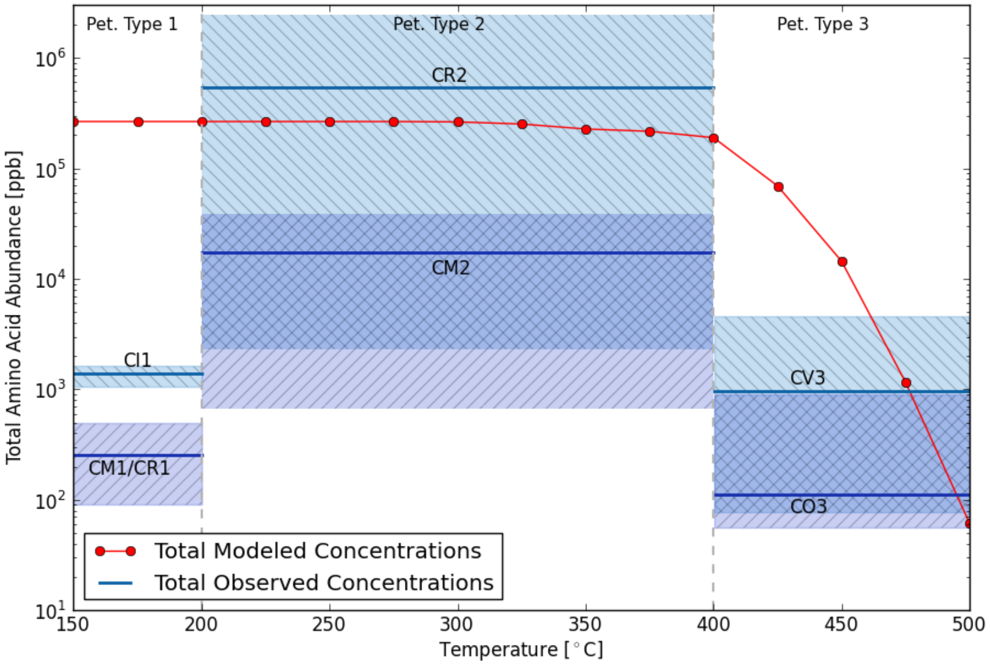

Figure 4.2: Theoretical total yield of amino acids in ppb. Each point on the red line represents the modeled total amino acid abundance at a given temperature, in intervals of 25°C. Amino acids included in the total concentration count are glycine, alanine, serine, aspartic acid, glutamic acid, valine, threonine, leucine, isoleucine, and lysine. Each blue horizontal line segment indicates the observed mean total amino acid concentration of a different carbonaceous chondrite subclass (CI1, CM1/CR1, CM2, CR2, CV3, and CO3), indicated by text adjacent to each line. The blue shaded boxes indicate the range in amino acid abundance for each subclass. The two dashed vertical lines separate the different petrologic types; type 1, associated with alteration temperatures 150°C to 200°C, type 2, associated with temperatures 200°C to 400°C, and type 3, associated with temperatures 400°C to 500°C.

In Fig. 4.2, data points from our model are shown by the red circles marked for intervals of 25°C for the temperature range 150°C to 500°C. Each data point represents the theoretical total amino acid yield. At each temperature point, the model reports some concentration value for each amino acid; we plot the total amino acid content. The modeled total amino acid yield at each temperature is a sum of the following amino acid abundances: glycine, alanine, serine, aspartic acid, glutamic acid, valine, threonine, leucine, isoleucine, and lysine.

Additionally, we plot observed total amino acid abundances as shaded blue regions. The upper and lower boundaries of each shaded blue region enclose the range of observed abundances for each subclass of meteorite (CI1, CM/CR1, CR2, CM2, CV3, and CO3). In each shaded region, a darker blue line segment indicates the mean value for that subclass, with the subclass label printed adjacent to the appropriate line.

Among subclasses CM2 and CR2, there is significant overlap in observed abundances; the minimum total abundance among CR2-types is lower than the maximum total abundance among CM2-types. There is similar overlap seen in the CV3- and CO3-types. Additionally, there are two grey vertical dashed lines indicating the temperatures which separate the petrologic types 1, 2, and 3. 150°C marks the boundary between types 1 and 2, and 450°C indicates the boundary between types 2 and 3.

We observe good agreement between our thermodynamic model and observed amino acid concentrations at temperatures higher than 200°C. Theoretical concentrations remain in the 10^5 ppb range throughout the entire range of temperatures associated with petrologic type 2 chondrites. This value, $\sim 3 * 10^5$ ppb, lies between the total CM2 concentration, $\sim 2*10^4$ ppb, and the total CR2 concentration, $\sim 5*10^5$ ppb.

There is also good agreement at the turnover point at temperatures just higher than 400°C. The classification scheme laid out in Fig. 3.1 shows the type 2-type 3 cutoff near to 400°C, and observed amino acid concentrations in meteorites mirror this. Our model shows a sharp decline in total amino acid concentrations when we move from the CM2 and CR2 meteorites into the petrologic type 3 meteorites, CV3 and CO3. Concentrations shift from 10^5 ppb to 10^4 ppb within 50°C of the turnover point, and reach levels as low as $\sim 6 * 10^1$ ppb within another 50°C change, around 500°C. These theoretical yields match very well the observed concentrations associated with petrologic type 3 meteorites. Total CV3 concentrations are near 10^3 ppb, and total CO3 value are approximately 10^2 ppb.

We see an exception to the generally good agreement between theory and observation near the cooler end of the temperature spectrum. Temperatures 150°C to 200°C are marked by meteorite falls which contain total amino acid concentrations lower by several orders of magnitude than the neighboring 200°C to 400°C range. These cooler temperatures are associated with petrologic type 1 meteorites, which are primarily the CI subclass, with a few CM/CR exceptions. Type 1 concentrations are observed to be near 10^3 ppb (for CI1 chondrites) and $2 * 10^2$ ppb (for CM/CR1 chondrites). Our ChemApp model does not recreate this low abundance pattern.

There could be numerous reasons for this discrepancy. Our model takes into account only the thermodynamics of a system in question as it is presently defined in ChemApp, with temperature, pressure, and chemical composition. Clearly thermodynamics explains well the second turnover point, around 400°C, with the temperatures, pressures, and initial organic abundances used in our model. That ChemApp does not recreate well the first turnover point, moving from 150°C to 200°C, indicates that this temperature range may be dominated by thermodynamic theory defined differently than its current parameters. A possible reason behind the lack in observed total amino acid abundance at cooler temperatures might have something to do with total water content; perhaps there is not enough liquid water in the interior of a parent body to create as many amino acids. Also, initial concentrations of organics might be different from what is currently defined in our model.

A significant factor behind this deviation is likely due to the initial uniform composition assumed by ChemApp. As discussed in Young et al. (1999), McSween Jr. et al. (2002), Gail et al. (2013), and Weiss & Elkins-Tanton (2013), parent bodies likely initially took on onion shell structures. The CI chondrites express significant water content and levels of aqueous alteration, but minimal abundance of amino acids. The origination point for CI-type meteorites might have been from different regions of the parent body, with different levels of initial organic reactants than were available for the CM and CR-types. ChemApp is only able to assume a uniform composition, which does not take into account this shell model for levels of available organics. This theory well explains the lack of amino acids in petrologic type 1 meteorites. Further calculations investigating the lack of amino acid presence at these temperatures are in progress.

4.4.2 Relative Frequencies

In addition to modeling the total amino acid yield, we investigate the relative frequencies of amino acids. Figure 9 in Cobb & Pudritz (2013a) (Fig. 3.9) shows the relative frequencies of 13 amino acids relative to glycine in the CM2 subclass. As the CM2 and CR2 subclasses contain the greatest concentrations and variety of amino acids, we selected one of these groups as a starting place for thermodynamic modeling.

We use the same ChemApp model used for calculating theoretical total amino acid yield to calculate relative frequencies. Our results are shown in Fig. 4.3. Theoretical frequencies are shown as red bars in the histogram. In the same figure, we include the frequencies observed in the CM2 subclass, shown by the blue bars in the histogram.

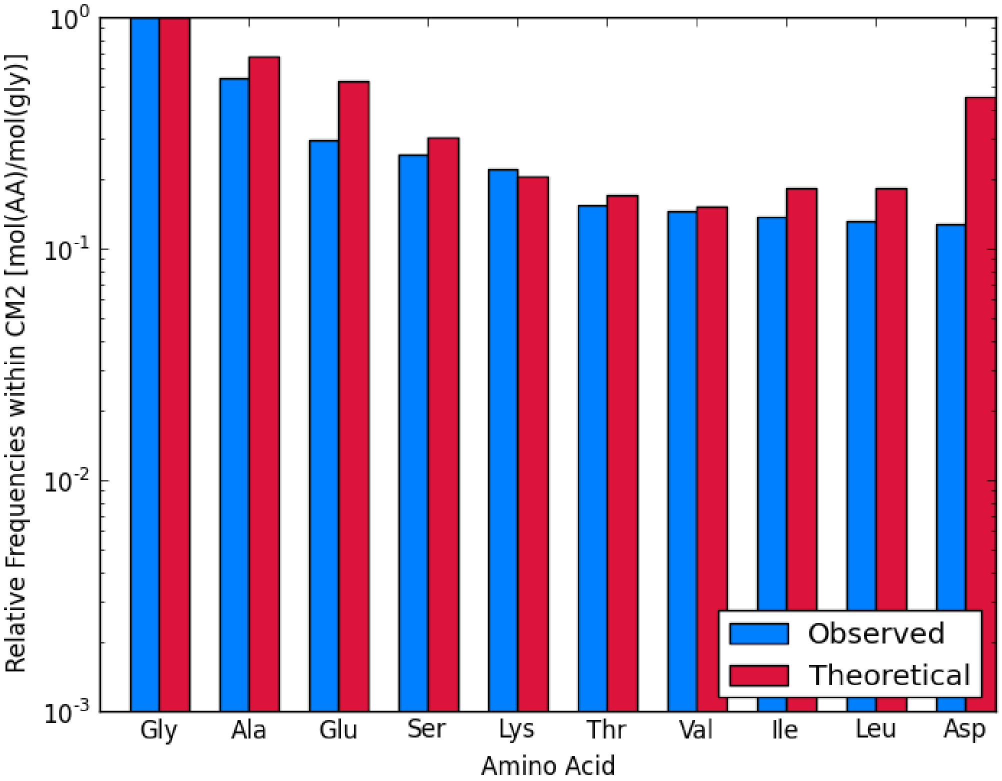

Figure 4.3: Relative frequencies of amino acids. Abundances of 10 amino acids are shown relative to glycine, reported in moles of amino acid/moles of glycine. Theoretical frequencies are indicated by the red histogram bars. Blue histogram bars indicate observed frequencies in the CM2 subclass. Amino acids include glycine (gly), alanine (ala), glutamic acid (glu), serine (ser), lysine (lys), threonine (thr), valine (val), isoleucine (ile), leucine (leu), and aspartic acid (asp), arranged in order of decreasing observed frequency.

The amino acid frequencies shown above correspond to a temperature of 200°C, selected arbitrarily as a representative temperature of the CM subclass. Each red column in the histogram represents a calculated frequency of an amino acid, normalized to glycine. The 10 amino acids included are glycine, alanine, glutamic acid, serine, lysine, threonine, valine, isoleucine, leucine, and aspartic acid. In addition to the theoretical frequencies, we include the observed relative frequencies of the same amino acids, shown in blue, for comparison. The amino acids have been arranged in order of decreasing observed frequency.

In general, we observe excellent agreement between our thermodynamic model and observed frequencies. All observed versus theoretical frequencies per amino acid match to well within an order of magnitude. Almost all, with one exception, match to within ~ 0.2, the single exception being aspartic acid, which matches to within ~ 0.3.

In almost every case, as well, the theoretical frequencies are greater than the observed frequencies, which we would expect. Our model is based on an ideal chemical system in equilibrium, and takes into account formation processes only. It does not consider degradation processes, which would occur in observed systems. The single exception to this is lysine, in which the observed concentration is slightly greater than the theoretical frequency.

We remind the reader that our current model has a limited number of aldehydes, as CHNOSZ does not contain the requisite data for every precursor aldehyde. Glycine, alanine, and serine are the only three amino acids which are modeled with their structurally correct aldehyde (those being formaldehyde, acetaldehyde, and glycolaldehyde, respectively), and we see a corresponding excellent agreement in relative frequencies between observation and theory for these three. The other seven amino acids are modeled with aldehydes which are close substitutes for the actual Strecker precursors. Valine and glutamic acid are modeled using butyraldehyde, threonine and aspartic acid are modeled using propionaldehyde, and leucine, isoleucine, and lysine are modeled using pentanaldehyde. This is one possible explanation for the discrepancy between observed frequencies and theoretical frequencies, especially among aspartic acid and lysine.

4.5 Conclusions

In general, we see good agreement between our thermodynamic computations and observed amino acid abundances. Thermodynamics well explains both the total amino acid concentrations and the relative frequencies we see in the CM2 subclass.

Observed total amino acid concentrations in the temperature range 200°C to 400°C vary between the total CM2 concentration, $\sim 2 * 10^4$, and the total CR2 concentrations, $\sim 5 * 10^5$ ppb. Output from ChemApp remains near a concentration value of $\sim 10^5$ ppb.

There is a sharp turnover point which occurs just after 400°C, when we move from petrologic type 2 chondrites into the petrologic type 3 range, associated with temperatures 400°C to 600°C. Observed abundances lay between the CO3 and CV3 total concentrations, $\sim 10^2$ ppb and $\sim 10^3$ ppb, respectively. Our model recreates this turnover point. Within 100°C, total concentrations decrease from $\sim 10^5$ ppb to $\sim 10^2$ ppb.

There is a second turnover point in the observed amino acid abundance levels, which occurs at the cooler end of the temperature spectrum. Among petrologic type 1 meteorites, associated with temperatures 150°C to 200°C, we do not observe the high levels of amino acids seen in our model. Observationally speaking, concentrations in this temperature range should remain near to $\sim 2 * 10^2 - 10^3$ ppb, associated with CM/CR1 and CI1 meteorites, respectively. Clearly, while thermodynamic theory as it is presently defined in ChemApp holds for the synthesis of amino acids in the temperature range 200°C to 500°C, there are additional factors which must be considered at lower temperatures. These factors may include, but are not limited to, overall water levels, a decrease in aldehyde content or concentrations of other initial reactants, and the possibility of amino acid degradation near the surfaces of meteoritic parent bodies. Our model explores the variation of amino acid abundances and frequencies as a consequence of thermal variation in parent bodies at a typical constant pressure and assumed uniform initial chemical composition.

Our model matches well for subclasses CM, CR, CV, and CO; abundance levels are well recreated assuming a simplified uniform composition and a single pressure. The petrologic type 1 meteorites, primarily CI-type meteorites, may originate from different regions of their parent bodies. There are no inhomogeneities taken into account in our current model in the fashion of an onion shell model.

Our model also accounts for the relative frequency pattern in amino acids among CM2 chondrites. The observed frequencies of 10 amino acids are shown relative to glycine, and compared to their theoretical yield. The observed and theoretical frequencies match well, to within an order of magnitude in all cases for a selected temperature of 200°C. The greatest deviation between theory and observation occurs for the amino acid aspartic acid, which still matches observation to within ~ 0.3 accuracy. In addition, in almost every case, the theoretical yields are higher than the observed frequencies, which is as we would expect. ChemApp assumes an ideal equilibrium state after synthesis of amino acids; it in no way accounts for the degradation processes which would surely be taking place in planetesimals. This explains why observed frequencies are lower than their theoretical counterparts. The single exception to this is the amino acid lysine. It is likely that our necessarily rudimentary treatment of substitute aldehydes has caused minor theoretical deviations from accuracy.

Chapter 5

Conclusions

This research investigates the abundances and relative frequencies of proteinogenic α-amino acids in carbonaceous chondrites, both in observed meteorite falls and in thermodynamic theory.

We collected and collated a wide variety of amino acid abundance data from a spectrum of meteorite types. The class of meteorite called carbonaceous chondrite is known for its high content of both water and organic material, including amino acids. Among carbonaceous chondrites, there is a range of subclasses, labeled CI, CM, CR, CV, CO, CH, CB, and CK, the first five of which we investigate in this thesis. The subclasses are organized according to bulk mineralogical composition and petrologic type, which varies from 1 to 6 and indicates the degree to which the interior of the meteorite has been altered. Petrologic type 1 meteorites (mostly CI chondrites, with a few CM and CR exceptions) have undergone the greatest degrees of aqueous alteration, an internal chemical process which occurs when liquid water and organic material are present, creating amino acids. However, we do not observe a peak in amino acid abundances for chondrites of this type. Petrologic type 2 meteorites (CM and CR-types) contain the greatest abundance and variety of amino acids. Petrologic type 3 meteorites have undergone relatively little to no degrees of alteration, and we see a correspondingly low amino acid content. Petrologic types 4 through 6, not investigated in this research, are characterized by a lack of water content and higher temperatures.

Primary results from the literature review are listed below:

- Type 1 meteorites, associated with the lowest alteration temperature range of 150°C to 200°C, show an average total amino acid concentration of $\sim 10^2$ parts-per-billion (ppb). Despite corresponding to the greatest degrees of internal aqueous alteration, which synthesizes organic material, we do not observe a peak in amino acid concentration.
- The 200°C to 400°C range corresponds to the petrologic type 2 chondrites, primarily in specimens of subclass CM2 and CR2. They show the greatest concentration ($\sim 10^5$ ppb) and variety of amino acids of all the carbonaceous chondrite subclasses.
- CO and CV meteorites are all petrologic type 3, associated with alteration temperatures 400°C to 600°C. These specimens are relatively unaltered from the time of their initial formation, and have a low amino acid content, $\sim 10^2$ ppb.
- As unveiled by this extensive literature review, we identify an optimal temperature range of 200°C to 400°C with regard to amino acid synthesis.
- Within this optimal temperature range, we compute the frequencies of amino acids relative to glycine. It should be possible to model computationally this pattern in relative frequencies via thermodynamic theory.

Given this extensive insight into observed amino acid concentrations and relative frequencies, we moved into the second phase of this research. We investigated computationally if temperature and aqueous conditions within a meteoritic parent body could account for total abundances and relative frequencies of amino acids using principles of thermodynamics.

As the thermodynamic modeling of amino acid synthesis has, to the best of our knowledge, not been attempted in such a way, we restricted our model to include only proteinogenic α-amino acids synthesized via a particular series of chemical reactions known as Strecker synthesis reactions. Strecker synthesis involves the reaction between an aldehyde molecule, ammonia, hydrogen cyanide, and water to create an α-amino acid. Altering the Strecker aldehyde precursor results in the synthesis of a different amino acid. We defined one Strecker-type reaction for each of 17 proteinogenic amino acids encoded for by our genetic code. Each chemical species in our set of Strecker reactions, including the variety of aldehydes, amino acids, and the reactants common to all reactions (water, ammonia, and hydrogen cyanide), has some Gibbs energy of formation associated with it. The Gibbs formation energies exist in thermochemical database called CHNOSZ. Given a set of Gibbs formation energies for each species, which vary independently according primarily to temperature and secondarily to pressure, we calculate the Gibbs energy of reaction for each of the Strecker-type reactions.

Our thermodynamic modeling software, called ChemApp, takes this Gibbs energy information as input, as well as a set of initial reactant concentrations which we extrapolated from cometary and/or meteoritic concentration values. The output from ChemApp is a set of amino acid concentrations, the synthesis of which minimizes the Gibbs free energy of the system and assumes a final chemical equilibrium.

The results of our modeling well match the abundance patterns seen in observation. We matched theory to observation twice-over, once in recreating the total amino acid concentration plot, measured in ppb, and again in the relative frequency plot, reported in moles of amino acid, normalized to glycine.

The theoretical total amino acid concentrations remain around $\sim 10^5$ ppb in the 200°C to 400°C range. This is in good agreement with observed concentrations seen in CM2 and CR2 chondrites. Total CM2 concentrations remain consistently around the $\sim 2 * 10^4$ ppb, and CR2 total concentrations are near $\sim 5 * 10^5$ ppb. Above 400°C, observed concentrations drop off sharply. This turnover point corresponds to the type 3 meteorites, CV3 and CO3, which have total concentrations of $\sim 10^3$ ppb and $\sim 10^2$ ppb, respectively. We see the same sharp decline in amino acid abundances in our model. Between 400°C and 500°C, total concentrations decrease from $\sim 10^5$ ppb to $\sim 10^2$ ppb.

Our model does not fit the total abundance plot between 150°C and 200°C. According to observed abundances, this temperature range should be associated with petrologic type 1 chondrites and a marked decrease in total concentrations. Observed CM/CR1 and CI1 total concentrations are $\sim 2 * 10^2 - 10^3$ ppb. We do not recreate this pattern using our current thermal model; simulated values remain high, near 10^5 ppb. There are several possible explanations for this, including a decrease in overall water content, which would limit the degrees to which Strecker synthesis could take place. Also, it is possible the levels of initial reactants, especially the aldehyde precursors, are different in the petrologic type 1 meteoritic parent body than for other parent bodies. Perhaps petrologic type 1 meteorites originate from layers of their parent bodies which limit the levels of all reactants, water, and lower the temperature, all factors which play a role in amino acid synthesis. This is in accordance with the onion shell model for parent body structures, which theorizes different shell depths as origins for various chondrite subclasses. The shell model implies an inherently inhomogeneous composition with regard to water content and levels of organics. Our current ChemApp model is restricted in its consideration of parent bodies, and currently treats parent bodies as being completely uniform in nature.

In addition to the total abundance curve, we use our computational model to recreate the pattern of relative frequencies of amino acids in the CM2 subclass. Thermodynamics also predicts this pattern well. In all cases, modeled values and observed frequencies for each amino acid within the CM2 subclass match to well within an order of magnitude, and only one case (aspartic acid) matches with less than ~ 0.2 accuracy. Also, with a single exception (lysine), theoretical frequencies are greater than observed frequencies, which we would expect due to the nature of our model. ChemApp considers only the synthesis of amino acids; it does not take into account any degradation processes, which would surely be occurring inside a parent body.

We know now that amino acid synthesis in meteoritic parent bodies is may be well explained using principles of thermodynamics. Our current studies are limited to meteorites originating within our solar system, but given that the synthesis of biomolecules is governed by universal principles, it is likely that biomolecules both form and are delivered to planetary systems far outside our solar neighborhood. It is also likely that distant worlds are being seeded with the *same* biomolecules; amino acids, sugars, nucleobases, etc. Evolution and natural selection eventually took over in determining the nature of life on Earth, but given the same starting chance and a location within a habitable zone, perhaps distant exoplanets have undergone similar evolutionary processes. The universe is big; it's vast and complicated and ridiculous. Perhaps we are not as alone in the universe as we once supposed.

Appendix A

Meteorite List

Type	Meteorite	Sample number, if applicable	Reference(s)
CI1	Ivuna	N.A.	Botta et al. (2002)
CI1	Orgueil	N.A.	Botta et al. (2002); Glavin et al. (2011)
CM1	Meteorite Hills	MET 01070	Glavin et al. (2011)
CM1	Scott Glacier	SCO 06043	Glavin et al. (2011)
CM2	Cold Bokkeveld	N.A.	Kaplan et al. (1963)
CM2	Mighei	N.A.	Kaplan et al. (1963); Botta et al. (2002)
CM2	Murray	N.A.	Kaplan et al. (1963); Botta et al. (2002)
CM2	Yamato	Yamato 791198	Shimoyama et al. (1985)
CM2	Nogoya	N.A.	Botta et al. (2002)
CM2	Essebi	N.A.	Botta et al. (2002)
CM2	Allan Hills	ALH 83100	Glavin et al. (2006)
CM2	Murchison	N.A.	Botta et al. (2002)
CM2	Murchison	Field Museum	Cronin & Pizzarello (1983)
CM2	Murchison	AZ State Univ.	Cronin & Pizzarello (1983)
CM2	Murchison	Smithsonian	Cronin & Pizzarello (1983)
CM2	Murchison	USNM 5453	Glavin et al. (2011)
CM2	Murchison	USNM 6650	Glavin et al. (2006)
CM2	Lonewolf Nunataks	LON 94102	Glavin et al. (2011)
CM2	Lewis Cliffs	LEW 90500	Glavin et al. (2006)
CM2	Bells	N.A.	Monroe & Pizzarello (2011)
CR2	Renazzo	N.A.	Botta et al. (2002)
CR2	Grosvenor Mountains	GRO 95577	Martins et al. (2007a); Glavin et al. (2011)

CR2	Elephant Moraine	EET 92042	Martins et al. (2007a); Glavin et al. (2011)
CR2	Graves Nunataks	GRA 95229	Martins et al. (2007a); Pizzarello (2009)
CR2	Lapaz	LAP 02342	Pizzarello (2009)
CR2	Shişr	Shişr 033	Martins et al. (2007b)
CR2	Queen Alexandra Range	QUE 99177	Glavin et al. (2011)
CV3	Allan Hills	ALH 84028	Burton et al. (2012)
CV3	Elephant Moraine	EET 96026	Burton et al. (2012)
CV3	LaPaz Icefield	LAP 02206	Burton et al. (2012)
CV3	Larkman Nunatak	LAR 06317	Burton et al. (2012)
CV3	Graves Nunataks	GRA 06101	Burton et al. (2012)
CV3	Allende	N.A.	Botta et al. (2002); Burton et al. (2012)
CO3	Miller Range	MIL 05013	Burton et al. (2012)
CO3	Dominion Range	DOM 08006	Burton et al. (2012)
CO3	Allan Hills	ALHA 77307	Burton et al. (2012)
CO3	Colony	N.A.	Chan et al. (2012)
CO3	Ornans	N.A.	Chan et al. (2012)

Appendix B

ChemApp Manual–A User's Guide

B. To Start a New Trial Run

Within a folder for any given amino acid, there are several files. To begin a new trial run, with different species, or to change temperature, or what have you, there are a few files we need to change. These are: ideal.f, streckerthermo.dat, and inputtemp. ideal.f is the main program that runs for each amino acid. This is the file you call in the terminal when you want to run ChemApp. To begin a new trial, first simply copy an existing (and working) run which already exists. The alteration steps to change it to a new run follow below.

B.1 Create a new AA folder that runs in ChemApp:

Select and copy an preexisting amino acid folder (for example, the Glycine folder, labeled 'G'). This will effectively start your new folder off with all of the necessary information, and all you need to do is alter the information contained within ideal.f and streckerthermo.dat to apply to the amino acid you are currently working on.

B.2 Alter ideal.f and streckerthermo.dat files

B.2.1 To the streckerthermo.dat file, do the following:

Each of the species in the new reaction you are considering will have an entry that looks like this:

```
C2H4O
1      1      2.0      4.0      0.0      1.0
513.15000      -302966.32      5010.8270      -863.77849      1.4508095
-.5721957E-03      6689820.7
```

In each entry, as above, the first line of text tells us the species, in this case, ethanal/acetaldehyde. Change this to match your species. The second line of text contains 6 numbers. Leave the first two numbers, the 1 and 1, alone. The last four numbers represent the number of molecules of carbon, hydrogen, nitrogen, and oxygen in your species. For ethanal, there are 2.0 carbon, 4.0 hydrogen, 0.0 nitrogen, and 1.0 oxygen molecules. The third and fourth lines are where the Gibbs coefficients go for the species being considered. The first number, the 523.15000, is the temperature, and should be left alone. The Gibbs coefficients come from our table of coefficients, computed using our coefficient linear regression code matching Eq. (4.3). The table of applicable values are located in Table 2.4. Replace the old coefficients with the coefficients of whatever species you are now considering. Ensure the format remains consistent.

Additionally, the second line of the streckerthermo.dat file needs to have a single number changed. The second line should read something like

```
4 2 0 x 0
```

The second to last number (labeled as 'x' in this example) needs to match the number of species in your system. For example, if you are running a trial which produces only glycine, you will have 5 species: water, HCN, ammonia, formaldehyde, and glycine.

B.2.2 To the ideal.f file, do the following:

Somewhere around lines 97 and 98 of ideal.f are two lines of code which read “Double Precision Conc(22)” and “Double Precision $d_{arr}(5)$”. The concentration array is telling us there are 22 species being considered in all of our ChemApp work. This number should not change (unless, several years from now, you are increasing the total number of considered species). The d_{arr} array is telling us there are 5 species being considered in the reaction you are currently working on. Again, this is applicable in the glycine-only example. This number should include all reactants and products in you reaction, and should match the number of species listed on the second line of the updated streckerthermo.dat file.

Near to line 375 in the ideal.f code will be a large, obvious section commented out with “Concentrations” numerous times. This section is where we list the species we want ChemApp to consider for the current reaction. There should be as many species listed here as were in the d_{arr} array and as were listed in streckerthermo.dat. Each species entry will look something like this:

```
Liquid Water (H2O)
CALL TQSETC(’ia ’, 1, 1, Conc(1),NUMCON,NOERR)
IF (NOERR .NE. 0) CALL CABORT(348,’TQSETC’,NOERR)
```

On the ’CALL’ line above, the second and third entries in the parentheses are little gold numbers. The first number should always be 1. The second number will change for each species and reaction. These numbers, for each species, need to match the order of species entered into streckerthermo.dat. For example, H2O has numbers 1 and 1. The 1 tells us that H2O was the first species listed in the corresponding streckerthermo.dat file. The fourth entry in the parentheses on the ’CALL’ line reads ’Conc(number)’. This number tells ChemApp where to take the initial value concentration from. These numbers must be changed to match the order of the species listed in species.dat. The species.dat file is located in the home directory where each individual amino acid folder is located (for example, my folder called "ones"). For example, in the species.dat file, alanine is the ninth species. So the alanine entry in ideal.f has a concentration array value of 'Conc(9)'.

Additionally, directly above the 'Concentrations' block of code are a couple of lines creating a dummy file of the appropriate size which replaces the original concentration values with the new ones being generated. In the line

DO dum=1, 22,

the second number again needs to match the universal number of species we are considering (22). (Not in this run specifically, but in the total ChemApp universe for this research.) The number will match the one listed in "Double Precision Conc(22)" near line 98 of this code.

Somewhere near line 515 is the last section of important information you need to change. This section will be commented out with large "Important!" statements. This section of code is responsible for taking the initial concentration values from concentration.dat, using them in ChemApp, and reporting them by putting them back into our output array (equilout). Again, there should be as many entries here as you have species considered in the reaction (should match the d_{arr} number). Each line looks like this:
Conc(9)=$d_{arr}(5)$

The Conc() number needs to be changed to match the order of the species listed in species.dat. The d_{arr} number needs to be changed to match the order of the species listed in streckerthermo.dat. For example, alanine is the ninth species listed in the species.dat file, so Conc(9), and the it is the fifth species listed in the streckerthermo.dat file, so $d_{arr}(5)$.

Again, we see the "DO dum=1, 22" command, and that second number should be the universal number of species we changed twice already.

B.3 Additional small changes

There are a few more small changes to various files which must be made before a new trial is ready to run. Now that streckerthermo.dat and ideal.f have been suitable modified for a new reaction, we are nearly ready to run ChemApp.

- ideal.f and streckerthermo.dat will be located in the same folder, likely called the name of the amino acid being considered. If you navigate up one directory, you should be located in a folder titled something similar (most of mine are also called after the amino acid in question). In this folder, there should be a concentration.dat file, a species.dat file, and an inputtemp file (along with the subfolder containing ideal.f and streckerthermo.dat).

- species.dat lists the universal list of species we use in ChemApp. In each run, you will pick and choose which species to consider, and change the corresponding lines of code in ideal.f (discussed above).

- concentration.dat contains the initial concentrations of organics discussed in Table 2.2. This file is overwritten with every run, and will need to be replaced before beginning a new trial. I keep a default concentration file on my desktop, which may be easily copied into the necessary folder for each new run.

- The file called inputtemp is where the temperatures may be changed. In inputtemp, the first block of code should read something like:

```
 Number Temp Points[K]: 8
    273.16
    323.15
    373.15
    423.15
    473.15
    523.15
    573.15
    623.15
Constant Pressure[bar]: 8.679
```

Each line with a number is a temperature, and ChemApp will perform a Gibbs minimization at each of these temperatures in every run. These temperatures may be changed. It should currently be set at 273 to 623 K (0°C to 350°C) in intervals of 50 K. This temperature range is in accordance with Travis & Schubert (2005) and the limitations of CHNOSZ, which cut off at 350°C. The additional blocks of code below this in inputtemp are for additional iterations. I do not consider multiple iterations in a single run, so tend to ignore these. Also, should you ever adapt our code to consider pressure changes, this is where that information would go (i.e., the line reading 'Constant Pressure[bar]: 8.679').

B.4 Ready to run

If everything is present, altered, and saved, open up a terminal (I prefer Konsole), change the directory to be the amino acid folder you are considering (G, for example), enter the 'make' command, enter, then the 'ideal' command, enter. The only real output file we are interested in is equilout, located in the subfolder containing streckthermo.dat and ideal.f. These concentrations will have changed according to the minimization of the Gibbs free energies for the species we input.

The reactants should be mostly used up (especially the aldehyde used and the hydrogen cyanide), and there will be a corresponding increase in the concentration(s) of the amino acid(s) of choice. Equilout reports separate blocks of code, one each for each of the temperatures in inputtemp. There are two columns of numbers, labeled appropriately. One column is concentration in percent normalized to water (comparable to the initial concentrations which were used as input), and a second column in molarity, which becomes relevant when we want to compare the computed concentrations to observations.

Finally, the reader is encouraged to refer to the official documentation for ChemApp. See GTT Technologies (2003).

Bibliography

Alexander, C. M. 2011, in IAU Symposium, Vol. 280, The Molecular Universe, ed. J. Cernicharo & R. Bachiller, 288–301

Bockelee-Morvan, D., Crovisier, J., Mumma, M. J., & Weaver, H. A. 2004, in Comets II, ed. M. Festou, H. U. Keller & H. A. Weaver, 391–423

Bockelee-Morvan, D., Lis, D. C., Wink, J. E., Despois, J. E., Crovisier, J., Bachiller, R., Benford, D. J., Biver, N., Colom, P., Davies, J. K., Gerard, E., Germain, B., Houde, M., Mehringer, D., Moreno, R., Paubert, G., Phillips, T. G., & Rauer, H. 2000, A&A, 353, 1101

Botta, O. 2005, in IAU Symposium, Vol. 231, Astrochemistry: Recent Successes and Current Challenges, ed. D. C. Lis, G. A. Blake, & E. Herbst, 479–488

Botta, O. & Bada, J. L. 2002, Surv. Geophys., 23, 411

Botta, O., Glavin, D. P., Kminek, G., & Bada, J. L. 2002, Orig. Life Evol. Biosph., 32, 143

Burton, A. S., Elsila, J. E., Callahan, M. P., Martin, M. G., Glavin, D. P., Johnson, N. M., & Dworkin, J. P. 2012, Meteorit. Planet. Sci., 47, 374

Burton, A. S., Elsila, J. E., Hein, J. E., Glavin, D. P., & Dworkin, J. P. 2013, Meteorit. Planet. Sci., 48, 390

Chan, H. S., Martins, Z., & Sephton, M. A. 2012, Meteorit. Planet. Sci., 47, 1502

Chyba, C. & Sagan, C. 1992, Nature, 355, 125

Chyba, C. & Sagan, C. 1997, in Comets and the Origin and Evolution of Life, ed. Thomas, P. J., Chyba, C. F. & McKay, C. P., 147–173

Chyba, C., Thomas, P. J., Brookshaw, L., & Sagan, C. 1990, Science, 249, 366

Cobb, A. K. & Pudritz, R. E. 2013a, in prep.

Cohen, B. A. & Coker, R. F. 2000, Icarus, 145, 369

Cronin, J. R. & Pizzarello, S. 1983, Adv. Space Res., 3, 5

Crovisier, J., Bockelee-Morvan, D., Colom, P., Biver, N., Despois, D., & Lis, D. C. 2004, A&A, 418, 1141

Dodd, R. T. 1981, in Meteorites, a Petrologic-chemical Synthesis (Cambridge University Press), 309–326

Ehrenfreund, P. & Charnley, S. B. 2000, ARA&A, 38, 427

Ehrenfreund, P., Glavin, D. P., Botta, O., Cooper, G., & Bada, J. L. 2001, PNAS, 98, 2138

Ehrenfreund, P., Irvine, W., Becker, L., Blank, J., Brucato, J. R., Colangeli, L., Derenne, S., Despois, D., Dutrey, A., Fraaije, H., Lazcano, A., Owen, T., & Robert, F. 2002, Rep. Prog. Phys., 65, 1427

Elsila, J. E., Dworkin, J. P., Bernstein, M. P., Martin, M. P., & Sandford, S. A. 2007, ApJ, 660, 911

Emberson, J. 2010, Amino Acid Synthesis in Meteoritic Parent Bodies, Undergraduate Honors Thesis, McMaster University

Engel, M. H. & Perry, R. S. 2008, in Proc. SPIE, Vol. 7097, Instruments, Methods, and Missions for Astrobiology

Espinosa-García, J. & Dóbé, S. 2005, J. Mol. Struct. THEOCHEM, 713, 119

Fernandes, D. 2013, Abiotic Amino Acid Synthesis in the Early Solar System, Undergraduate Honors Thesis, McMaster University

Gaidos, E. & Selsis, F. 2007, in Protostars and Planets V, ed. B. Reipurth, D. Jewitt, & K. Keil, Proc. SPIE (University of Arizona Press), 929–944

Gail, H. P., Breuer, D., Spohn, T., Kleine, T., & Trieloff, M. 2013, Protostars & Planets VI Conference, Based on PPVI Conference Presentation in Heidelberg, Germany. PPVI book in prep.

Glavin, D. P., Callahan, M. P., Dworkin, J. P., & Elsila, J. E. 2011, Meteorit. Planet. Sci., 45, 1948

Glavin, D. P. & Dworkin, J. P. 2009, PNAS, 106, 5487

Glavin, D. P., Dworkin, J. P., Aubrey, A., Botta, O., Doty III, J. H., Martins, Z., & Bada, J. L. 2006, Meteorit. Planet. Sci., 41, 889

Grimm, R. E. & McSween Jr., H. Y. 1989, Icarus, 82, 244

GTT Technologies. 2003, ChemApp Programmer's Manual: ChemApp - the Thermochemical Library for your Software

Hayes, J. M. 1967, Geochim. Cosmochim. Acta, 31, 1395

Hein, J. 2012, private communication

Higgs, P. G. & Pudritz, R. E. 2009, Astrobiology, 9, 483

Jungclaus, G. A., Yuen, G. U., Moore, C. B., & Lawless, J. G. 1976, Meteorit. Planet. Sci., 11, 231

Kaplan, I. R., Degens, E. T., & Reuter, J. H. 1963, Geochim. Cosmochim. Acta, 27, 805

Martins, Z., Alexander, C. M. O. D., Orzechowska, G. E., Fogel, M. L., & Ehrenfreund, P. 2007a, Meteorit. Planet. Sci., 42, 2125

Martins, Z., Hoffman, B. A., Gnos, E., Greenwood, R. C., Verchovsky, A., Franchi, I. A., Jull, A. J. T., Botta, O., Glavin, D. P., Dworkin, J., & Ehrenfreund, P. 2007b, Meteorit. Planet. Sci., 42, 1581

McSween Jr., H. Y., Ghosh, A., Grimm, R. E., Wilson, L., & Young, E. D. 2002, in Asteroids III, ed. W.F. Bottke Jr., A. Cellino, P. Paolicchi, & R.P. Binzel (University of Arizona Press), 559–571

McSween Jr., H. Y. & Weissman, P. R. 1989, Geochim. Cosmochim. Acta, 53, 3263

Meteoritical Bulletin Database. 2013, The Meteoritical Society, International Society for Meteoritics and Planetary Science. Lunar and Planetary Institute. Available online at http://www.lpi.usra.edu/meteor/

Monroe, A. A. & Pizzarello, S. 2011, Geochim. Cosmochim. Acta, 75, 7585

Morbidelli, A., Lunine, J. I., O'Brien, D. P., Raymond, S. N., & Walsh, K. J. 2012, Annu. Rev. Earth Planet. Sci., 40, 251

Mumma, M. J. & Charnley, S. B. 2011, ARA&A, 49, 471

Peltzer, E. T., Bada, J. L., Schlesinger, G., & Miller, S. L. 1984, Adv. Space Res., 4, 69

Pizzarello, S. 2009, J. Mex. Chem. Soc., 53, 253

Pizzarello, S. & Holmes, W. 2009, Geochim. Cosmochim. Acta, 73, 2150

Rimola, A., Sodupe, M., & Ugliengo, P. 2010, Phys. Chem. Chem. Phys., 12, 5285

Schulte, M. & Shock, E. 1995, Orig. Life Evol. Biosph., 25, 161

—. 2004, Meteorit. Planet. Sci., 39, 1577

Sephton, M. 2002, Nat. Prod. Rep., 19, 292

Sephton, M. A. & Botta, O. 2005, Int. J. Astrobiol., 4, 269

Shimoyama, A., Harada, K., & Yanai, K. 1985, Chem. Lett., 14, 1183

Taylor, G. J. 2011, PSRD

The Catalogue of Meteorites. 2012, Natural History Museum Catalogue of Meteorites, fifth edition. ed. M.M. Grady. Available online at http://www.nhm.ac.uk/research-curation/research/projects/metcat/

Travis, B. J. & Schubert, G. 2005, Earth Planet. Sci. Lett., 240, 234

Warren, P. H. 2012, Meteorit. Planet. Sci., 47, 209

Weisberg, M. K., McCoy, T. J., & Krot, A. N. 2006, in Meteorites and the Early Solar System II, ed. D. S. Lauretta, & H. Y. McSween Jr., Vol. 943 (University of Arizona Press), 19–52

Weiss, B. P. & Elkins-Tanton, L. T. 2013, Annu. Rev. Earth Planet. Sci., 41, 529

Young, E. D., Ash, R. D., England, P., & Rumble III, D. 1999, Science, 286, 1331